Dynamic regulation of phosphatidylinositol 3,5-bisphosphate and its upstream lipid kinase Fab1/PIKfyve

By
Michael J. Lang

A dissertation submitted in partial fulfillment
of the requirements for the degree of
Doctor of Philosophy
(Cell and Developmental Biology)
in the University of Michigan
2016

Doctoral committee:

Professor Billy Tsai, Chair
Assistant Professor Mara Duncan
Professor Lois Weisman
Associate Professor Zhaohui Xu

“*O passi graviora, dabit deus his quoque finem.*”
Virgil, The Aeneid

ACKNOWLEDGEMENTS

This dissertation is the result of countless hours of study, thought, work, experimentation, and analysis.

I would like to thank past and present members of the Weisman lab for their valuable insight into my thesis work and helpful advice on protocols: Dr. Yanling Zhang, Dr. Richard Gar Wai Yau, Steven Merz, Dr. Sai Srinivas Panapakkam Giridharan, Camille Akeman, Rachel Chung, Noah Steinfield, Sara Wong, Emily Kauffman, Nadia (supa fly) Azad, and Dr. Bethany Strunk. I thank past lab members Dr. Jason Duex and Dr. Jason Petersen for beginning the preliminary work of my dissertation. I thank Drs. William Brown and James Delproposto for their advice on protein construct design and purification. I thank Dr. Scott Emr (Cornell) for providing the pRS416-Mss4-GFP strain that allowed me to broaden the scope of my work.

I thank my thesis committee members and their laboratories for their enthusiasm and mentorship. I thank Dr. Lois Weisman for allowing me to work in her lab, for the opportunity to mentor an undergraduate student, and for her mentorship. I thank Dr. Zhaohui Xu and his graduate student Dr. Cody Vild for their mentorship in protein construct design, expression, and purification as well as the generous aliquots of Mach1 cells and expression vectors ppSUMO2 and ppSUMO7B. I thank Dr. Billy Tsai for his mentorship and for taking on the position as my committee chair. I thank Dr. Mara

Duncan for taking me into her lab when I was a college student with almost no benchwork experience as well as for her invaluable training, advice, and mentorship I received while I worked in her lab. I cut my teeth at the bench in Mara's lab and owe the success of many experiments to her. Mara continues to advise me today as part of my doctoral committee for which I am grateful.

Finally, I thank my family for their support, encouragement, and advice: Mom, Dad, Alex, Daniel, and the dogs.

TABLE OF CONTENTS

LIST OF FIGURES

LIST OF TABLES

LIST OF ABBREVIATIONS

ABD	Adaptor-binding domain
ALS	Amyotrophic Lateral Sclerosis
AD	Gal4-Activation Domain
BD	Gal4-Binding Domain
CCR	Conserved cysteine-rich domain
CCT	TriC/CCT/Thermosome-like domain
CMT4J	Charcot Marie-Tooth syndrome
DEP	Disheveled, Egl-10, and pleckstrin domain
DSB	Double-stranded break
FYVE	Fab1, YOTB, Vac1, and EEA1 zinc finger domain
GST	Glutathione S-transferase
HEAT	Huntingtin, elongation factor 3, protein phosphatase 2A, and the yeast kinase TOR1 domain
HOG	High Osmolarity Glycerol response
MBP	Maltose Binding Protein
mTOR	Mechanistic target of rapamycin
PI3K	Phosphoinositide 3-kinase
PI4K	Phosphoinositide 4-kinase
PI	Phosphatidylinositol
$PI(3,4)P_2$	Phosphatidylinositol 3,4-bisphosphate
$PI(3,4,5)P_3$	Phosphatidylinositol 3,4,5-trisphosphate
$PI(3,5)P_2$	Phosphatidylinositol 3,5-bisphosphate
$PI(4,5)P_2$	Phosphatidylinositol 4,5-bisphosphate
PI3P	Phosphatidylinositol 3-phosphate
PI4P	Phosphatidylinositol 4-phosphate
PI5P	Phosphatidylinositol 5-phosphate
PIK	Phosphatidylinositol kinase
PIPK	Phosphatidylinositol phosphate kinase
PLAAC	Prion-Like Amino Acid Composition
PPI	Phosphorylated phosphoinositide lipids
PX	Phox homology domain
TRPML	Transient receptor potential mucolipin
V-ATPase	V-ATPase proton pump
WT	Wild Type
Y2H	Yeast two-hybrid assay

ABSTRACT

Eukaryotes maintain homeostatic balance in part via signal transduction cascades, which generate cellular adaptations in response to extracellular cues. Some of these cascades are regulated in part via phosphorylated phosphoinositide lipids (PPIs), which are low-abundance signaling molecules. The PPI phosphatidylinositol (3,5)-bisphosphate ($PI(3,5)P_2$) is generated from phosphatidylinositol 3-phosphate (PI3P) by the conserved lipid kinase Fab1/PIKfyve, which resides in a multiprotein complex known as the Fab1 complex. $PI(3,5)P_2$ controls multiple pathways including calcium storage, lysosomal pH, and TORC1 signaling. $PI(3,5)P_2$ is essential for multiple organ systems. Moreover, defects in the dynamic regulation of $PI(3,5)P_2$ are linked to human diseases, especially those of the nervous system. However, few mechanisms that regulate $PI(3,5)P_2$ have been identified. Here, we report a new mechanism that regulates Fab1 and dynamically controls cellular $PI(3,5)P_2$ synthesis. Using multiple sequence alignment and secondary structure prediction we report a defined domain architecture of each member of the Fab1 complex. We identify new domains in Fab1/PIKfyve and Vac7, a Fab1 activator. Using a forward genetic screen optimized for the isolation of dominant-active Fab1 alleles, we identify point mutations within each domain of Fab1 that alter the dynamic regulation of $PI(3,5)P_2$ levels. We characterize a subset of these dominant-active alleles and show that they disrupt a newly identified, inhibitory, intramolecular interaction between the yeast Fab1 kinase region and an upstream

conserved cysteine-rich (CCR) domain. We report preliminary evidence that this mechanism may be conserved in a second lipid kinase—the PI4 5-kinase, Mss4. Point mutations in Mss4 were generated based on Fab1 dominant-active alleles. These Mss4 mutations increase Mss4 activity under basal conditions and in response to stimulus-induced Mss4 activation. These studies identify a mechanism of regulation that may be conserved among lipid kinases to dynamically control PPI levels in response to external stimuli.

CHAPTER 1

INTRODUCTION[1]

Phosphorylated phosphoinositide lipids

Phosphorylated phosphoinositide lipids (PPIs) are low-abundance signaling molecules that control signal transduction pathways and are necessary for cellular homeostasis (De Camilli *et al.*, 1996). PPIs are generated from phosphatidylinositol (PI). Although PI represents only a small percentage of total cellular lipids, it plays a critical role in the maintenance of signal transduction as the precursor to second messenger PPI molecules. PPIs can be differentially phosphorylated or dephosphorylated to give rise to seven different PPIs (Figure 1.1). Highly regulated PPI kinases, phosphatases, and lipases generate and turn over these lipid species.

Interconvertability of PPIs allows rapid changes in identity of the signaling lipid, which will in turn quickly affect downstream signaling pathways. For instance, the PPI phosphatidylinositol 3-phosphate (PI3P) has been identified at early and late endosomes and lysosomes (Falkenburger *et al.*, 2010).SNARE proteins on endosomes and lysosomes have been shown to bind PI3P in order to mediate homotypic fusion of

[1] Sections of this chapter are adapted from a published literature review: Jin N, Lang MJ, Weisman LS. 2016. Phosphatidylinositol 3,5-bisphosphate: regulation of cellular events in space and time. Biochem Soc Trans. Feb;44(1):177-84. DOI: 10.1042/BST20150174.

endolysosomal compartments (Cheever *et al.*, 2001; Boeddinghaus *et al.*, 2002). However, an additional effector of PI3P, the PI3P 5-kinase Fab1, can bind PI3P via its FYVE domain and phosphorylate the 5-hydroxyl to produce phosphatidylinositol 3,5-bisphosphate ($PI(3,5)P_2$) (Dove *et al.*, 1997; Gary *et al.*, 1998), which does not recruit the machinery for homotypic vacuole fusion. Instead, the generation of $PI(3,5)P_2$ recruits a distinct set of $PI(3,5)P_2$ binding proteins.

To date, PI3P, phosphatidylinositol 4-phosphate (PI4P), phosphatidylinositol 4,5-bisphosphate ($PI(4,5)P_2$), and $PI(3,5)P_2$ have been identified in *S. cerevisiae*. Phosphatidylinositol 3,4,5-trisphosphate has been identified in the fission yeast (*Schizosaccharomyces pombe*), but not in *S. cerevisiae* (Wera *et al.*, 2001; Mitra *et al.*, 2004). Higher eukaryotes synthesize the five PPIs found in fungi as well as PI5P (Viaud *et al.*, 2014; Li and Marshall, 2015). A total of six PPIs have been identified; however, for this thesis I will focus on the regulation of those PPIs identified in *S. cerevisiae*. Through their dynamic regulation, PPI lipids provide spatial and temporal control of complex protein machines and downstream effectors.

The enzymes that phosphorylate phosphatidylinositol and its derivatives are termed phosphoinositide kinases. Phosphoinositide kinases are grouped into three general

families: phosphoinositide 3-kinases (PI3Ks), phosphoinositide 4-kinases (PI4Ks), and phosphorylated phosphoinositide kinases (PIPKs) (Strahl and Thorner, 2007). The majority of PPI kinases are conserved throughout evolution. Evidence that PI was phosphorylated in fungi was first presented in 1972 (Wheeler *et al.*, 1972), and later work identified a total of seven PPI kinases. The first PPI kinase isolated and cloned was yeast VPS34, which encoded a PI 3-kinase (Schu *et al.*, 1993), and within the same year yeast PIK1 was identified as a PI 4-kinase (Flanagan *et al.*, 1993). Later Stt4 was identified as a second yeast PI 4-kinase, which generates a PI4P pool distinct from the Pik1-generated PI4P pool (Trotter *et al.*, 1998; Audhya *et al.*, 2000). Together Pik1 and Stt4 generate ~95% of total PI4P in yeast (Audhya *et al.*, 2000); the remaining 5% is currently proposed to be generated from Lsb6, a type II PI 4-kinase that localizes to the plasma membrane and vacuole in yeast (Han *et al.*, 2002; Shelton *et al.*, 2003). While the function of Lsb6 activity is largely unknown it is hypothesized that a third pool of PI4P may exist in yeast (Chang *et al.*, 2005). In yeast, two PIPKs have been identified. Mss4 is an essential gene encoding a PI4 5-kinase (Desrivieres *et al.*, 1998). Fab1 is a PI3 5-kinase encoding a protein of 2278 amino acids in *S. cerevisiae*—the largest PPI kinase in yeast (Yamamoto *et al.*, 1995). These kinases will be discussed in greater detail in Chapter 5. Together, these kinases synthesize the five yeast PPIs.

The enzymes that turn over PPIs are lipid phosphatases and lipases (Strahl and Thorner, 2007; McCartney *et al.*, 2014). PLC1 encodes a lipase that hydrolyzes PI(4,5)P_2 into IP3 and DAG (Flick and Thorner, 1993). PLC1 is a significant source of turnover of PI(4,5)P_2, but not other PPIs (Cutler *et al.*, 1997). *S. cerevisiae* is predicted

to contain at least seven PPI phosphatases (Strahl and Thorner, 2007). These PPI phosphatases include Sac1, Inp51-4, Fig4, and Ymr1 (Guo *et al.*, 1999; Whisstock *et al.*, 2002; Clague and Lorenzo, 2005). Current literature on the specific activity of yeast lipid phosphatases is limited. Often, *in vivo* phenotypes require multiple lipid phosphatase deletions before a phenotype is observed and biochemical assays are limited due to instability of purified proteins (Gary *et al.*, 2002; Botelho *et al.*, 2008). Improved genetic and biochemical assays are needed to determine the activity and specificity of lipid phosphatases.

PI(3,5)P_2

The presence of PI(3,5)P_2 within cells was first proposed in 1989 (Auger *et al.*, 1989). However, another decade was to pass until, in 1997, two groups independently confirmed the presence of PI(3,5)P_2 in mouse fibroblasts, yeast, and Cos-7 cells (Dove *et al.*, 1997; Whiteford *et al.*, 1997). PI(3,5)P_2 is of extreme low abundance even by the low-abundance standards of other PPIs. PI(3,5)P_2 is present at about 0.08% and 0.04% of total phosphatidylinositol in yeast and mammalian fibroblasts, respectively. Comparatively, this is ~17-fold and 125-fold lower than phosphatidylinositol 4,5-bisphosphate PI(4,5)P_2 in yeast and mammalian cells, respectively (Bonangelino *et al.*, 2002; Duex *et al.*, 2006a; Duex *et al.*, 2006b; Jin *et al.*, 2008; Zolov *et al.*, 2012a). In cells, PI(3,5)P_2 is found on early endosomes, late endosomes, and lysosomes where it regulates downstream effectors (McCartney *et al.*, 2014).

The Role of PI(3,5)P_2 in Human Health

$PI(3,5)P_2$ deficiencies are linked to human diseases, especially those of the nervous system. For instance, mutations predicted to have a modest effect on the ability of cells to dynamically elevate $PI(3,5)P_2$ levels underlie a severe form of Charcot Marie-Tooth syndrome (CMT4J) (Chow *et al.*, 2007; Lenk *et al.*, 2011; Nicholson *et al.*, 2011), a peripheral neuropathy, as well as some cases of amyotrophic lateral sclerosis (ALS) (Chow *et al.*, 2009). Recently, a homozygous missense mutation in Fig4, a Fab1/PIKfyve regulator, was found to be the causal allele in a consanguineous family with multiple neurological problems: temporo-occipital polymicrogyria, epilepsy, and psychiatric indications including suicide and aggressive behavior (Baulac *et al.*, 2014).

Mutations with more severe deficiencies in the regulation of $PI(3,5)P_2$ underlie additional neurological diseases. For instance, a mutation predicted to lower $PI(3,5)P_2$ to 1/3 of its normal levels causes Yunis-Varon syndrome, which results in infant mortality and severe pathological effects on multiple tissues, including the brain(Campeau *et al.*, 2013). Importantly, the defects observed in Yunis-Varon syndrome fit closely with phenotypes observed in mice with a homozygous deletion of Fig4 (Chow *et al.*, 2007) as well as mice homozygous for a hypomorphic mutation in PIKfyve, PIKfyve-βgeo/βgeo (Zolov *et al.*, 2012a).

$PI(3,5)P_2$ levels are dynamically controlled by the Fab1 complex

A complex of proteins, which includes Fab1/PIKfyve, Vac4, and Fig4, dynamically controls the biosynthesis of $PI(3,5)P_2$ within the cell. Fab1 was initially identified in Baker's yeast and was shown to function as a PI3P-5 kinase, and reside on the

vacuolar membrane (Yamamoto *et al.*, 1995; Cooke *et al.*, 1998; Gary *et al.*, 1998). Homologs have been identified in *C. elegans (Nicot et al., 2006)*, *D. melanogaster* (Oppelt *et al.*, 2013), plants (Hirano *et al.*, 2011; Hirano and Sato, 2011), and mammals (Sbrissa *et al.*, 1999). In yeast, Fab1 is the sole PI3P 5-kinase (Gary *et al.*, 2002). Similarly, the human homolog, PIKfyve, is the sole PI3P 5-kinase (Zolov *et al.*, 2012b). Within this dissertation Fab1 will refer to the yeast protein, PIKfyve will refer to mammalian Fab1, and Fab1/PIKfyve will refer to all known Fab1 homologs.

Several PI(3,5)P_2 modulators have been identified in yeast including Vac7, Vac14, Fig4 and Atg18. Fab1 and its regulators localize on the vacuole membrane (Bonangelino *et al.*, 1997; Gary *et al.*, 1998; Dove *et al.*, 2002; Dove *et al.*, 2004b; Jin *et al.*, 2008). Vac7 and Vac14 were first identified as novel vacuolar proteins required for vacuole inheritance and morphology (Wang *et al.*, 1996; Bonangelino *et al.*, 1997). Deletion of Vac7, Vac14 or Fab1 increases vacuole size and causes a defect in the synthesis of PI(3,5)P_2 under basal conditions as well as during hyperosmotic shock (Bonangelino *et al.*, 1997; Gary *et al.*, 1998; Dove *et al.*, 2002) (Figure 1.2), which provides an indication that Vac7 and Vac14 positively regulate Fab1 lipid kinase activity. The connection between Fig4 and Fab1 came from a yeast genetic screen for mutants that suppress the temperature sensitivity of a *vac7Δ* mutant (Gary *et al.*, 2002). Fig4 has a Sac1 phosphatase domain that is found in several lipid phosphatases including Inp51, 52 and 53 (Gary *et al.*, 2002). Although Fig4 functions as a PI(3,5)P_2-specific phosphoinositide phosphatase *in vitro* (Rudge *et al.*, 2004) and *in vivo* (Duex *et al.*, 2006a), paradoxically, deletion of Fig4 causes a defect in the acute synthesis of PI(3,5)P_2 during hyperosmotic

shock (Duex *et al.*, 2006a). This suggests that Fig4 has dual roles for the synthesis and turnover of $PI(3,5)P_2$. Atg18 is a regulator of autophagy (Dove *et al.*, 2004b; Efe *et al.*, 2005, 2007). However, deletion of Atg18 results in an enlarged vacuole, similar to mutants with defects in the levels of $PI(3,5)P_2$. Unexpectedly, the ***atg18Δ*** mutant has increased levels of $PI(3,5)P_2$ both under basal conditions and during hyperosmotic shock (Dove *et al.*, 2004a). These observations indicate that Atg18 negatively modulates Fab1 activity. Note that Atg18 binds PI(3)P and $PI(3,5)P_2$ with high affinity via two sites (Watanabe *et al.*, 2012) and associates with the vacuole membrane through binding to $PI(3,5)P_2$. Association of Atg18 with the vacuole membrane is required for its regulation of Fab1 (Efe *et al.*, 2005, 2007). Together, yeast Vac14, Fig4, and Atg18 work in both positive and negative regulatory mechanisms to control $PI(3,5)P_2$ levels.

In mammalian cells, Vac14 and Fig4 are evolutionally and functionally conserved and are also referred to as ArPIKfyve (Sbrissa *et al.*, 2004) and Sac3 (Ikonomov *et al.*, 2009a; Ikonomov *et al.*, 2009b) respectively. Similar to yeast, mammalian PIKfyve, Vac14 and Fig4 are localized on early and late endosomes as well as lysosomes (Sbrissa *et al.*, 2007; Zhang *et al.*, 2007; Zhang *et al.*, 2012; Zolov *et al.*, 2012b). Vac7 homologues have only been observed in fungi and it is not clear whether functional homologues are present in other species. Atg18 belongs to a large family of proteins known as PROPPINS, which are found in most eukaryotes (Dove *et al.*, 2004b; Krick *et al.*, 2012). PROPPIN proteins have predicted β-propeller folds and the presence of an FRRG motif required for phosphoinositide binding. Mammals have four PROPPINS, WIPI-1,2,3 and 4 which have sequence similarity with yeast Atg18 (Dove *et al.*, 2004b;

Krick *et al.*, 2012). Moreover, like Atg18, WIPI-1,2 and 4 bind PI(3)P and PI(3,5)P_2 with high affinity (Baskaran *et al.*, 2012). WIPI-3 has not yet been tested due to instability. Despite the similarities between Atg18 and WIPI-1,2,3 and 4, it is not clear whether WIPI proteins regulate PI(3,5)P_2 levels in mammalian cells. Together, these studies suggest that the functions of Fab1, Vac14, and Fig4 are conserved from yeast to humans; the roles and conservation of Vac7 and Atg18 are less clear.

Response to hyperosmotic stress in yeast

When exposed to hyperosmotic stress the yeast *S. cerevisiae* initiates a complex series of adaptive responses, which include a short-term and long-term adaption response. Short-term adaption is accomplished through a controlled elevation in synthesis of PI(3,5)P_2 (Duex *et al.*, 2006a). The long-term adaptive response includes (1) the adjustment of transcription and translation patterns (2) the temporary arrest of the cell cycle, and (3) the synthesis and maintenance of elevated levels of glycerol. These long-term adaptive changes are regulated via the HOG (High Osmolarity Glycerol response) pathway (reviewed in (Saito and Posas, 2012)).

During short-term adaption to hyperosmotic media, yeast cells modulate levels of all PPIs (Duex *et al.*, 2006a). For example, following hyperosmotic shock the level of PI3P decreases at a rate similar to the rate of elevation seen in PI(3,5)P_2, and accounts for a concomitant increase in PI(3,5)P_2 levels (Duex *et al.*, 2006a) (Figure 1.3). While the decrease in PI3P is only a small fraction of total PI3P, the elevation in PI(3,5)P_2 is much more dramatic. Within 5 minutes post hyperosmotic shock, PI(3,5)P_2 levels rise over

fifteen-fold, plateau for ten minutes, then precipitously return to basal levels over a sixty minute timecourse (Duex *et al.*, 2006a). Concomitant with the fifteen-fold rise in $PI(3,5)P_2$ levels, the yeast vacuole fragments (Duex *et al.*, 2006a). While the biological significance for this acute regulation of PPI levels in response to introduction into hyperosmotic media remains unclear, investigators have taken advantage of these acute changes to gain mechanistic insights into the regulation of PPIs (Jin *et al.*, 2008).

PI4P and $PI(4,5)P_2$ are elevated during hyperosmotic shock. PI4P levels spike one minute after hyperosmotic shock stimulation; however, by the second minute PI4P levels quickly begin to decline for the remainder of the time course (Duex *et al.*, 2006a). This decrease in PI4P levels is likely due to the synthesis of $PI(4,5)P_2$, which begins at five minutes post hyperosmotic shock, peaks at fifteen minutes, then returns to basal levels after sixty minutes (Duex *et al.*, 2006a). In Chapter Five of this thesis, I take advantage of this observation to probe a mechanism for the regulation of the yeast PI4P 5-kinase, Mss4.

$PI(3,5)P_2$ regulates the vacuole and signaling pathways that occur on the vacuolar membrane

One of the hallmarks of eukaryotic cells is the compartmentalization of cellular processes via organelles within each cell. This compartmentalization allows for separation of specific catabolic and anabolic processes that occur simultaneously within the cell. Additional levels of control are exerted via controlling the relative concentrations of ions and metabolites within specific subcellular organelles. This

aspect of cellular storage is often overlooked in the characterization of the yeast vacuole, which is the main storage organelle in yeast. Exponentially growing yeast cells have between 2-4 vacuoles, which share multiple similarities to the mammalian lysosome (Klionsky *et al.*, 1990; Chan and Marshall, 2014). The vacuole has a role in the degradation of proteins as well as the storage and regulation of many essential macro and micronutrients. Indeed, the yeast vacuole stores large pools of amino acids, polyphosphate, and inorganic ions such as calcium and other heavy metals (Klionsky *et al.*, 1990). While it has not yet been critically tested, $PI(3,5)P_2$ may control many of these processes. Three emerging examples of how $PI(3,5)P_2$ may control the contents of the vacuole and signaling on the vacuolar membrane are exemplified in studies of (1) the yeast YVC1 Ca^{+2} channel (2) the vacuolar V-ATPase proton pump and (3) $PI(3,5)P_2$ dependent TORC1 signaling.

$PI(3,5)P_2$ is a positive regulator of the YVC1/TRPML Ca^{+2} channel

One example of how $PI(3,5)P_2$ may regulate the vacuole is demonstrated through studies of the mammalian TRPML1 calcium transporter (Dong *et al.*, 2010a). TRPML1 is a member of the transient receptor potential (TRP) mucolipin (ML) family, which in turn is a family member of a superfamily of Ca^{+2}-permeable cation channels (Dong *et al.*, 2010b). TRPML1 is primarily localized on membranes of late endosomes and lysosomes (Dong *et al.*, 2010b). Through a modified patch-clamp technique developed in the laboratory of Dr. Haoxing Xu, it was determined that $PI(3,5)P_2$ activates TRPML1 channels in endolysosomal membranes in both HEK293T and Cos-1 cells. In yeast, induction of vacuolar Ca^{+2} release is through Yvc1/TRPY1, a TRP channel homologue

(Palmer *et al.*, 2001). Deletion of YVC1 causes a defect in the release of Ca^{+2} (Denis and Cyert, 2002). Excitingly, in a *fab1Δ* strain, vacuolar Ca^{+2} release in response to hyperosmotic shock is defective similar to a *yvc1Δ* yeast strain (Dong *et al.*, 2010b). This data suggests that Yvc1 releases Ca^{+2} from the vacuole in a $PI(3,5)P_2$ dependent manner. Additional experiments confirmed this hypothesis. Overexpression of TRPML1 in wild-type (WT) yeast increases Ca^{+2} release in response to hyperosmotic shock and that in *yvc1Δ* cells, overexpression of TRPML1, but not a non-functional pore mutant of TRPML1 (TRPML1-KK), rescues Ca^{+2} release during hyperosmotic shock (Dong *et al.*, 2010b). However, overexpression in a *fab1Δ* mutant strain fails to significantly increase the Ca^{+2} release response. Together this data suggests that PI(3,5)P2 is a positive regulator of the Ca^{+2} channel mammalian TRPML1 and its yeast homolog YVC1.

$PI(3,5)P_2$ positively regulates the V-ATPase and maintains vacuolar acidification

Vacuoles are the most acidic component of the yeast cell, with an average pH of ~6.2 and a range of <5.0-6.5 depending on growth conditions (Preston *et al.*, 1989; Plant *et al.*, 1999; Padilla-Lopez and Pearce, 2006; Martinez-Munoz and Kane, 2008). This acidification is maintained through the V-ATPase proton pump (V-ATPase). The V-ATPase uses energy generated by ATP hydrolysis to pump protons across the vacuolar membrane and into the vacuolar lumen. The activity of the *S. cerevisiae* V-ATPase pump results in a decrease in the vacuolar pH and a membrane potential of 75mV (Kakinuma *et al.*, 1981). The V-ATPase is a multisubunit proton pump, with evolutionary relationships to F-type ATP synthases and archaeral ATPases (Gruber *et al.*, 2014). The V-ATPase is composed of two subunits: the peripheral (V_1) subunit and the

membrane bound (V_0) subunit, which contains the proton pore (Kane and Smardon, 2003). The assembly and disassembly of these subunits are controlled by upstream cues such as glucose availability and external pH (Ramos *et al.*, 2016). Importantly, work from our lab and Dr. Patricia Kane's lab has shown that PI(3,5)P_2 stabilizes the association between the V_1 and V_0 sectors and activates the V-ATPase (Li *et al.*, 2014). Indeed, PI(3,5)P_2 levels are directly correlated with an increase in the assembly of the V-ATPase and subsequent acidification of the vacuolar lumen.

Defects in the V-ATPase proton pump lead to an increase in the alkalization of the yeast vacuole, and subsequent defects associated with an increase in vacuolar pH (Preston *et al.*, 1989; Diakov and Kane, 2010) (Tarsio *et al.*, 2011). Importantly, yeast strains deleted of FAB1, VAC14, or VAC7 are poorly acidified (Bonangelino *et al.*, 1997; Cooke *et al.*, 1998; Bonangelino *et al.*, 2002; Dove *et al.*, 2002), which demonstrates that PI(3,5)P_2 production and maintenance is important for V-ATPase function.

PI(3,5)P_2 positively regulates TORC1 signaling

PI(3,5)P_2 is a positive regulator of TORC1 activity (Jin *et al.*, 2014). The mechanistic target of rapamycin (mTOR) is an evolutionarily conserved protein kinase responsible for homeostatic control of cell growth and metabolism (reviewed in (Kim and Guan, 2009; Loewith and Hall, 2011; Powis and De Virgilio, 2016)). mTOR functions within two distinct complexes, TORC1 and TORC2 (Loewith *et al.*, 2002). In yeast, TORC1 consists of four proteins: Tor1 or Tor2, the Raptor homolog Kog1, the mLST8/GβL

homolog Lst8, and Tco89. TORC1 localizes to the vacuole membrane in yeast, and this localization is required for full activity of the complex (Sturgill *et al.*, 2008).

In addition to TORC1, vacuolar localization of two major TORC1-activators, the EGO complex and the V-ATPase, is required for TORC1 activity. The EGO Complex, which is the fungal equivalent of the mammalian regulator complex, is composed Ego1, Gtr2, and Ego3, and localizes to the limiting membrane of the vacuole (Dubouloz *et al.*, 2005; Binda *et al.*, 2009; Kogan *et al.*, 2010; Sancak *et al.*, 2010). The EGO complex is activated by Vam6, where it targets TORC1 to the vacuolar surface and mediates nutrient sensing (Sancak *et al.*, 2010). The V-ATPase resides on the vacuolar/lysosomal membrane and, in addition to its role as a proton pump, positively regulates the regulator complex in mammalian cells in an amino acid-dependent manner (Zoncu *et al.*, 2011). Studies have not yet confirmed this in yeast; however, the conservation of other mechanisms within this pathway would indicate that this role of the V-ATPase is similarly conserved.

$PI(3,5)P_2$ physically interacts with subunits of the TORC1 complex as well as downstream targets of the TORC1 pathway. In addition to the previously discussed positive regulation of the V-ATPase by $PI(3,5)P_2$, *in vitro* the TORC1 subunit Raptor directly binds $PI(3,5)P_2$ (Bridges *et al.*, 2012) and this interaction is necessary to recruit TORC1 to the lysosomal membrane in mammalian cells. Additionally, the yeast homolog of Raptor, Kog1, also binds $PI(3,5)P_2$ (Jin *et al.*, 2014).

In vivo, PI(3,5)P_2 defective mutants are highly sensitive to rapamycin indicating that TORC1 function is impaired in cells with reduced PI(3,5)P_2 levels (Jin *et al.*, 2014). Moreover, PI(3,5)P_2 is required for TORC1-dependent phosphorylation of Sch9, the yeast homolog of mammalian S6K, which in yeast is localized to the vacuole in a PI(3,5)P_2-dependent fashion (Jin *et al.*, 2014). These findings reveal that PI(3,5)P_2 regulates multiple steps within the TORC1 pathway.

That PI(3,5)P_2 regulates vacuolar calcium flux, vacuolar pH, and TORC1 function indicates that this lipid regulates diverse pathways. Moreover, the pleiotropic defects in a *fab1Δ* strain suggests that several pathways likely rely on PI(3,5)P_2. Discovery of additional downstream effectors will reveal these pathways. However, there are currently no bioinformatic approaches to identify these effectors. Moreover, biochemical and genetic approaches are not straightforward.

Another gap in current knowledge of PI(3,5)P_2 is the mechanisms required for its dynamic regulation. I propose that at least two categories of effects dynamically regulate PI(3,5)P_2: (1) upstream, unknown pathways that regulate the Fab1 complex (2) the large Fab1 complex, which directly synthesizes PI(3,5)P_2 from PI3P. For this thesis I choose to focus on the mechanism of regulation of the Fab1 complex, which generates and turns over PI(3,5)P_2 through lipid kinase and lipid phosphatase activity.

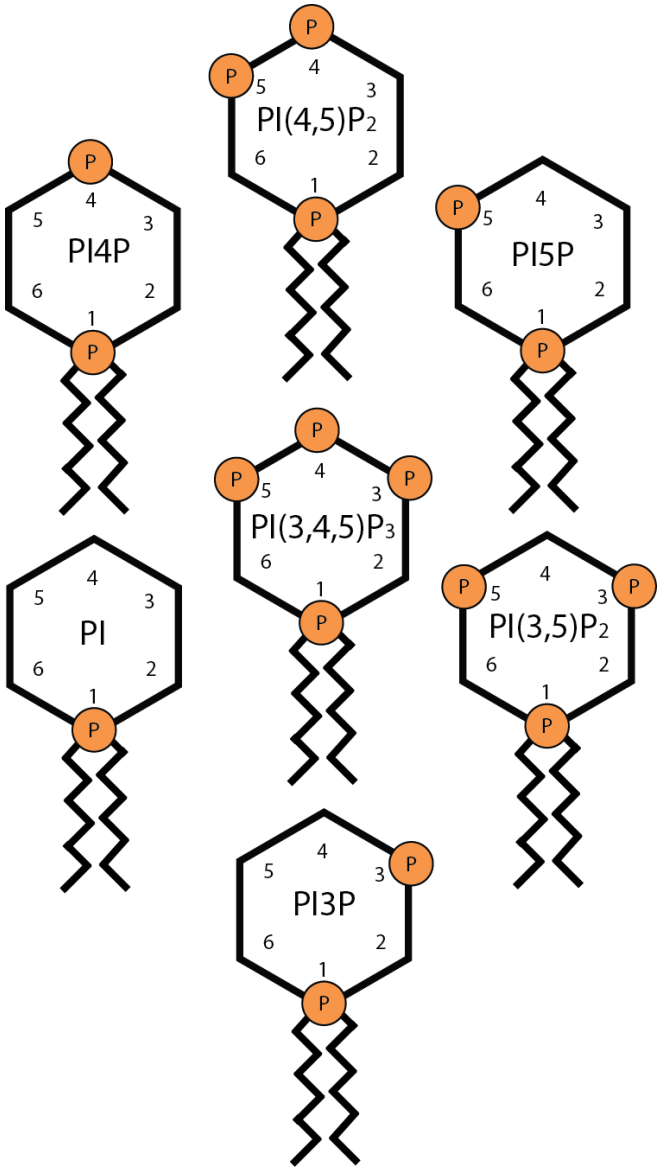

Figure 1.1. Phosphatidylinositol can be differentially phosphorylated or dephosphorylated to give rise to seven different PPIs. Center: phosphatidylinositol 3,4,5-triphosphate ($PI(3,4,5)P_3$) Clockwise from top left: phosphatidylinositol 4-phosphate (PI4P), phosphatidylinositol 4,5-bisphosphate ($PI(4,5)P_2$), phosphatidylinositol 5-phosphate (PI5P), phosphatidylinositol 3,5-bisphosphate ($PI(3,5)P_2$), phosphatidylinositol 3-phosphate (PI3P), and phosphatidylinositol.

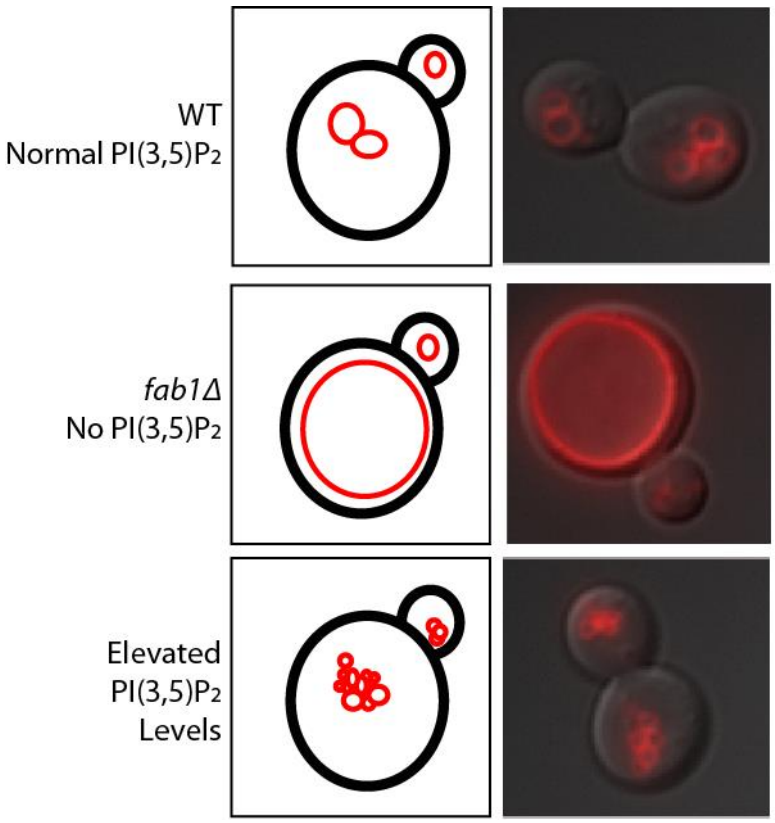

Figure 1.2. In most cases the size of the lysosome (vacuole in yeast) is inversely correlated with the amount of PI(3,5)P_2. From top to bottom: Wild-type yeast contain two to four vacuoles. A Fab1 null (No PI(3,5)P_2) is comprised of a single, swollen vacuole. Yeast with elevated levels of PI(3,5)P_2 display a fragmented phenotype consisting of many small vacuoles.

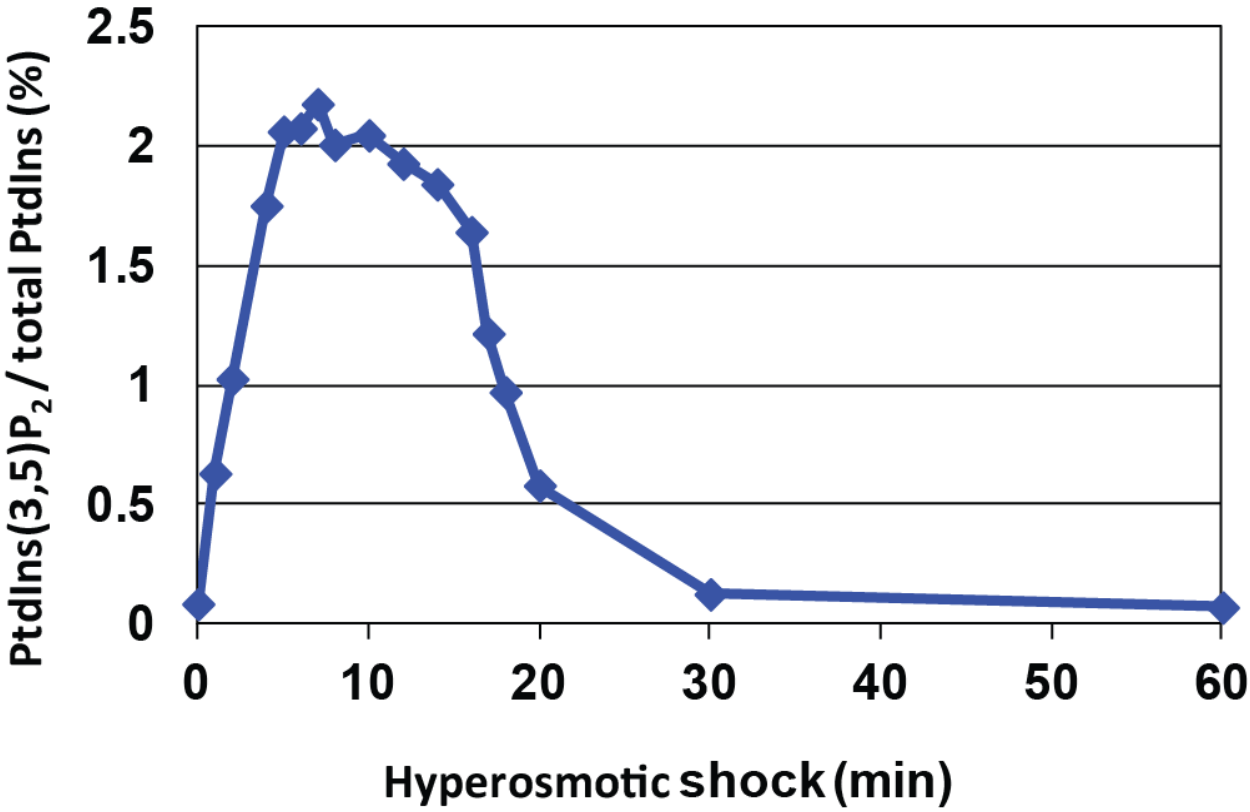

Figure 1.3. The synthesis of PI(3,5)P_2 is tightly regulated. PI(3,5)P_2 levels transiently change in response to specific stimuli. A prolonged single stimulus, introduction of yeast into hyperosmotic media, causes a transient elevation of PI(3,5)P_2. Within 5 min, PI(3,5)P_2 levels rise over 15-fold, plateau for 10 min, then rapidly return to basal levels. That levels of PI(3,5)P_2 are tightly controlled suggests that there are multiple layers of regulation. Data modified from (Duex *et al.*, 2006a).

Bibliography

Audhya, A., Foti, M., and Emr, S.D. (2000). Distinct roles for the yeast phosphatidylinositol 4-kinases, Stt4p and Pik1p, in secretion, cell growth, and organelle membrane dynamics. Mol Biol Cell *11*, 2673-2689.

Auger, K.R., Carpenter, C.L., Cantley, L.C., and Varticovski, L. (1989). Phosphatidylinositol 3-kinase and its novel product, phosphatidylinositol 3-phosphate, are present in Saccharomyces cerevisiae. J Biol Chem *264*, 20181-20184.

Baskaran, S., Ragusa, M.J., Boura, E., and Hurley, J.H. (2012). Two-site recognition of phosphatidylinositol 3-phosphate by PROPPINs in autophagy. Molecular cell *47*, 339-348.

Baulac, S., Lenk, G.M., Dufresnois, B., Bencheikh, B.O.A., Couarch, P., Renard, J., Larson, P.A., Ferguson, C.J., Noé, E., Poirier, K., Hubans, C., Ferreira, S., Guerrini, R., Ouazzani, R., El, K.H., Hachimi, K.H.E., Meisler, M.H., and Leguern, E. (2014). Role of the phosphoinositide phosphatase FIG4 gene in familial epilepsy with polymicrogyria. Neurology *(in press)*.

Binda, M., Peli-Gulli, M.P., Bonfils, G., Panchaud, N., Urban, J., Sturgill, T.W., Loewith, R., and De Virgilio, C. (2009). The Vam6 GEF controls TORC1 by activating the EGO complex. Mol Cell *35*, 563-573.

Boeddinghaus, C., Merz, A.J., Laage, R., and Ungermann, C. (2002). A cycle of Vam7p release from and PtdIns 3-P-dependent rebinding to the yeast vacuole is required for homotypic vacuole fusion. J Cell Biol *157*, 79-89.

Bonangelino, C.J., Catlett, N.L., and Weisman, L.S. (1997). Vac7p, a novel vacuolar protein, is required for normal vacuole inheritance and morphology. Molecular and cellular biology *17*, 6847-6858.

Bonangelino, C.J., Nau, J.J., Duex, J.E., Brinkman, M., Wurmser, A.E., Gary, J.D., Emr, S.D., and Weisman, L.S. (2002). Osmotic stress-induced increase of phosphatidylinositol 3,5-bisphosphate requires Vac14p, an activator of the lipid kinase Fab1p. The Journal of cell biology *156*, 1015-1028.

Botelho, R.J., Efe, J.A., Teis, D., and Emr, S.D. (2008). Assembly of a Fab1 phosphoinositide kinase signaling complex requires the Fig4 phosphoinositide phosphatase. Mol Biol Cell *19*, 4273-4286.

Bridges, D., Ma, J.T., Park, S., Inoki, K., Weisman, L.S., and Saltiel, A.R. (2012). Phosphatidylinositol 3,5-bisphosphate plays a role in the activation and subcellular localization of mechanistic target of rapamycin 1. Mol Biol Cell *23*, 2955-2962.

Campeau, P.M., Lenk, G.M., Lu, J.T., Bae, Y., Burrage, L., Turnpenny, P., Corona-Rivera, J.R., Morandi, L., Mora, M., Reutter, H., Vulto-van Silfhout, A.T., Faivre, L., Haan, E., Gibbs, R.A., Meisler, M.H., and Lee, B.H. (2013). Yunis-Varón syndrome is caused by mutations in FIG4 encoding a phosphoinositide phosphatase. American Journal of Human Genetics *92*, 781-791.

Chan, Y.H., and Marshall, W.F. (2014). Organelle size scaling of the budding yeast vacuole is tuned by membrane trafficking rates. Biophys J *106*, 1986-1996.

Chang, F.S., Han, G.S., Carman, G.M., and Blumer, K.J. (2005). A WASp-binding type II phosphatidylinositol 4-kinase required for actin polymerization-driven endosome motility. J Cell Biol *171*, 133-142.

Cheever, M.L., Sato, T.K., de Beer, T., Kutateladze, T.G., Emr, S.D., and Overduin, M. (2001). Phox domain interaction with PtdIns(3)P targets the Vam7 t-SNARE to vacuole membranes. Nat Cell Biol *3*, 613-618.

Chow, C.Y., Landers, J.E., Bergren, S.K., Sapp, P.C., Grant, A.E., Jones, J.M., Everett, L., Lenk, G.M., McKenna-Yasek, D.M., Weisman, L.S., Figlewicz, D., Brown, R.H., and Meisler, M.H. (2009). Deleterious variants of FIG4, a phosphoinositide phosphatase, in patients with ALS. American journal of human genetics *84*, 85-88.

Chow, C.Y., Zhang, Y., Dowling, J.J., Jin, N., Adamska, M., Shiga, K., Szigeti, K., Shy, M.E., Li, J., Zhang, X., Lupski, J.R., Weisman, L.S., and Meisler, M.H. (2007). Mutation of FIG4 causes neurodegeneration in the pale tremor mouse and patients with CMT4J. Nature *448*, 68-72.

Clague, M.J., and Lorenzo, O. (2005). The myotubularin family of lipid phosphatases. Traffic *6*, 1063-1069.
Cooke, F.T., Dove, S.K., McEwen, R.K., Painter, G., Holmes, A.B., Hall, M.N., Michell, R.H., and Parker, P.J. (1998). The stress-activated phosphatidylinositol 3-phosphate 5-kinase Fab1p is essential for vacuole function in S-cerevisiae. Current Biology *8*, 1219-1222.
Cutler, N.S., Heitman, J., and Cardenas, M.E. (1997). STT4 is an essential phosphatidylinositol 4-kinase that is a target of wortmannin in Saccharomyces cerevisiae. J Biol Chem *272*, 27671-27677.
De Camilli, P., Emr, S.D., McPherson, P.S., and Novick, P. (1996). Phosphoinositides as regulators in membrane traffic. Science *271*, 1533-1539.
Denis, V., and Cyert, M.S. (2002). Internal Ca(2+) release in yeast is triggered by hypertonic shock and mediated by a TRP channel homologue. J Cell Biol *156*, 29-34.
Desrivieres, S., Cooke, F.T., Parker, P.J., and Hall, M.N. (1998). MSS4, a phosphatidylinositol-4-phosphate 5-kinase required for organization of the actin cytoskeleton in Saccharomyces cerevisiae. J Biol Chem *273*, 15787-15793.
Diakov, T.T., and Kane, P.M. (2010). Regulation of vacuolar proton-translocating ATPase activity and assembly by extracellular pH. J Biol Chem *285*, 23771-23778.
Dong, X.P., Shen, D., Wang, X., Dawson, T., Li, X., Zhang, Q., Cheng, X., Zhang, Y., Weisman, L.S., Delling, M., and Xu, H. (2010a). PI(3,5)P(2) controls membrane trafficking by direct activation of mucolipin Ca(2+) release channels in the endolysosome. Nat Commun *1*, 38.
Dong, X.P., Shen, D., Wang, X., Dawson, T., Li, X., Zhang, Q., Cheng, X., Zhang, Y., Weisman, L.S., Delling, M., and Xu, H. (2010b). PI(3,5)P(2) controls membrane trafficking by direct activation of mucolipin Ca(2+) release channels in the endolysosome. Nature communications *1*.
Dove, S.K., Cooke, F.T., Douglas, M.R., Sayers, L.G., Parker, P.J., and Michell, R.H. (1997). Osmotic stress activates phosphatidylinositol-3,5-bisphosphate synthesis. Nature *390*, 187-192.
Dove, S.K., McEwen, R.K., Mayes, A., Hughes, D.C., Beggs, J.D., and Michell, R.H. (2002). Vac14 controls PtdIns(3,5)P-2 synthesis and Fab1-dependent protein trafficking to the multivesicular body. Current Biology *12*, 885-893.
Dove, S.K., Piper, R.C., McEwen, R.K., Yu, J.W., King, M.C., Hughes, D.C., Thuring, J., Holmes, A.B., Cooke, F.T., Michell, R.H., Parker, P.J., and Lemmon, M.A. (2004a). Svp1p defines a family of phosphatidylinositol 3,5-bisphosphate effectors. EMBO J *23*, 1922-1933.
Dove, S.K., Piper, R.C., McEwen, R.K., Yu, J.W., King, M.C., Hughes, D.C., Thuring, J., Holmes, A.B., Cooke, F.T., Michell, R.H., Parker, P.J., and Lemmon, M.A. (2004b). Svp1p defines a family of phosphatidylinositol 3,5-bisphosphate effectors. Embo Journal *23*, 1922-1933.
Dubouloz, F., Deloche, O., Wanke, V., Cameroni, E., and De Virgilio, C. (2005). The TOR and EGO protein complexes orchestrate microautophagy in yeast. Mol Cell *19*, 15-26.
Duex, J.E., Nau, J.J., Kauffman, E.J., and Weisman, L.S. (2006a). Phosphoinositide 5-phosphatase Fig 4p is required for both acute rise and subsequent fall in stress-induced phosphatidylinositol 3,5-bisphosphate levels. Eukaryotic cell *5*, 723-731.
Duex, J.E., Tang, F., and Weisman, L.S. (2006b). The Vac14p-Fig4p complex acts independently of Vac7p and couples PI3,5P2 synthesis and turnover. The Journal of cell biology *172*, 693-704.
Efe, J.A., Botelho, R.J., and Emr, S.D. (2005). The Fab1 phosphatidylinositol kinase pathway in the regulation of vacuole morphology. Curr Opin Cell Biol *17*, 402-408.
Efe, J.A., Botelho, R.J., and Emr, S.D. (2007). Atg18 regulates organelle morphology and Fab1 kinase activity independent of its membrane recruitment by phosphatidylinositol 3,5-bisphosphate. Mol Biol Cell *18*, 4232-4244.
Falkenburger, B.H., Jensen, J.B., Dickson, E.J., Suh, B.C., and Hille, B. (2010). Phosphoinositides: lipid regulators of membrane proteins. The Journal of physiology *588*, 3179-3185.

Flanagan, C.A., Schnieders, E.A., Emerick, A.W., Kunisawa, R., Admon, A., and Thorner, J. (1993). Phosphatidylinositol 4-kinase: gene structure and requirement for yeast cell viability. Science *262*, 1444-1448.
Flick, J.S., and Thorner, J. (1993). Genetic and biochemical characterization of a phosphatidylinositol-specific phospholipase C in Saccharomyces cerevisiae. Mol Cell Biol *13*, 5861-5876.
Gary, J.D., Sato, T.K., Stefan, C.J., Bonangelino, C.J., Weisman, L.S., and Emr, S.D. (2002). Regulation of Fab1 phosphatidylinositol 3-phosphate 5-kinase pathway by Vac7 protein and Fig4, a polyphosphoinositide phosphatase family member. Molecular biology of the cell *13*, 1238-1251.
Gary, J.D., Wurmser, A.E., Bonangelino, C.J., Weisman, L.S., and Emr, S.D. (1998). Fab1p is essential for PtdIns(3)P 5-kinase activity and the maintenance of vacuolar size and membrane homeostasis. The Journal of cell biology *143*, 65-79.
Gruber, G., Manimekalai, M.S., Mayer, F., and Muller, V. (2014). ATP synthases from archaea: the beauty of a molecular motor. Biochim Biophys Acta *1837*, 940-952.
Guo, S., Stolz, L.E., Lemrow, S.M., and York, J.D. (1999). SAC1-like domains of yeast SAC1, INP52, and INP53 and of human synaptojanin encode polyphosphoinositide phosphatases. J Biol Chem *274*, 12990-12995.
Han, G.S., Audhya, A., Markley, D.J., Emr, S.D., and Carman, G.M. (2002). The Saccharomyces cerevisiae LSB6 gene encodes phosphatidylinositol 4-kinase activity. J Biol Chem *277*, 47709-47718.
Hirano, T., Matsuzawa, T., Takegawa, K., and Sato, M.H. (2011). Loss-of-Function and Gain-of-Function Mutations in FAB1A/B Impair Endomembrane Homeostasis, Conferring Pleiotropic Developmental Abnormalities in Arabidopsis. Plant Physiology *155*, 797-807.
Hirano, T., and Sato, M.H. (2011). Arabidopsis FAB1A/B is possibly involved in the recycling of auxin transporters. Plant Signal Behav *6*, 583-585.
Ikonomov, O.C., Sbrissa, D., Fenner, H., and Shisheva, A. (2009a). PIKfyve-ArPIKfyve-Sac3 core complex: contact sites and their consequence for Sac3 phosphatase activity and endocytic membrane homeostasis. The Journal of biological chemistry *284*, 35794-35806.
Ikonomov, O.C., Sbrissa, D., Ijuin, T., Takenawa, T., and Shisheva, A. (2009b). Sac3 is an insulin-regulated phosphatidylinositol 3,5-bisphosphate phosphatase: gain in insulin responsiveness through Sac3 down-regulation in adipocytes. The Journal of biological chemistry *284*, 23961-23971.
Jin, N., Chow, C.Y., Liu, L., Zolov, S.N., Bronson, R., Davisson, M., Petersen, J.L., Zhang, Y., Park, S., Duex, J.E., Goldowitz, D., Meisler, M.H., and Weisman, L.S. (2008). VAC14 nucleates a protein complex essential for the acute interconversion of PI3P and PI(3,5)P(2) in yeast and mouse. The EMBO journal *27*, 3221-3234.
Jin, N., Mao, K., Jin, Y., Tevzadze, G., Kauffman, E.J., Park, S., Bridges, D., Loewith, R., Saltiel, A.R., Klionsky, D.J., and Weisman, L.S. (2014). Roles for PI(3,5)P2 in nutrient sensing through TORC1. (in revision).
Kakinuma, Y., Ohsumi, Y., and Anraku, Y. (1981). Properties of H+-translocating adenosine triphosphatase in vacuolar membranes of SAccharomyces cerevisiae. J Biol Chem *256*, 10859-10863.
Kane, P.M., and Smardon, A.M. (2003). Assembly and regulation of the yeast vacuolar H+-ATPase. J Bioenerg Biomembr *35*, 313-321.
Kim, E., and Guan, K.L. (2009). RAG GTPases in nutrient-mediated TOR signaling pathway. Cell Cycle *8*, 1014-1018.
Klionsky, D.J., Herman, P.K., and Emr, S.D. (1990). The fungal vacuole: composition, function, and biogenesis. Microbiol Rev *54*, 266-292.
Kogan, K., Spear, E.D., Kaiser, C.A., and Fass, D. (2010). Structural conservation of components in the amino acid sensing branch of the TOR pathway in yeast and mammals. J Mol Biol *402*, 388-398.
Krick, R., Busse, R.A., Scacioc, A., Stephan, M., Janshoff, A., Thumm, M., and Kuhnel, K. (2012). Structural and functional characterization of the two phosphoinositide binding sites of PROPPINs, a beta-propeller

protein family. Proceedings of the National Academy of Sciences of the United States of America *109*, E2042-2049.
Lenk, G.M., Ferguson, C.J., Chow, C.Y., Jin, N., Jones, J.M., Grant, A.E., Zolov, S.N., Winters, J.J., Giger, R.J., Dowling, J.J., Weisman, L.S., and Meisler, M.H. (2011). Pathogenic mechanism of the FIG4 mutation responsible for Charcot-Marie-Tooth disease CMT4J. PLoS genetics *7*, e1002104.
Li, H., and Marshall, A.J. (2015). Phosphatidylinositol (3,4) bisphosphate-specific phosphatases and effector proteins: A distinct branch of PI3K signaling. Cell Signal *27*, 1789-1798.
Li, S.C., Diakov, T.T., Xu, T., Tarsio, M., Zhu, W., Couoh-Cardel, S., Weisman, L.S., and Kane, P.M. (2014). The signaling lipid PI(3,5)P(2) stabilizes V(1)-V(o) sector interactions and activates the V-ATPase. Mol Biol Cell *25*, 1251-1262.
Loewith, R., and Hall, M.N. (2011). Target of rapamycin (TOR) in nutrient signaling and growth control. Genetics *189*, 1177-1201.
Loewith, R., Jacinto, E., Wullschleger, S., Lorberg, A., Crespo, J.L., Bonenfant, D., Oppliger, W., Jenoe, P., and Hall, M.N. (2002). Two TOR complexes, only one of which is rapamycin sensitive, have distinct roles in cell growth control. Mol Cell *10*, 457-468.
Martinez-Munoz, G.A., and Kane, P. (2008). Vacuolar and plasma membrane proton pumps collaborate to achieve cytosolic pH homeostasis in yeast. J Biol Chem *283*, 20309-20319.
McCartney, A.J., Zhang, Y., and Weisman, L.S. (2014). Phosphatidylinositol 3,5-bis phosphate: Low abundance. High significance. . Bioessays *36*, 52-64.
Mitra, P., Zhang, Y., Rameh, L.E., Ivshina, M.P., McCollum, D., Nunnari, J.J., Hendricks, G.M., Kerr, M.L., Field, S.J., Cantley, L.C., and Ross, A.H. (2004). A novel phosphatidylinositol(3,4,5)P3 pathway in fission yeast. J Cell Biol *166*, 205-211.
Nicholson, G., Lenk, G.M., Reddel, S.W., Grant, A.E., Towne, C.F., Ferguson, C.J., Simpson, E., Scheuerle, A., Yasick, M., Hoffman, S., Blouin, R., Brandt, C., Coppola, G., Biesecker, L.G., Batish, S.D., and Meisler, M.H. (2011). Distinctive genetic and clinical features of CMT4J: a severe neuropathy caused by mutations in the PI(3,5)P(2) phosphatase FIG4. Brain *134*, 1959-1971.
Nicot, A.S., Fares, H., Payrastre, B., Chisholm, A.D., Labouesse, M., and Laporte, J. (2006). The phosphoinositide kinase PIKfyve/Fab1p regulates terminal lysosome maturation in Caenorhabditis elegans. Mol Biol Cell *17*, 3062-3074.
Oppelt, A., Lobert, V.H., Haglund, K., Mackey, A.M., Rameh, L.E., Liestol, K., Schink, K.O., Pedersen, N.M., Wenzel, E.M., Haugsten, E.M., Brech, A., Rusten, T.E., Stenmark, H., and Wesche, J. (2013). Production of phosphatidylinositol 5-phosphate via PIKfyve and MTMR3 regulates cell migration. EMBO Rep *14*, 57-64.
Padilla-Lopez, S., and Pearce, D.A. (2006). Saccharomyces cerevisiae lacking Btn1p modulate vacuolar ATPase activity to regulate pH imbalance in the vacuole. J Biol Chem *281*, 10273-10280.
Palmer, C.P., Zhou, X.L., Lin, J., Loukin, S.H., Kung, C., and Saimi, Y. (2001). A TRP homolog in Saccharomyces cerevisiae forms an intracellular Ca(2+)-permeable channel in the yeast vacuolar membrane. Proc Natl Acad Sci U S A *98*, 7801-7805.
Plant, P.J., Manolson, M.F., Grinstein, S., and Demaurex, N. (1999). Alternative mechanisms of vacuolar acidification in H(+)-ATPase-deficient yeast. J Biol Chem *274*, 37270-37279.
Powis, K., and De Virgilio, C. (2016). Conserved regulators of Rag GTPases orchestrate amino acid-dependent TORC1 signaling. Cell Discov *2*, 15049.
Preston, R.A., Murphy, R.F., and Jones, E.W. (1989). Assay of vacuolar pH in yeast and identification of acidification-defective mutants. Proc Natl Acad Sci U S A *86*, 7027-7031.
Ramos, J., Kschischo, M., and Sychrova, H. (2016). Yeast Membrane Transport. Preface. Adv Exp Med Biol *892*, v.
Rudge, S.A., Anderson, D.M., and Emr, S.D. (2004). Vacuole size control: Regulation of PtdIns(3,5)P-2 levels by the vacuole-associated Vac14-Fig4 complex, a PtdIns(3.5)P-2-specific phosphatase. Molecular Biology of the Cell *15*, 24-36.

Saito, H., and Posas, F. (2012). Response to hyperosmotic stress. Genetics *192*, 289-318.
Sancak, Y., Bar-Peled, L., Zoncu, R., Markhard, A.L., Nada, S., and Sabatini, D.M. (2010). Ragulator-Rag complex targets mTORC1 to the lysosomal surface and is necessary for its activation by amino acids. Cell *141*, 290-303.
Sbrissa, D., Ikonomov, O.C., Fu, Z.Y., Ijuin, T., Gruenberg, J., Takenawa, T., and Shisheva, A. (2007). Core protein machinery for mammalian phosphatidylinositol 3,5-bisphosphate synthesis and turnover that regulates the progression of endosomal transport - Novel sac phosphatase joins the arpikfyve-pikfyve complex. Journal of Biological Chemistry *282*, 23878-23891.
Sbrissa, D., Ikonomov, O.C., and Shisheva, A. (1999). PIKfyve, a mammalian ortholog of yeast Fab1p lipid kinase, synthesizes 5-phosphoinositides - Effect of insulin. Journal of Biological Chemistry *274*, 21589-21597.
Sbrissa, D., Strakova, J., Ikonomov, O.C., Dondapati, R., Mlak, K., Deeb, R., Silver, R., and Shisheva, A. (2004). ArPIKfyve: A mammalian ortholog of yeast Vac14 that associates with and up-regulates PIKfyve phosphoinositide 5-kinase activity. Molecular Biology of the Cell *15*, 437a-437a.
Schu, P.V., Takegawa, K., Fry, M.J., Stack, J.H., Waterfield, M.D., and Emr, S.D. (1993). Phosphatidylinositol 3-kinase encoded by yeast VPS34 gene essential for protein sorting. Science *260*, 88-91.
Shelton, S.N., Barylko, B., Binns, D.D., Horazdovsky, B.F., Albanesi, J.P., and Goodman, J.M. (2003). Saccharomyces cerevisiae contains a Type II phosphoinositide 4-kinase. Biochem J *371*, 533-540.
Strahl, T., and Thorner, J. (2007). Synthesis and function of membrane phosphoinositides in budding yeast, Saccharomyces cerevisiae. Biochim Biophys Acta *1771*, 353-404.
Sturgill, T.W., Cohen, A., Diefenbacher, M., Trautwein, M., Martin, D.E., and Hall, M.N. (2008). TOR1 and TOR2 have distinct locations in live cells. Eukaryot Cell *7*, 1819-1830.
Tarsio, M., Zheng, H., Smardon, A.M., Martinez-Munoz, G.A., and Kane, P.M. (2011). Consequences of loss of Vph1 protein-containing vacuolar ATPases (V-ATPases) for overall cellular pH homeostasis. J Biol Chem *286*, 28089-28096.
Trotter, P.J., Wu, W.I., Pedretti, J., Yates, R., and Voelker, D.R. (1998). A genetic screen for aminophospholipid transport mutants identifies the phosphatidylinositol 4-kinase, STT4p, as an essential component in phosphatidylserine metabolism. J Biol Chem *273*, 13189-13196.
Viaud, J., Boal, F., Tronchere, H., Gaits-Iacovoni, F., and Payrastre, B. (2014). Phosphatidylinositol 5-phosphate: a nuclear stress lipid and a tuner of membranes and cytoskeleton dynamics. Bioessays *36*, 260-272.
Wang, Y.X., Zhao, H., Harding, T.M., Gomes de Mesquita, D.S., Woldringh, C.L., Klionsky, D.J., Munn, A.L., and Weisman, L.S. (1996). Multiple classes of yeast mutants are defective in vacuole partitioning yet target vacuole proteins correctly. Mol Biol Cell *7*, 1375-1389.
Watanabe, Y., Kobayashi, T., Yamamoto, H., Hoshida, H., Akada, R., Inagaki, F., Ohsumi, Y., and Noda, N.N. (2012). Structure-based analyses reveal distinct binding sites for Atg2 and phosphoinositides in Atg18. J Biol Chem *287*, 31681-31690.
Wera, S., Bergsma, J.C., and Thevelein, J.M. (2001). Phosphoinositides in yeast: genetically tractable signalling. FEMS Yeast Res *1*, 9-13.
Wheeler, G.E., Michell, R.H., and Rose, A.H. (1972). Phosphatidylinositol kinase activity in Saccharomyces cerevisiae. Biochem J *127*, 64P.
Whisstock, J.C., Wiradjaja, F., Waters, J.E., and Gurung, R. (2002). The structure and function of catalytic domains within inositol polyphosphate 5-phosphatases. IUBMB Life *53*, 15-23.
Whiteford, C.C., Brearley, C.A., and Ulug, E.T. (1997). Phosphatidylinositol 3,5-bisphosphate defines a novel PI 3-kinase pathway in resting mouse fibroblasts. Biochem J *323 (Pt 3)*, 597-601.

Yamamoto, A., Dewald, D.B., Boronenkov, I.V., Anderson, R.A., Emr, S.D., and Koshland, D. (1995). Novel Pi(4)P 5-Kinase Homolog, Fab1p, Essential for Normal Vacuole Function and Morphology in Yeast. Molecular Biology of the Cell *6*, 525-539.
Zhang, Y., McCartney, A.J., Zolov, S.N., Ferguson, C.J., Meisler, M.H., Sutton, M.A., and Weisman, L.S. (2012). Modulation of synaptic function by VAC14, a protein that regulates the phosphoinositides PI(3,5)P(2) and PI(5)P. EMBO J *31*, 3442-3456.
Zhang, Y., Zolov, S.N., Chow, C.Y., Slutsky, S.G., Richardson, S.C., Piper, R.C., Yang, B., Nau, J.J., Westrick, R.J., Morrison, S.J., Meisler, M.H., and Weisman, L.S. (2007). Loss of Vac14, a regulator of the signaling lipid phosphatidylinositol 3,5-bisphosphate, results in neurodegeneration in mice. Proceedings of the National Academy of Sciences of the United States of America *104*, 17518-17523.
Zolov, S.N., Bridges, D., Zhang, Y., Lee, W.-W., Riehle, E., Verma, R., Lenk, G.M., Converso-Baran, K., Weide, T., Albin, R.L., Saltiel, A.R., Meisler, M.H., Russell, M.W., and Weisman, L.S. (2012a). In vivo, Pikfyve generates PI(3,5)P2, which serves as both a signaling lipid and the major precursor for PI5P. Proceedings of the National Academy of Sciences *109*, 17472-17477.
Zolov, S.N., Bridges, D., Zhang, Y., Lee, W.W., Riehle, E., Verma, R., Lenk, G.M., Converso-Baran, K., Weide, T., Albin, R.L., Saltiel, A.R., Meisler, M.H., Russell, M.W., and Weisman, L.S. (2012b). In vivo, Pikfyve generates PI(3,5)P2, which serves as both a signaling lipid and the major precursor for PI5P. Proc Natl Acad Sci U S A *109*, 17472-17477.
Zoncu, R., Bar-Peled, L., Efeyan, A., Wang, S., Sancak, Y., and Sabatini, D.M. (2011). mTORC1 senses lysosomal amino acids through an inside-out mechanism that requires the vacuolar H(+)-ATPase. Science *334*, 678-683.

CHAPTER 2:

BIOINFORMATIC ANALYSIS OF THE FAB1/PIKFYVE COMPLEX[2]

Introduction

The field of structure prediction is rapidly improving. Indeed, during this doctoral work, the secondary structure prediction program JPred underwent a large re-optimization from version three to version four (Drozdetskiy *et al.*, 2015). Therefore, it is highly likely that previous reports of the domain boundaries of Fab1 and its regulators may not be correct. Additionally, it is likely that the new analyses reported in this chapter will become outdated as future advances enhance the ability to predict functional units of secondary structure within polypeptide chains.

In lieu of relying on previous reviews and journal articles to report putative domains of the Fab1 complex, I took a *tabula rasa* approach. I used secondary structure prediction software (JPred4) in conjunction with multiple sequence alignment (ClustalOmega) to define regions that likely function as distinct domains (Thompson *et al.*, 1994; Edgar and Batzoglou, 2006; Drozdetskiy *et al.*, 2015). In order to predict areas of secondary structure, I first identified a list of homologs from yeast to humans. This list includes organisms representing fungi, plants, and animals. In fungi, I include common model

[2] Sections of this chapter are adapted from a published literature review: Jin N, Lang MJ, Weisman LS. 2016. Phosphatidylinositol 3,5-bisphosphate: regulation of cellular events in space and time. Biochem Soc Trans. Feb;44(1):177-84. DOI: 10.1042/BST20150174.

organisms (*Y. lipolytica*, *S. pombe*) as well as more divergent species (*C. albicans*, *C. thermophilium*). For plants I include the model organism *Arabidopsis thaliana* as well as rice (*O. sativa*) and maize (*Z. mays*). For animals, I use the invertebrates *D. melanogaster* and *C. elegans*, the non-mammalian vertebrates *X. tropicalis*, *D. rerio*, and *G. gallus* and the mammals *M. musculus* and *H. sapiens*. I performed a multiple sequence alignment using the ClustalOmega multiple sequence alignment program (Thompson *et al.*, 1994), and analyzed this alignment with Jpred4 to generate a prediction of secondary structure of either *S. cerevisiae* or *H. sapiens* based only on the selected homologs. The analysis was performed using this strategy because using JPred4 software without specifying specific homologs for comparison results in poor predictions based on comparison with unrelated proteins.

Last, I determined by eye where specific domains started and ended. In general I capped domains based on the results from secondary structure analysis, but added 1-3 amino acids to the end of the predicted domain based on advice from Dr. Clay Brown in the laboratory of Dr. Janet Smith. In situations where a proline was within 5 residues of a predicted domain boundary, I ended the domain one residue before the proline.

Proline residues often start or end alpha helicies (Ncap-1 or Ccap+1 respectively) (Kim and Kang, 1999); therefore, when possible I used them to end or begin a domain if they were proximal to the domain boundary. For instance, the CCR domain of Fab1 has no secondary structure predicted after residue 1498, and encounters a proline at residue 1501. Therefore, I chose the end of the domain to be 1500.

In addition to secondary structure prediction, I used Phyre 2.0 and the latest version of I-TASSER to generate three-dimensional models of predicted domains (Kelley *et al.*, 2015; Yang *et al.*, 2015). While the I-TASSER suite is considered the current best modeling program, I often used Phyre 2.0 to predict areas with known, inherent unstructured areas such as the activation loop of the Fab1 kinase domain. Phyre 2.0 will exclude the unstructured activation loop based on solved structures of other kinase domains while I-TASSER will attempt to predict secondary structure for the activation loop, which often causes a low overall score of prediction for the entire structure. For Vac7 I use RaptorX (Peng and Xu, 2011), which has previously been noted as the best structure prediction software for poorly conserved polypeptides (Adhikari *et al.*, 2012). The software used for each prediction will be indicated within the figure.

Domain architecture of Fab1/PIKfyve

Both Fab1 and PIKfyve are larger than other PI 5-kinases and are composed of 2278 and 2098 amino acids, respectively (Strahl and Thorner, 2007). Therefore, it is likely that regions outside of the kinase domain contribute to the modulation of kinase activity. The first two major reviews to predict domains with Fab1/PIKfyve identified five unique domains (Efe et al., 2005; Michell et al., 2006). From N- to C-terminus these reviews identify the FYVE domain, the DEP domain in mammalian PIKfyve, the CCT domain (TriC/CCT/Thermosome-like domain), the CCR domain (conserved cysteine rich domain), and the kinase domain.

The Fab1/PIKfyve FYVE domain

The phosphoinositide phosphatidylinositol 3-phosphate (PI3P) is typically 2.28±0.05% of total PI in log-phase WT yeast cells (unpublished data, N=4, error=SEM) (Bonangelino *et al.*, 2002; Duex *et al.*, 2006a), and is hypothesized to reside on yeast endosomes and vacuoles (Gillooly *et al.*, 2000). To date, two known domains have been found that bind to PI3P. First identified was the FYVE (Fab1, YOTB, Vac1, and EEA1) zinc finger domain (Stenmark *et al.*, 1996) Subsequently the Phox homology (PX) domain was identified as a second PI3P binding-domain (Cheever *et al.*, 2001; Ellson *et al.*, 2001; Kanai *et al.*, 2001; Xu *et al.*, 2001). The FYVE domain is the PI3P-binding domain found in Fab1/PIKfyve.

The FYVE domain is a divergent 60-residue polypeptide built around a pair of antiparallel beta-strands and two loops that coordinate the four zinc ions through CxxC motifs (Hayakawa *et al.*, 2004). Specifically, the FYVE domain contains a WxxD motif and a R(R/K)HHCR motif. The WxxD motif and the R(R/K)HHCR motif coordinate the inositol 4-OH and 5/6-OH of PI3P, respectively. Additionally, the first arginine of the R(R/K)HHCR motif interacts with the 1-phosphate of PI3P (Stenmark *et al.*, 2002).

My analysis predicts the FYVE domain of Fab1 to be from residue 230-320. The FYVE domain from PIKfyve is predicted to span from 143-234. While the majority of FYVE domains are sixty residues in length (Hayakawa *et al.*, 2004), the Fab1-FYVE domain and the PIKfyve FYVE domain span lengths of 90 amino acids and 91 amino acids, respectively. My analysis is in agreement with a previous report that generated a Fab1-FYVE domain construct from residue 207 to residue 317 (Botelho *et al.*, 2008).

Expressed in yeast, this Fab1-FYVE domain localizes to the vacuole both in WT cells and *vac7Δ* or *fab1Δ* cells, which are deficient in generating $PI(3,5)P_2$. That the Fab1-FYVE domain localizes to the vacuole in the absence of $PI(3,5)P_2$ indicates that the FYVE domain likely does not bind $PI(3,5)P_2$. It is currently assumed that the Fab1 and the PIKfyve FYVE domains bind PI3P; however, this has not been experimentally determined.

The PIKfyve DEP domain has no known function

PIKfyve, but not Fab1, contains a DEP domain. Within Fab1 the region best-aligned to the PIKfyve DEP domain has no predicted secondary structure and is 15% conserved between the two proteins. Therefore, my analysis indicates that there is no DEP domain in Fab1. The DEP domain is a protein module of about 100 amino acids, which was first identified in signaling proteins such as disheveled, Egl-10, and pleckstrin (Ponting and Bork, 1996). Currently, six subfamilies of the DEP domain have been identified, one of which consists solely of the PIKfyve DEP domain (Civera *et al.*, 2005). My analysis indicates that the PIKfyve DEP domain spans from residue 368 to residue 438, which is in agreement with residues 367-438 reported previously (Civera *et al.*, 2005).

Currently, no known functional role is attributed to the PIKfyve DEP domain; however, based on detailed analysis of the DEP domain in Pleckstrin I hypothesize that the PIKfyve-DEP domain regulates the PIKfyve-FYVE domain. Pleckstrin is a small protein consisting, from N- to C-terminus, of a PH domain, a DEP domain, and a second PH domain (Tyers *et al.*, 1988; Hu *et al.*, 1999). The PH domain of Pleckstrin binds

$PI(4,5)P_2$ (Harlan *et al.*, 1994). The Pleckstrin DEP domain does not bind $PI(4,5)P_2$ (Civera *et al.*, 2005). $PI(4,5)P_2$-binding experiments comparing the PH domain alone versus a Pleckstrin construct containing both the PH and the DEP domains indicate that the phosphoinositide binding site of the PH domain is blocked via the DEP domain (Civera *et al.*, 2005). Moreover, phosphorylation of the linker connecting the PH and the DEP domain by PKC is required for Pleckstrin function and membrane localization (Abrams *et al.*, 1995). An analogous regulatory mechanism of the FYVE domain by PIKfyve-DEP may be present within PIKfyve. The PIKfyve DEP domain is the closest domain to the FYVE domain—124 residues away. Studies to determine the function of the PIKfyve DEP domain should include an analysis of a potential protein-protein interaction with the FYVE domain, as well as a potential role in regulating the access of the Fab1-FYVE domain to PI3P.

The CCT domain binds the Vac14 scaffolding protein

Based on the conservation between Fab1 residues 700-1000 and a regulatory region of the CCT/TCP-1/Cpn60 chaperonins, the CCT domain was proposed to associate with regulatory proteins (Efe *et al.*, 2005; Michell *et al.*, 2006; Botelho *et al.*, 2008). Indeed, the CCT domain is essential for the interaction of Fab1 with the scaffold protein Vac14 (Jin *et al.*, 2008b). Mutation within a conserved region of the CCT domain (T1017I) produces an enlarged vacuolar phenotype, an inability of cells to grow at 38ºC, mislocalization of Vac14 from a vacuolar localization to cytosolic localization, and roughly half normal levels of $PI(3,5)P_2$ (Botelho *et al.*, 2008). Therefore, it is clear that the CCT domain plays an important role in the regulation of $PI(3,5)P_2$ levels.

My analysis indicates that yeast Fab1-CCT spans residues 796-1096, which contrasts with a previous analysis that found Fab1-CCT spanning 770-1054 (McCartney *et al.*, 2014) (Figure 2.1). The PIKfyve CCT domain is 766-1039, and was previously reported to be 588-874 (McCartney *et al.*, 2014). These new boundaries are slightly different from previously published estimations of the boundaries of the CCT domain (McCartney *et al.*, 2014). In McCartney 2014, these domains were determined solely based on multiple sequence alignment (McCartney *et al.*, 2014). Here, the use of both sequence alignments and secondary structure prediction likely provides a more definitive demarcation of the domain's boundaries.

The CCR domain likely coordinates a metal ion

The CCR (conserved cysteine rich) domain is conserved in all known Fab1 proteins (Cooke, 2002; Efe *et al.*, 2005; Michell *et al.*, 2006; Botelho *et al.*, 2008). The CCR domain was initially identified via alignment of multiple PIKfyve sequences using the gap-tolerant alignment tool Dialign (Morgenstern *et al.*, 1998; Michell *et al.*, 2006). The most prominent feature of this domain is the conservation of several cysteine and histidine residues (Cooke, 2002). BLAST searches of genome databases retrieve only other Fab1 homologs; no other protein has detectable sequence similarity to the CCR domain (Michell *et al.*, 2006). Little is known about the CCR domain, except that it is required for Fab1 activity (Botelho *et al.*, 2008). Mutation of a conserved cysteine within this domain does not perturb Fab1 localization; yet leads to loss of Fab1 function as exhibited by temperature sensitivity, a defect in vacuolar morphology, and greatly

reduced PI(3,5)P_2 levels (Botelho *et al.*, 2008). These findings indicate that the CCR domain is critical for the regulation of PI(3,5)P_2 levels.

Bioinformatic analysis of the CCR domain demonstrates that the domain is a continuous region of secondary structure of roughly 400 residues both in Fab1 and PIKfyve (Figure 2.1). The yeast Fab1 CCR domain is residue 1181-1500. The PIKfyve CCR domain is 1157-1524.

The conserved cysteines and histidines of the CCR domain may coordinate a metal ion. Cysteines and histidines are biologically important for the coordination of metal ions within proteins (Pace and Weerapana, 2014). The conservation of multiple cysteines and histidines within the CCR domain leads to the hypothesis that this domain is a novel metal binding domain. To date no data has been published that Fab1 coordinates metal ions; however, the presence of a zinc-coordinating FYVE domain indicates that Fab1/PIKfyve likely coordinates zinc. Current bioinformatic programs such as DiANNA, MetSite, and FINDSITE-metal (Sodhi *et al.*, 2004; Ferre and Clote, 2006; Levy *et al.*, 2009) are limited to predicting metal-binding sites on solved or predicted protein structures. Thus I used MetalDetector 2.0, which predicts both metal coordination and disulfide bond formation based on the primary sequence of a polypeptide chain (Passerini *et al.*, 2011). MetalDetector 2.0 predicts a potential metal binding site in the Fab1-CCR domain and no disulfide bonds within this region. The metal is predicted to be coordinated by Fab1-C1289, Fab1-C1292, Fab1-C1324, and Fab1-H1326. Similarly, although the PIKfyve-CCR domain is only 29% identical with yeast Fab1-CCR,

MetalDetector 2.0 predicts that PIKfyve residues PIKfyve-C1316, PIKfyve-C1319, PIKfyve-C1359 and PIKfyve-H1361 coordinate a metal ion. Importantly, these latter residues align with the putative metal coordinating residues within yeast Fab1-CCR suggesting that these domains share a common metal binding site. As a positive control, I assayed the FYVE domain of Fab1 using MetalDetector 2.0. In agreement with solved FYVE domain structures where four CxxC motifs bind four Zinc ions (Hayakawa *et al.*, 2004), MetalDector 2.0 finds four metal coordinating sites in the Fab1-FYVE domain consisting of the CxxC Zinc coordinating loops. The secondary structure data in conjunction with the MetalDetector 2.0 data provides a better definition of the boundaries of the CCR domain and additionally predicts a conserved metal binding motif within the domain.

The kinase domain of Fab1/PIKfyve generates PI(3,5)P_2 from PI3P

The kinase domain of Fab1 phosphorylates PI3P in order to produce PI(3,5)P_2 (Gary *et al.*, 1998). Kinase function can largely be abolished through mutation of the GGxxG glycine triad motif containing Gly2042 and Gly2045 of Fab1, which is reminiscent of the highly conserved GxGxxG motif present in the nucleotide binding site of numerous protein kinases (Gary *et al.*, 1998). In agreement with previous alignments (Rao *et al.*, 1998; McCartney *et al.*, 2014), the kinase domain spans amino acids 1990-2268 and 1759-2084 in yeast Fab1 and PIKfyve, respectively. Overexpression of the yeast kinase domain (residues 1723-2278) in WT yeast does not alter vacuolar morphology (Figure 2.3D). Moreover, overexpression of the kinase domain in WT yeast has no effect on PI(3,5)P_2 levels under basal conditions or in response to a hyperosmotic shock (Figure

2.3C). However, immunoprecipitation followed by western blot analysis demonstrates that this kinase domain construct is stable and expressed in WT cells (Figure 2.3B). It is possible that the kinase domain construct has enzymatic activity but cannot access the substrate. Alternatively, additional levels of regulation may be required to properly activate the kinase domain.

The PrD, L1, L2, and L3 domains are four new domains within Fab1/PIKfyve

In addition to previously predicted domains, I predict four new domains within Fab1/PIKfyve. Three of the new areas have predicted secondary structure. The fourth domain is predicted to be unstructured.

Three conserved regions of predicted secondary structure that I coin the L1, L2, and L3 domains, are either conserved in all metazoans, all fungi, or in all eukaryotes, respectively (Figure 2.1). The L1 domain is situated between the CCT domain and CCR domain of PIKfyve and spans from residue 1037-1090. It has no known function. The L2 domain is conserved only in fungi and spans from residue 1649-1700. In Chapter 3 I will present *in vivo* data indicating that this domain has a role in the regulation of Fab1 activity. Last, the L3 domain is found in all Fab1/PIKfyve proteins. In yeast the L3 domain is predicted to start at residue 1821 and end at 1905. Importantly, data from Chapter 3 as well as previously published data indicate that this domain has a functional role in the regulation of $PI(3,5)P_2$ (Duex *et al.*, 2006c). Specifically: conserved dominant-active mutations can be made in this domain that elevate Fab1 activity. Moreover, both this domain and the dominant-active mutations are conserved in PIKfyve. The L3

domain of PIKfyve spans from 1618 to 1693. Conserved dominant-active yeast residues are homologous to PIKfyve-E1620 and PIKfyve N1630. Mutation of these PIKfyve residues in conjunction with a third residue (PIKfyve-S2068) produce a dominant-active PIKfyve allele. This data indicates that the L3 domain has a conserved regulatory function in both Fab1 and PIKfyve. Together, three additional areas of predicted secondary structure which have structural and sequence conservation in all species (L3), in all fungi (L2) or in metazoans (L1) have been identified, and which likely contribute to the regulation of $PI(3,5)P_2$.

The fourth new Fab1 domain identified is unstructured and harbors a polyasparagine stretch. Polyasparagine and polyglutamine stretches (known as (Q/N)-rich domains) have a propensity to form self-propagating amyloid fibrils and are implicated in prion-based inheritance in yeast and aggregation of neurodegenerative proteins in human diseases (Ross *et al.*, 1998; Perutz, 1999; Michelitsch and Weissman, 2000; Uptain and Lindquist, 2002). Recently, software was developed that has successfully predicted prionogenic regions within yeast proteins (Alberti *et al.*, 2009). In this study the authors generate an algorithm, which in addition to identifying the known prionogenic yeast protein Sup35, identifies Mot3 as a prion-forming yeast ORF. Interestingly, using the computational prion-prediction program used in this publication, we find that out of every yeast ORF, Fab1 is ranked 53rd in terms of highest probability of harboring a prionogenic region. Specifically, using the Prion-Like Amino Acid Composition (PLAAC) program we find that the unstructured region from residue 456 to residue 607 is considered a prionogenic-like domain (PrD) (Figure 2.4). In this schematic, a red line

indicates the probability that a polypeptide sequence is prion-like, which is defined based on amino acid similarity to previously published prions and as having a length close to or greater than 60 residues. A black line indicates background amino acid frequencies for *S. cerevisiae*. Figure 2.4 suggests the existence of a prionogenic domain from residues 456-607 in yeast Fab1 but not in mammalian PIKfyve.

Domain architecture of Vac14

Vac14 is predicted to be entirely composed of HEAT repeats, each containing two anti-parallel helices connected by a short loop (Jin *et al.*, 2008a). To independently search for repeats, I used Jpred4 secondary structure prediction and ClustalOmega multiple sequence alignment to determine the boundaries of possible domains. For both yeast and human Vac14, the tailored use of the software HHpred was used in addition to the above analysis. HHPred is used to identify HEAT repeats in both proteins with solved structures as well as proteins of unknown domain composition (Kippert and Gerloff, 2009). For analysis with HHPred, I first identify a probable HEAT repeat on the prediction from Jpred4 of two anti-parallel alpha helices connected by a loop. This sequence is then run through HHPred, which will identify the probability of a HEAT repeat and the PDB file to which the sequence was aligned.

In agreement with previous analyses, I find that both yeast and human Vac14 are composed of tandem HEAT repeats (Figure 2.1). In Figure 2.1 the colored boxes indicate homology of HEAT repeats between yeast and human Vac14. Hashed boxes indicate degenerate sequences which may be HEAT repeats, but that are only weakly

predicted using available programs. In HEAT repeats Table 2.1 and Table 2.2 of yeast and human Vac14: # indicates which HEAT repeat number, “residue start” indicates where the domain starts, and “residue stop” indicates where the domain stops. PDB indicates which PDB file the HEAT repeat was scored against and “info” provides information of what the PDB code references. Unless otherwise stated, only candidate domains with a predicted likelihood of HEAT repeat less than 0.1 (0 is 100% HEAT repeat, 1 is not a HEAT repeat) were specified as a predicted HEAT repeat. For instance, yeast HEAT repeat #1 starts at residue 1, ends at residue 33, and, based off of the *S. cerevisiae* Stu2 crystal structure (PDB file 2QK2), HHPred predicts this to be a *bona fide* HEAT repeat (p=1e-5).

Yeast Vac14 HEAT repeat #20 provides further clarification of the analysis. This area of the protein is predicted to be composed of the characteristic alpha helix turn alpha helix fold of a HEAT repeat by Jpred4; however, HHPred does not strongly predict this sequence of yeast Vac14 to contain a HEAT repeat. While it is below the threshold for detection of a HEAT repeat using HHPred it is useful to note that the program does identify the *E. coli* protein Tram (A HEAT repeat containing protein) as having some sequence similarity to this region. Due to the loose evidence in favor of having a HEAT repeat, Vac14 #20 is displayed in Figure 2.1 with hash marks.

Domain architecture of Fig4

Fig4 has a Sac1 phosphatase domain (Figure 2.1) that is found in several lipid phosphatases including Inp51, 52 and 53 (Gary *et al.*, 2002). Although Fig4 functions as

a PtdIns(3,5)P_2 specific phosphoinositide phosphatase *in vitro* (Rudge *et al.*, 2004) and *in vivo* (Gary *et al.*, 2002; Duex *et al.*, 2006b), paradoxically, deletion of Fig4 causes a defect in the acute synthesis of PtdIns(3,5)P_2 during hyperosmotic shock (Duex *et al.*, 2006b). This suggests that Fig4 has dual roles for the synthesis and turnover of PtdIns(3,5)P_2. Bioinformatic analysis of the Fig4 phosphatase indicates a single Sac1 phosphatase domain of predicted secondary structure spanning 157-598 and 144-617 in yeast and human Fig4, respectively (Figure 2.1).

Domain architecture of Vac7

Vac7 is found only in some fungi. BLAST searches of genome databases indicates a total of fourteen identifiable homologs of Vac7 (Table 2.3). Using this list of Vac7 homologs, our lab identified domains and regions of conservation within yeast Vac7 that may play functional roles in the regulation of Vac7 and of PI(3,5)P_2 levels. For Vac7, boundaries of each domain were determined using multiple techniques that delineate domains of predicted structure as well as unstructured regions. Vac7 contains a 14-residue coiled-coil domain (80% certainty using COILS) from residues 497-510 (Figure 2.7A-C); two transmembrane domains spanning regions 921-941 and 966-986 (Figure 2.5A-C); two conserved regions of no predicted structure at regions 423-460 and 668-703 (Figure 2.6A-C); four prionogenic-like regions 361-398, 467-488, 529-549, and 833-886 (Figure 2.7A-B); and a C-terminal structured domain of unknown function from 1038-1161 (Figure 2.9A-B).

Domain architecture of Atg18

Atg18 is similar to mammalian WIPI1 and WIPI2; however, it is not known if these WIPI proteins regulate PIKfyve (Dove *et al.*, 2004). Atg18, WIPI1 and WIPI4 domain boundaries were determined from ClustalOmega multiple sequence alignment with Hsv2 (Homologous with SVP1/ATG18), a related protein where high-resolution structures are available (Baskaran *et al.*, 2012; Krick *et al.*, 2012; Watanabe *et al.*, 2012). Seven WD40 (WD or beta-transducin repeat) blades are depicted in green (Figure 2.2B). A hydrophobic lipid-associated region is highlighted in blue. The beige Atg18 loop is a predicted unstructured region between β-sheet 2 and 3 of blade 4. WIPI2 (not depicted) is structurally similar to WIPI1 and both contain an unstructured C-terminal tail with 31% similarity to each other. WIPI3 (not depicted) is structurally similar to WIPI4. Residue pockets predicted to bind PI(3)P and PI(3,5)P_2 are highlighted for ATG18, WIPI1 and WIPI4 (Figure 2.2B). The fact that these regions are conserved indicates that Atg18, WIPI1, WIPI4 as well as their paralogs likely interact with phospholipids in a similar manner.

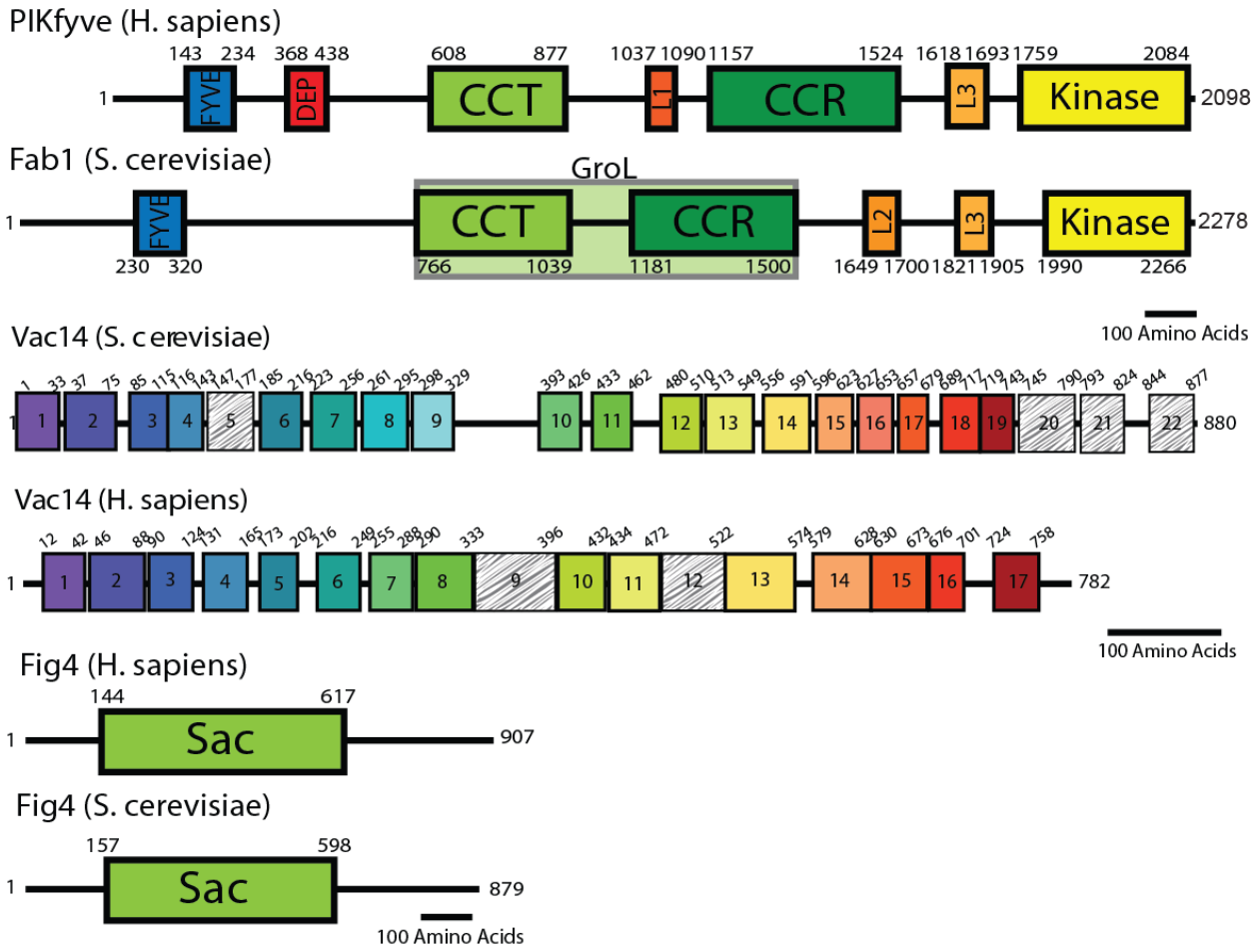

Figure 2.1. Domains of Fab1/PIKfyve, Vac14 and Fig4. Boundaries of each domain were determined using a combination of Jpred4 secondary structure prediction and ClustalOmega multiple sequence alignment. For Vac14, in addition to the above techniques, tailored HHpred alignments of select predicted HEAT repeats were performed. Fab1/PIKfyve contains previously described domains (FYVE, DEP, CCT, CCR and kinase); I identify three additional areas of predicted secondary structure which have structural and sequence conservation in all species (L3), in all fungi (L2) or in metazoans (L1). Vac14 is composed of tandem HEAT repeats. Colored boxes indicate homology of HEAT repeats between yeast and human Vac14. Hashed boxes indicate degenerate sequences which may be bona fide HEAT repeats. Fig4 contains a single Sac1 phosphatase domain. Black lines represent 100 amino acids.

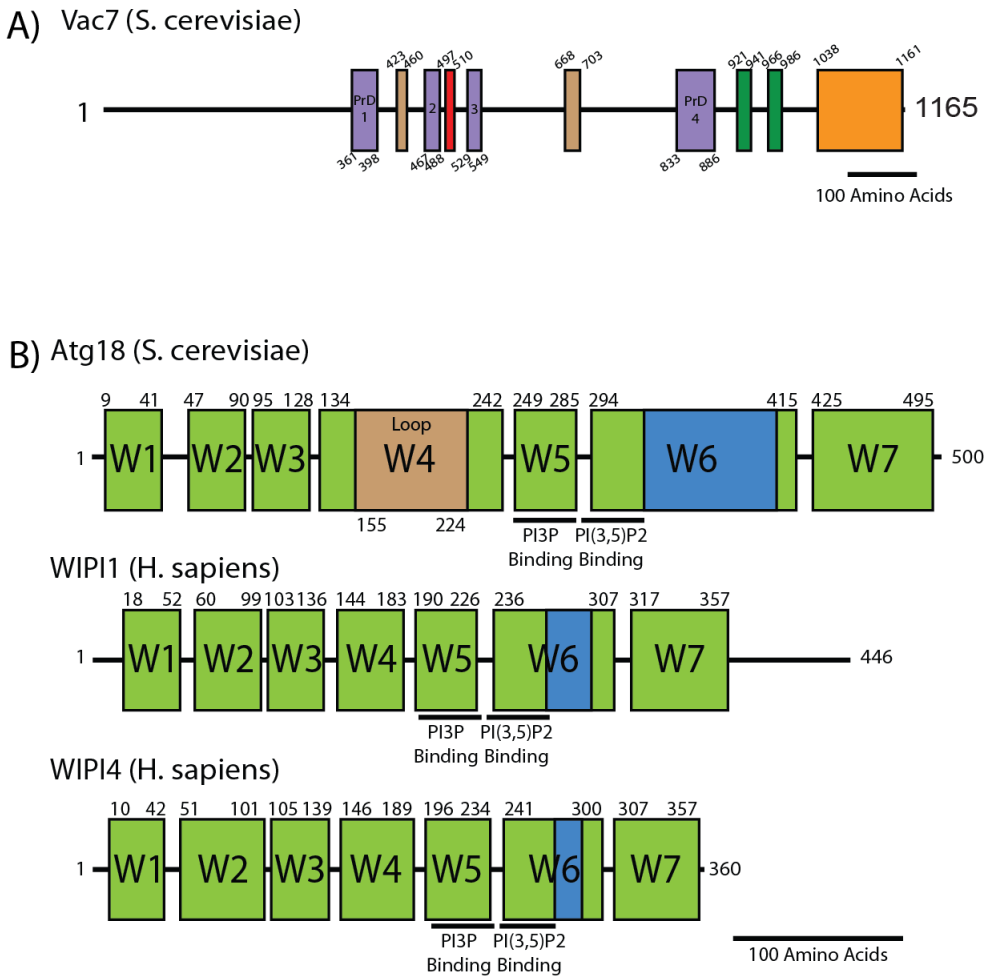

Figure 2.2. Domain architecture of Vac7 and Atg18. Vac7 is found only in some fungi. Atg18 is similar to mammalian WIPI1 and WIPI2; however, it is not known if these WIPI proteins regulate PIKfyve. For Vac7, boundaries of each domain were determined using a combination of Jpred4 secondary structure prediction and ClustalOmega multiple sequence alignment. Vac7 contains a coiled-coil domain (red domain, 80% certainty using COILS), two transmembrane domains (green domains), four prion-like domains (purple PrD domains), two regions of conservation but no predicted secondary structure (tan domains), and a C-terminal structured region (orange). Atg18, WIPI1 and WIPI4 domain boundaries were determined from ClustalOmega multiple sequence alignment with Hsv2 (Homologous with SVP1/ATG18), a related protein where high-resolution structures are available. Seven WD40 (WD or beta-transducin repeat) blades are depicted in green. A hydrophobic lipid-associated region is highlighted in blue. The beige Atg18 loop is a predicted unstructured region between β-sheet 2 and 3 of blade 4. WIPI2 (not depicted) is structurally similar to WIPI1 and both contain an unstructured C-terminal tail with 31% similarity to each other. WIPI3 (not depicted) is structurally similar to WIPI4. Regions predicted to bind PI(3)P and PI(3,5)P_2 are highlighted for ATG18, WIPI1 and WIPI4. The fact that these regions are conserved indicates that Atg18, WIPI1, WIPI4 as well as their paralogues likely interact with phospholipids in a similar manner. Black lines represent 100 amino acids.

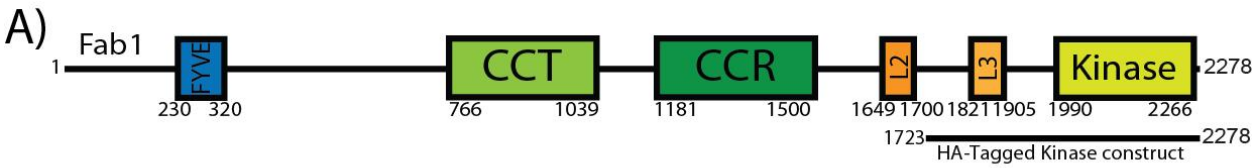
A)
Fab1
1
FYVE
230 320
CCT
766 1039
CCR
1181 1500
L2
1649 1700
L3
1821 1905
Kinase
1990 2266
2278
1723
2278
HA-Tagged Kinase construct

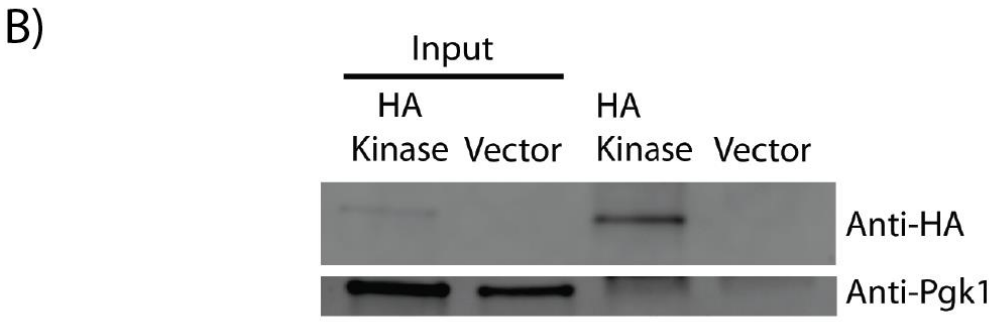
B)
Input
HA Kinase
Vector
HA Kinase
Vector
Anti-HA
Anti-Pgk1

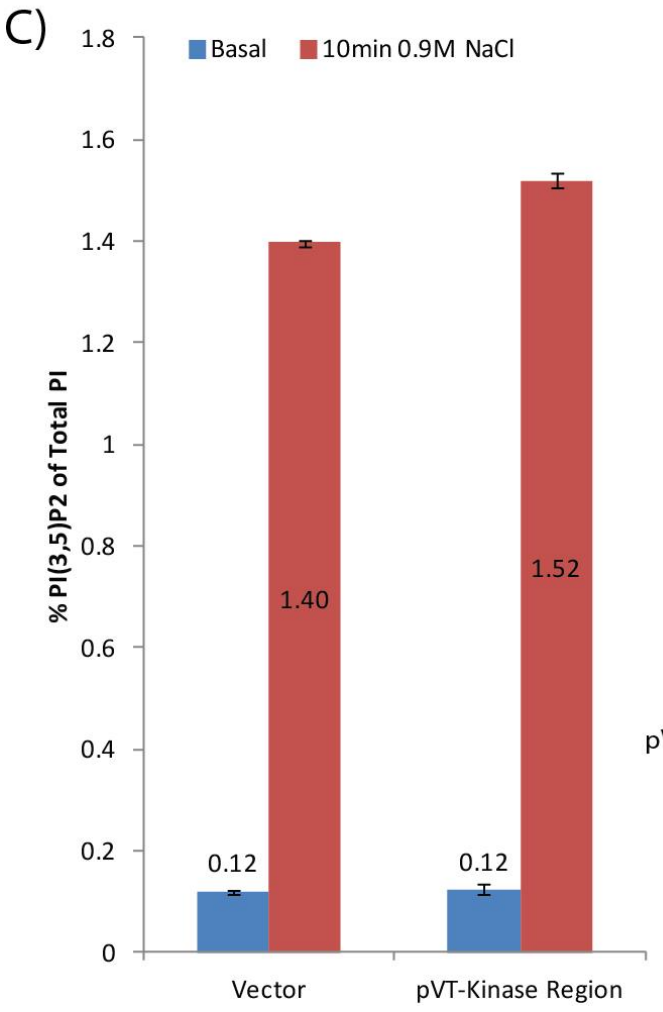
C)
Basal
10min 0.9M NaCl
% PI(3,5)P2 of Total PI
1.8
1.6
1.4
1.2
1
0.8
0.6
0.4
0.2
0
0.12
1.40
0.12
1.52
Vector
pVT-Kinase Region

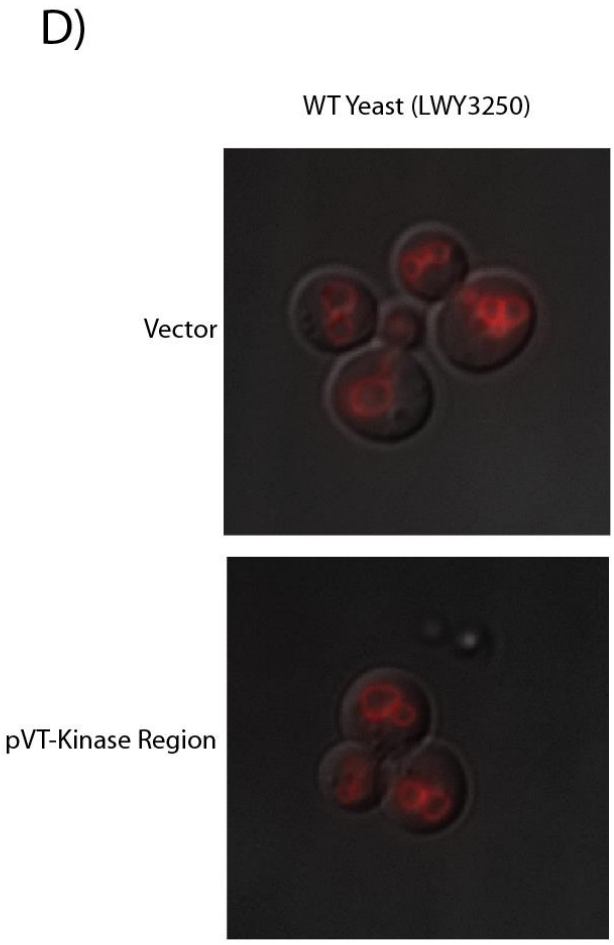
D)
WT Yeast (LWY3250)
Vector
pVT-Kinase Region

Figure 2.3. Overexpression of the yeast kinase domain has no detectable phenotype. A) An HA-tagged kinase domain construct (residues 1723-2278) under the control of the high-expression yeast ADH1 promoter was generated to test the effect of overexpression of the Fab1 kinase domain in yeast *in vivo*. **B)** Immunoprecipitation of either pADH1-HA-Kinase domain or vector demonstrates that the kinase domain construct is expressed in vivo. Pgk1 as load control. **C)** $PI(3,5)P_2$ levels were measured in WT yeast expressing either empty vector (Vector) or overexpressed kinase domain (pVT-Kinase Region) at both basal levels and at the peak (10 min) of hyperosmotic-shock induced $PI(3,5)P_2$ production. No drastic difference is observed between vector and Kinase domain construct. **D)** vacuolar morphology is unchanged in yeast cells expressing overexpression vector alone (Vector) or overexpressed Kinase Region (pVT-Kinase Region).

A)

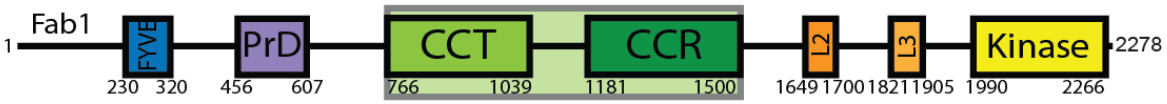

B)

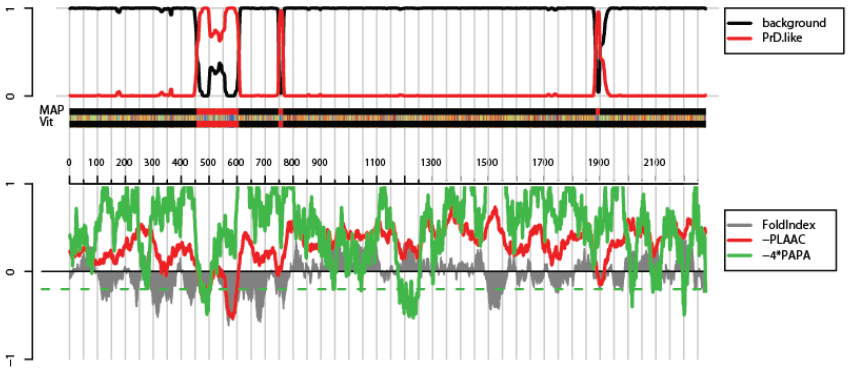


```
1    MSSEEPHASISFPDGSHVRSSSTGTSSVNTIDATLSRPNYIKKPSLHIMSTSTTSTTTDLVTNPILSNISVPKISPPTSSSIATATSTSHVTGTASHSNI
101  KANANTSTSVNKKNLPPTTSGRIPSSTIKRYPSRYKPSHSLQLPIKNDSNFKRSSIYASKSTVTAIPIRNNRPISMQNSYARTPDSDHDDVGDEVSSIKS
201  ASSSLTASLSKSFLFAFYNNRKKDKTSNNGVLSKEYWMKDESSKECFSCGKTFNTFRRKHHCRICGQIFCSSCTLLIDGDRFGCHAKMRVCYNCYEHADT
301  YEDSSDEENDSTMQLNEPRSRSRSRSSNTNPYSHSHSHLHLISQDNHNGTDLHDPVAATDNPQQQNEVYLLNDDDVQSIMTSGEDSKLFISTPPPPPKMA
401  IPATKQGGSLEISFDSENDRALHYQDDNPGRHHHLDSVPTRYTIRDMDNISHYDTNSNSTLRPHYNTNNSTITINNLNNTTSNNSNYNNTNSNSNINNPA
501  HSLRRSIFHYVSSNSVNKDSNNSSATPASSAQSSSILDPANRIIGNYAHRNYKFKFNYNSKGPSQQNDTANGNNDNNNNNNNNNNNNSASGIADNNN
601  IPSNDNGTTFTLDKKKRNPLTKSKSTSAYLEYPLNEEDSSEDEGSMSIYSVLNDDHKTDNPIRSMRNSTKSFQRAQASLQRMRFRRKSKSKHFPNNSKSS
701  IYRDLNFLTNSTPNLLSVVSDDNLYDDSSPLQDKASSSAASRLTDRKFSNSSGSNNNSNSNSNINTDPWKRIASISGFKLKKEKKRELNEVSLLHMHALL
801  KQLLNDQEISNLQEWITLLDGALRKVLRTILNARDLNTLDFRQTYVKIKRISGGSPQNSEYIDGVVFSKALPSKTMPRHLKNPRILLIMFPLEYQKNNNH
901  FLSIESVFRQEREYLDKLVSRLKSLHPDIIYVGANVSGYALELLNDSGIVVQFNMKPQVIERIAKLTEADIAISVDKLATNIKMGECETFEVKSYIYGNI
1001 SKTYTFLRGCNPELGGTILLRGDSLENLRKIKQVSEFMVYAIFSLKLESSFFNDNFIQLSTDVYLKRAESKKLQVFEGYFADFLIKFNNRITVSPTVDF
1101 PIPFLLEKARGLEKKLIERINQYESESDLDRQTQLNMLQGLESTITKKHLGNLIKFLHEMEIENLELEFQKRSRQMEVSYSSSQNLLGTGSHQSITVLYS
1201 MVSTKTATPCVGPQIVTIDYFWDSDISIGQFIENVVGTARYPCQQGCNGLYLDHYRSYVHGSGKVDVLIEKFQTRLPKLKDIITWSYCKKCGTSTPILQ
1301 ISEKTWNHSFGKYLEVMFWSYKDSVTGIGKCPHDFTKDHVKYFGYNDLVVRLEYSDLEVHELITPPRKIKWKPHIDIKLKVELYYKILEKINNFYGSVLS
1401 RLERIKLDSMFKDKVLSGQAKIIELKSNATEEQKLMLQDLDTFYADSPCDQHLPLNLVIKSLYDKAVNWISTFAIFAKSYLPSETDISRITAKQLKKLFY
1501 DSSRKDSEDKKSLHDEKAKTRKPEKNELPLEGLKDVEKPKIDSKNTTENRDRTNEPQNAVTITTFKDDTPIITPTSGTSHLTVTPSASSVSSSLTPQTEER
1601 PPISRSGTGISMFHDKSTRPNIRKMSSDSSLCGLASLANEYSKNNKVSKLATFFDQMHFDALSKEFELERERERLQLNKDKYQAIRLQTSTPIVEIYKNV
1701 KDAVDEPLHSRSSGNNLSSANVKTLEAPVGEHSRANNCNPPNLDQNLETELENSISQWGENILNPSGKTTASTHLNSKPVVKETSENPKSIVRESDNSKS
1801 EPLPPVITTTTVNKVESTPQPEKSLLMKTLSNFWADRSAYLWKPLVYPTCPSEHIFTDSDVIIREDEPSSLIAFCLSTSDYRNKMMNLNVQQQQQQQTAE
1901 AAPAKTGGNSGGTTQTGDPSVNISPSVSTTSHNKGRDSEISSLVTTKEGLLNTPPIEGARDRTPQESQTHSQANLDTLQELEKIMFKKTATHLRYQFEEG
2001 LTVMSCKIFFTEHFDVFRKICDCQENFIQSLSRCVKWDSNGGKSGSGFLKTLDDRFIIKELSHAELEAFIKFAPSYFEYMAQAMFHDLPTTLAKVFGFYQ
```

C)

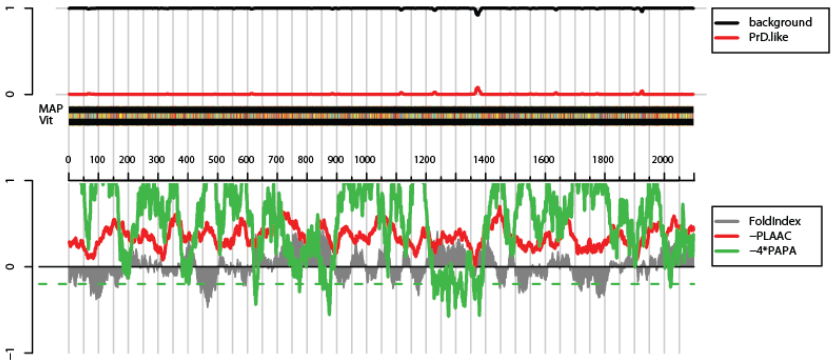


```
1    MATDDKTSPTLDSANDLPRSPTSPSHLTHFKPLTPDQDEPPFKSAYSSFVNLFRFNKERAEGGQSEQQPLSGSWTSPQLPSRTQSVRSPTPYKKQLNEEL
101  QRRSSALDTRRKAEPTFGGHDPRTAVQLRSLSTVLKRLKEIMEGKSQDSDLKQYWMPDSQCKECYDCSEKFTTFRRRHHCRLCGQIFCSRCCNQEIPGKF
201  MGYTGDLRACTYCRKIALSYAHSTDSNSIGEDLNALSDSACSVSVLDPSEPRTPVGSRKASRNIFLEDDLAWQSLIHPDSSNTPLSTRLVSVQEDAGKSP
301  ARNRSASITNLSLDRSGSPMVPSYETSVSPQANRTYVRTETTEDERKILLDSVQLKDLWKKICHHSSGMEFQDHRYWLRTHPNCIVGKELVNWLIRNGHI
401  ATRAQAIAIGQAMVDGRWLDCVSHHDQLFRDEYALYRPLQSTEFSETPSPDSDSVNSVEGHSEPSWFKDIKFDDSDTEQIAEEGDDNLANSASPSKRTSV
501  SSFQSTVDSDSAASISLNVELDNVNFHIKKPSKYPHVPPHPADQKEYLISDTGGQQLSISDAFIKESLFNRRVEEKSKELPFTPLGWHHNNLELLREENG
601  EKQAMERLLSANHNHMMALLQQLLHSDSLSSSVRDIIVSLVCQVVQTVRPDVKNQDDDMDIRQFVHIKKIPGGKKFDSVVVNGFVCTKNIAHKKMNSCIK
701  NPKILLLKCSIEYLYREETKFTCIDPIVLQERE FLKNYVQRIVDVRPTLVLVEKTVSRIAQDMLLEHGITLVINVKSQVLERISRMTQGDLVMSMDQLLT
801  KPHLGTCHKFYMQIFQLPNEQTIKTLMFFEGCPQHLGCTIKLRGGSDYELARVKEILIFMICVAYHSQLEISFLMDEFAMPPTLMQNPSFHSLIEGRGHEG
901  AVQEQYGGGSIPWDPDIPPESLPCDDSSLLESRIVFEKGEQENKNLPQAVASVKHQEHSTTACPAGLPCAFFAPVPESLLPLPVDDQQDALGSELPESLQ
1001 QTVVLQDPKSQIRAFRDPLQDDTGLYVTEEVTSSEDKRKTYSLAFKQELKDVILCISPVITFREPFLLTEKGMRCSTRDYFAEQVYWSPLLNKEFKEMEN
1101 RRKKQLLRDLSGLQGMNGSIQAKSIQVLPSHELVSTRIAEHLGDSQSLGRMLADYRARGGRIQPKNSDPFAHSKDASSTSSGKSGSKNEGDEERGLILSD
1201 AVWSTKVDCLNPINHQRLCVLFSSSSAQSSNAPSACVSPWIVTMEFYGKNDLTLGIFLERYCFRPSYQCPSMFCDTPMVHHIRRFVHGQGCVQIILKELD
1301 SPVPGYQHTILTYSWCRICKQVTPVVALSNESWSMSFAKYLELRFYGHQYTRRANAEPCGHSIHHDYHQYFSYNQMVASFSYSPILLEVCVPLPKIFIK
1401 RQAPLKVSLLQDLKDFFQKVSQVYVAIDERLASLKTDTFSKTREEKMEDIFAQKEMEGEFKNWIEKMQARLMSSVDTPQQLQSVFESLIAKKQSLCEV
1501 LQAWNNRLQDLFQQEKGRKRPSVPPSPGRLRQGEESKISAMDASPRNISPGLQNGEKEDRFLTTLSSQSSTSSTHLQLPTPPEVMSEQSVGGPPELDTAS
1601 SSEDVFDGHLLGSTDSQVKEKSTMKAIFANLLPGNSYNPIPFPFDPDKHYLMYEHERVPIAVCEKEPSSIIAFALSCKEYRNALEELSKATQWNSAEEGL
1701 PTNSTSDSRPKSSSPILRLPEMSGGQTNRTTETEPQPTKKASGMLSFFRGTAGKSPDLSSQKRETLRGADSAYYQVGQTGKEGTENQGVEPQDEVDGGDTQ
1801 KKQLINPHVELQFSDANAKFYCRLYYAGEFHKMREVILDSSEEDFIRSLSHSSPWQARGGKSGAAFYATEDDRFILKQMPRLEVQSFLDFAPHYFNYITN
1901 AVQQKRPTALAKILGVYRIGYKNSQNNTEKKLDLLVMENLFYGRKMAQVFDLKGSLRNRNVKTDTGKESCDVVLLDENLLKMVRDNPLYIRSHSKAVLRT
2001 SIHSDSHFLSSHLIIDYSLLVGRDDTSNELVVGIIDYIRTFTWDKKLEMVVKSTGILGGQGKMPTVVSPELYRTRFCEAMDKYFLMVPDHWTGLGLNC
```

Figure 2.4. Yeast Fab1 but not mammalian PIKfyve contains a prion-like domain (PrD). A) Schematic representation of *S. cerevisiae* Fab1 with the PrD domain from residues 456-607. **B)** Prion-like amino acid composition (PLAAC) (Lancaster *et al.*, 2014) analysis of *S. cerevisiae* Fab1. **Top graph:** black line indicates background of yeast ORFs. Red line indicates probability of prion-like domain where 1=extremely likely 0=not likely. **Bottom graph:** PLAAC comparison with other unfolded protein prediction programs FoldIndex and 4*PAPA. **Bottom:** Vac7 protein sequence: red indicates prion-like domains. **C)** Prion-like amino acid composition (PLAAC) (Lancaster *et al.*, 2014) analysis of *H. sapien* PIKfyve indicates no PrD. **Top graph:** black line indicates background of yeast ORFs. Red line indicates probability of prion-like domain where 1=extremely likely 0=not likely. **Bottom graph:** PLAAC comparison with other unfolded protein prediction programs FoldIndex and 4*PAPA. **Bottom:** Vac7 protein sequence: red indicates prion-like domains.

A)

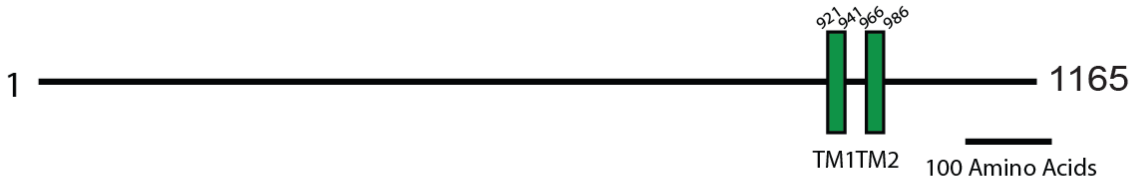

B)

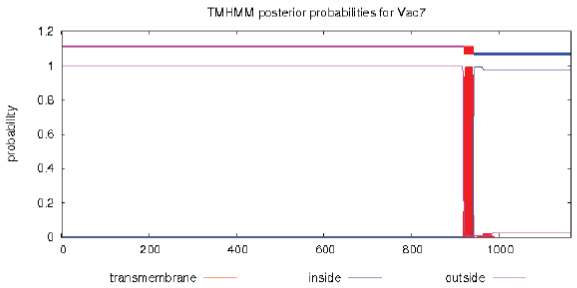

# AA	inside	membrane	outside
919 N	0.00172	0.14931	0.84897
920 F	0.00021	0.79289	0.2069
921 L	0.00002	**0.93183**	0.06815
922 Y	0.00001	**0.97200**	0.02799
923 L	0.00000	**0.98527**	0.01473
924 A	0.00000	**0.99136**	0.00864
925 F	0.00000	**0.99256**	0.00744
926 V	0.00000	**0.99280**	0.0072
927 I	0.00000	**0.99283**	0.00717
928 S	0.00000	**0.99283**	0.00717
929 S	0.00000	**0.99283**	0.00717
930 L	0.00000	**0.99283**	0.00717
931 L	0.00000	**0.99283**	0.00717
932 M	0.00000	**0.99283**	0.00717
933 T	0.00000	**0.99283**	0.00717
934 G	0.00000	**0.99283**	0.00717
935 F	0.00000	**0.99283**	0.00717
936 I	0.00001	**0.99282**	0.00717
937 L	0.00006	**0.99277**	0.00718
938 G	0.00077	**0.99202**	0.00721
939 F	0.00317	**0.98959**	0.00724
940 L	0.01933	**0.97333**	0.00735
941 L	0.04571	**0.94687**	0.00742
942 A	0.25673	0.73545	0.00783
943 T	0.86556	0.12528	0.00916
944 N	0.97372	0.01694	0.00934

C)

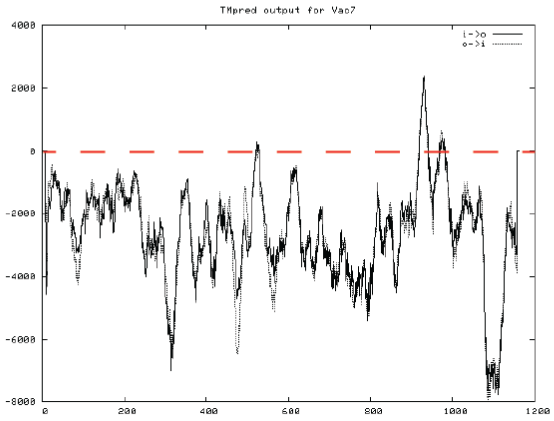


```
2 strong transmembrane helices, total score : 3002
# from   to length
1  924  941 (18)
2  966  986 (21)
```

Figure 2.5. Vac7 may contain two transmembrane domains. A) S. cerevisiae Vac7 contains two transmembrane domains from 921-941 (TM1) and 966-968 (TM2). B) TMHMM (Krogh *et al.*, 2001) predictes a single transmembrane domain from Vac7 residues 921-941. C) TMpred (Ikeda *et al.*, 2003) predicts two transmembrane domains from 924-941 and 966-986. TMPred is a more recent algorithm and likely a better predictor of TM domains.

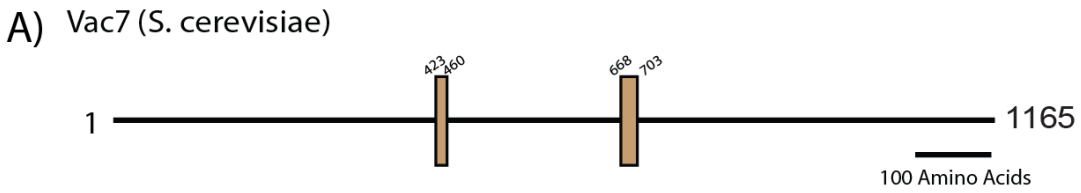

B)

```
Kluyveromyces_marxianus_Vac7      SESVRRLNKESSSKADFFAARLATAVGENEISDSEETFVYQSTANSVKNASLNDASSMQN  448
Kluyveromyces_lactis              SESVRKLNKESSSKADFFAARLATAVGENEISDSEETFVYQSTANSVKNASINDVSATPN  384
Ashbya_gossypii                   -----RHSKEPSTKADFFAARLASAVGENEISDSEETFVYESTANSTKNSYEPISSNLV-  241
Zygosaccharomyces_bailii          -----SESLHKPTKADFFAARLASAVGENEISDSEETFIYESAANSTKNAVAGGTTEALP  191
Torulaspora_delbrueckii           -----LDSLQKPTKADFFAARLASAVGENEISDSEETFIYESAANSTKNAIAPPAFD---  342
Zygosaccharomyces_rouxii          -----TDSLHKPTKADFFAARLASAVGENDISDSEETFIYESAANSTKNAVPSGVGNNSI  351
Candida_glabrata                  TQTTESSNAHRPTKTDFFAARLASAVGENEVSDSEETFVYESAANSTKNMIYPSTSKIND  367
S288c_Vac7                        NDDSHESNSEKPTKADFFAARLATAVGENEISDSEETFVYESAANSTKNLIFPDSSSQQQ  471
Saccharomyces_arboricola          NDDSHDDTSEKPTKADFFAARLATAVGENEISDSEETFVYESAANSTKNLIYPDSSNQQQ  484
Kazachstania_naganishii           QSPDEVDASQKPNRTDFFAARLASAVGENEISDSEETFVYESAANSTKNLIYPSASSMAL  468
Kazachstania_africana             SQFGLDGSSQKPTKADFFAARLASAVGENEGSDSEETFVYESAANSTKNLIYPNASSVAL  408
Naumovozyma_castellii             STDNDQDQSQIPTKTDFFAAKLASAVGDNEISDSEETFVYESAANSTKNMILPSTMEAIQ  334
Vanderwaltozyma_polyspora         TISQDTDSLQKPTKADIFAAKLASAVGENEISDSEETFVYESTANSSKNVKLANPQEMLN  375
                                           .  .::*:***:**:***:*: *******:*:*:*** **
```

C)

```
Kluyveromyces_marxianus_Vac7      KGHNRT---------SSRPGENKKGVTTLRTRSSKVFDPNG--SSLRRYSGVPDDVNLED  669
Kluyveromyces_lactis              QNHRRT---------SSKPGDSKK--SALRTRSSKVFDPNG--SSLRRYSGVPDDVNLED  602
Ashbya_gossypii                   -G-NSG----------TLK-MKNNHLYPLRTTASRIFDANG--ASLRRYSGVPDNINLED  433
Zygosaccharomyces_bailii          ----------------SKP-DPPSFKRKLRTTASKIFDPNG--A--RRYSGIPDDVNLED  448
Torulaspora_delbrueckii           AGTARGK-------FVTKP-DGDNNKRNLRTTASKIFDANG--APLRRYSGVPDDVNLED  549
Zygosaccharomyces_rouxii          MGVPRA-----------KP-EPTGFKRKLRTTASKIFDANG--APLRRYSGVPDDVNLED  585
Candida_glabrata                  HNQ----RAKTGAAQKNASKASIENKNTLRTTVSKIFDANG--ASLRRYSGVPDNVNLED  591
S288c_Vac7                        N-----------------SNYGDNKRPLRTTVSKIFDSNPNGAPLRRYSGVPDHVNLED  699
Saccharomyces_arboricola          N-----------------STYGDNKRPLRTTVSKIFDSNPNGAPLRRYSGVPDHVNLED  718
Kazachstania_naganishii           ---------------LRLNKKRDGKRVLRTTISKIFDTTG--APARRYSGVPDNVNLED  695
Kazachstania_africana             K----------MNLEDSANNYNPDSKRVLRTTVSKIFDSNN--TPLRRYSGVPDHINLED  658
Naumovozyma_castellii             NNNNNNNNNNNPNTPRGTKNEPMGNKRKLRTTVSKIFDGNG-NQPLRRYSGVPDNINLED  584
Vanderwaltozyma_polyspora         HRIPSNA---------NNGIVRTNSKRRLRTTASKIFDTNG--APLRRYSGVPDHVNLED  599
                                                        ***  *::** .      *****:**.:****

Kluyveromyces_marxianus_Vac7      FVDQYDGEFDLTVSRQQKGNDKKALKYYHP------SNAASQREISSGIRHDQY---D--  718
Kluyveromyces_lactis              FVDQYDGEFDIKMHRPSRTTEKKSNNQQHQ------SNAASQRGTYSSDNHIQY---E--  651
Ashbya_gossypii                   YVEQENGELTPNKFTYRS---S-------------------------------------  452
Zygosaccharomyces_bailii          YIEQQQPLEPHRIGHELADDQQSTIQEEDAE---YGGGGAEGAKIFDPNGARRYSGIP--  503
Torulaspora_delbrueckii           FIEQSNGHYMTNPSNQRDDRTRNFLE-----------NNHNNDK----------------  582
Zygosaccharomyces_rouxii          YIEQHPSQDTKRLGHD--------LG-----------GIDDQQS----------------  610
Candida_glabrata                  FIEQNDLYTNQGLNSKEKKLSR--QQKYMPSRHSISGAHTRGSERSSPIDADYLKGITRH  649
S288c_Vac7                        YIEQPHNYPTMQNSVKKDEF----YN----SRN--------------------------  724
Saccharomyces_arboricola          YIEQSHNYPTVQNSVKKDEF----FN----NRN--------------------------  743
Kazachstania_naganishii           YIEQSDEVSDMGTDNNAGPI----KTGNNNNHA------------------SHRGPDNN  732
Kazachstania_africana             YIEQANDYNVVNSHQNPHNS----NGSLMHSNSV-------------KINSSYLTNNNDS  701
Naumovozyma_castellii             YIEQSDEYYHPSSVK----M----NNNYMPNGA-----------------NYYNAP-DY  617
Vanderwaltozyma_polyspora         YIEQSNFSPMSNSVIKHEPV----NDYFEPKKV-----------------NYIRD----  633
                                  :::*
```

Figure 2.6. Vac7 contains two unstructured regions with high conservation in all identified Vac7 homologs. A) Vac7 contains two areas of sequence conservation first from 423-460 and second from 668-703. **B)** ClustalOmega alignment of all known Vac7 homologs shows sequence conservation from residues 423-460. **C)** ClustalOmega alignment of all known Vac7 homologs shows sequence conservation from residues 668-703. *S. cerevisiae* Vac7 is indicated based on its strain name Vac7_S288C.

A) Vac7 (S. cerevisiae)

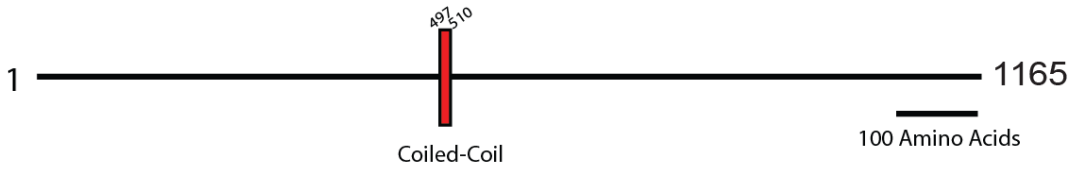

B)

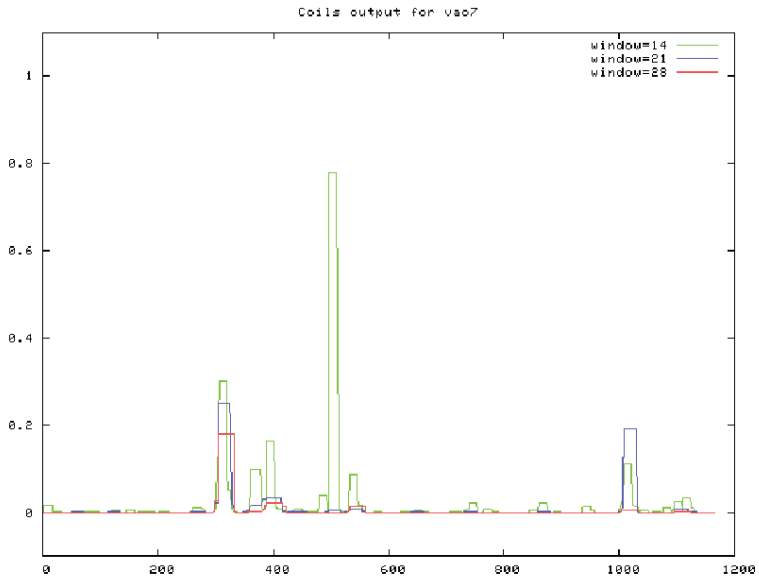

C)

Amino Acid Number	Amino Acid Residue	14-Coil	21-Coil	28-Coil
495	A	0.005	0.001	0
496	P	0.008	0.001	0
497	**L**	**0.779**	0.004	0
498	**L**	**0.779**	0.004	0
499	**N**	**0.779**	0.004	0
500	**N**	**0.779**	0.004	0
501	**N**	**0.779**	0.004	0
502	**K**	**0.779**	0.004	0
503	**K**	**0.779**	0.004	0
504	**L**	**0.779**	0.004	0
505	**L**	**0.779**	0.004	0
506	**S**	**0.779**	0.004	0
507	**R**	**0.779**	0.004	0
508	**L**	**0.779**	0.004	0
509	**K**	**0.779**	0.004	0
510	**N**	**0.779**	0.004	0
511	S	0.435	0.004	0
512	R	0.435	0.004	0
513	H	0.109	0.004	0

Figure 2.7. Vac7 contains a single 14-residue coiled-coil domain from residues 497-510. A) S. cerevisiae Vac7 schematic depicting a coiled-coil domain from residues 497-510. **B)** COILS (Lupas *et al.*, 1991) graph indicating an 80% certainty of a coiled coil domain at indicated residues. **C)** residue chart depicting COILS graph indicating a 14-residued coiled coil from Vac7 residues 497-510.

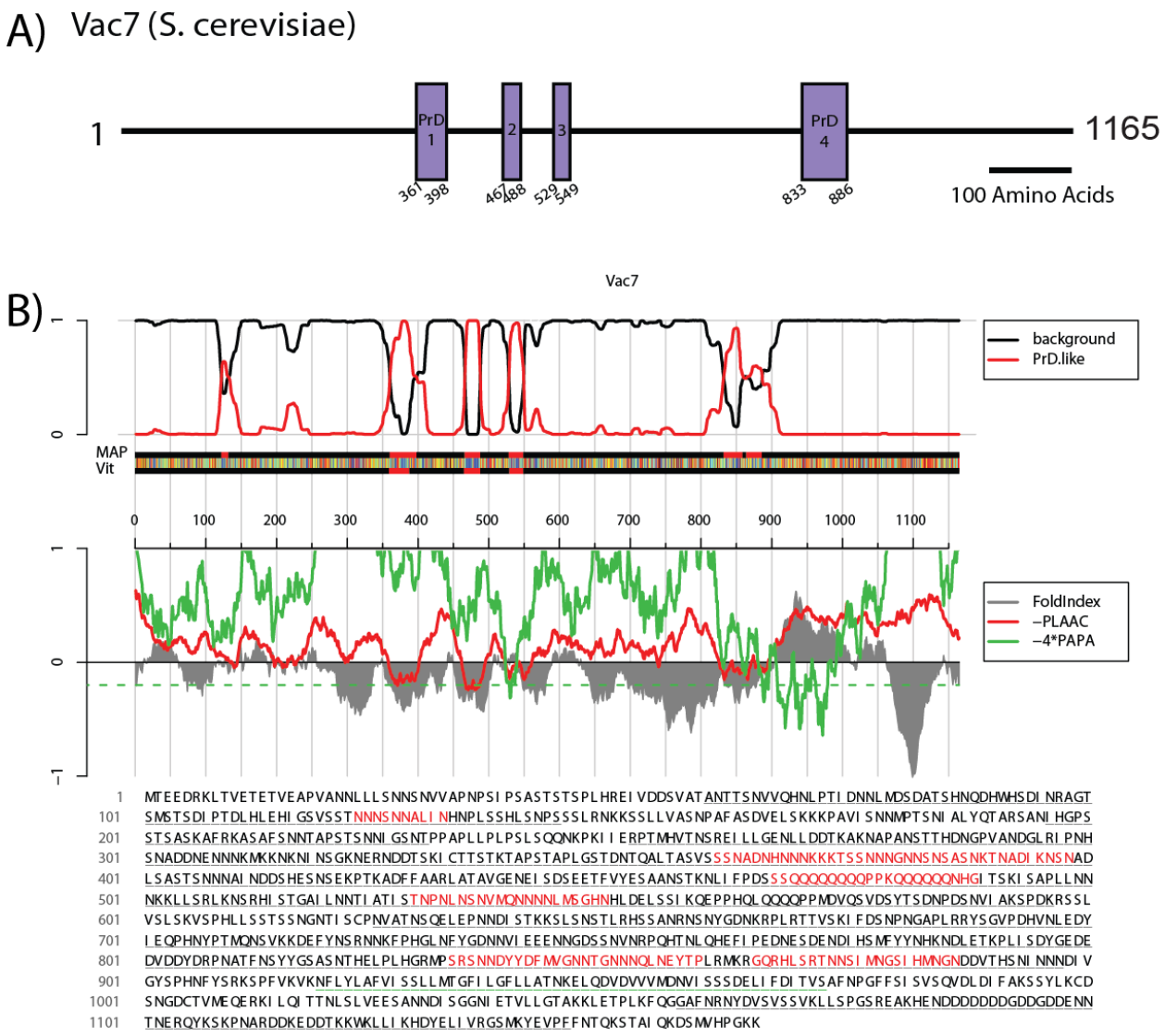

Figure 2.8. Vac7 contains four prion-like domains (PrD domains). A) Schematic representation of *S. cerevisiae* Vac7 with four PrD domains from residues 361-398, 467-488, 529-549, and 833-886. **B)** Prion-like amino acid composition (PLAAC) (Lancaster *et al.*, 2014) analysis of *S. cerevisiae* Vac7. **Top graph:** black line indicates background of yeast ORFs. Red line indicates probability of prion-like domain where 1=extremely likely 0=not likely. **Bottom graph:** PLAAC comparison with other unfolded protein prediction programs FoldIndex and 4*PAPA. **Bottom:** Vac7 protein sequence: red indicates prion-like domains.

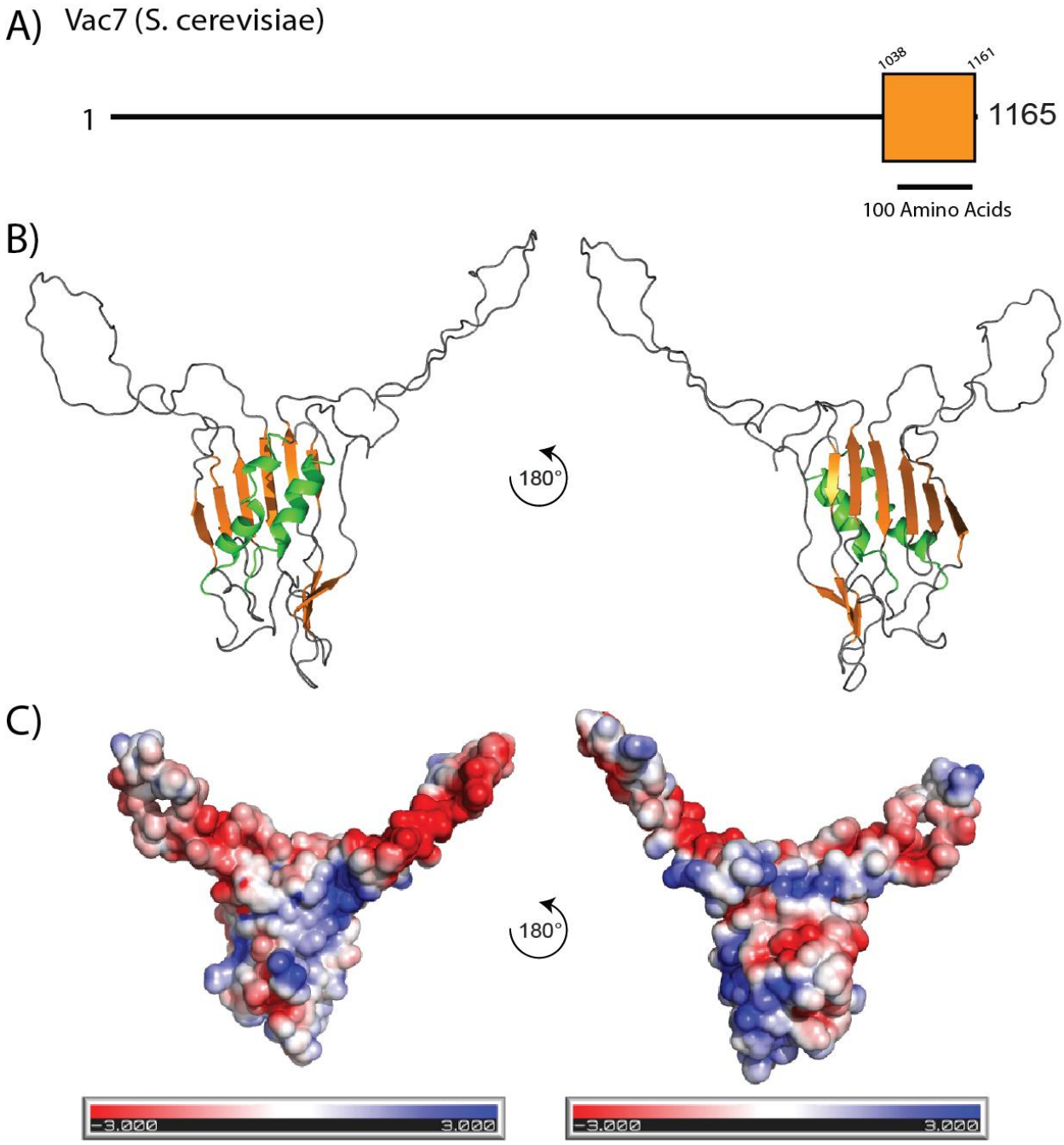

Figure 2.9. The C-terminal region of Vac7 contains a domain with secondary structure. A) Schematic representation of *S. cerevisiae* Vac7 with C-terminal structured region from 1038-1161. **B)** Raptor X secondary structure prediction of C-terminal Vac7. Green: transmembrane helicies TM1 and TM2. Orange: C-terminal domain composed of beta-sheets spanning from residues 1038-1161. Structure prediction is based off of the crystal structure of Osh6. **C)** electrostatic potential map of structure depicted in B. Saturating red indicates $\varphi < -3$ kT/e, and saturating blue indicates $\varphi > 3$ kT/e, where T = 25°C and pH=7.0. Unstructured loops of predicted Vac7 structured domain are electrostatically negative and thus are likely not membrane insertion loops.

Table 2.1. HEAT repeats of *S. cerevisiae* Vac14

#	Residue start	Residue stop	PDB	Info
1	1	33	2QK2	*S. cerevisiae* Stu2
2	37	75	2QK2	*S. cerevisiae* Stu2
3	85	115	4G3A	*D. melanogaster* CLIP-associating protein
4	116	143	4G3A	*D. melanogaster* CLIP-associating protein
5	147	177	2QK2	No HEAT repeat strongly detected
6	185	216	2QK2	*S. cerevisiae* Stu2
7	223	256	4G3A	*D. melanogaster* CLIP-associating protein
8	261	295	4G3A	*D. melanogaster* CLIP-associating protein
9	298	329	4G3A	*D. melanogaster* CLIP-associating protein
10	393	426	4G3A	*D. melanogaster* CLIP-associating protein
11	433	462	4G3A	*D. melanogaster* CLIP-associating protein
12	480	510	2QK2	*S. cerevisiae* Stu2
13	513	549	2QK2	*S. cerevisiae* Stu2
14	556	591	4G3A	*D. melanogaster* CLIP-associating protein
15	596	623	4G3A	*D. melanogaster* CLIP-associating protein
16	627	653	1ZAV	*T. maritima* 50S ribosomal protein L10
17	657	679	3BQO	*H. sapiens* Telomeric repeat-binding factor 1
18	689	717	2J4B	*E. cuniculi* TFIID subunit 72/90-100 KDA
19	719	743	4J2G	*L. thermotolerans* Atg13
20	745	790	3OMY	*E. coli* Protein tram, Not likely a HEAT repeat
21	793	824	3OMY	*E. coli* Protein tram, Not likely a HEAT repeat
22	844	877	3K7I	*H. sapiens* Indian hedgehog protein, Not likely a HEAT repeat

Table 2.2. HEAT repeats of *H. sapiens* Vac14

#	Residue start	Residue stop	PDB	Info
1	12	42	2QK2	*S. cerevisiae* Stu2
2	46	88	2QK2	*S. cerevisiae* Stu2
3	90	124	2QK2	*S. cerevisiae* Stu2
4	131	165	2QK2	*S. cerevisiae* Stu2
5	173	202	2QK2	*S. cerevisiae* Stu2
6	216	249	2QK2	*S. cerevisiae* Stu2
7	255	288	4G3A	*D. melanogaster* CLIP-associating protein
8	290	333	4G3A	*D. melanogaster* CLIP-associating protein
9	333	396		No HEAT repeat strongly detected
10	396	432	4G3A	*D. melanogaster* CLIP-associating protein
11	434	472	4G3A	*D. melanogaster* CLIP-associating protein
12	472	522		No HEAT repeat strongly detected
13	522	574	5CHS	Vesicular stomatitis indiana virus RNA-directed RNA polymerase L
14	579	628	5CHS	Vesicular stomatitis indiana virus RNA-directed RNA polymerase L
15	630	673	4KKO	Human immunodeficiency virus 1 HIV-1 reverse transcriptase, p66 subunit
16	676	701	4WZX	*H. sapiens* Serine/threonine-protein kinase ULK3
17	724	758	4WZX	*H. sapiens* Serine/threonine-protein kinase ULK3

Table 2.3. Vac7 homologs are limited to fungi

Species	Vac7 Accession number
S. Cerevisiae S288c	YNL054W
Kluyveromyces marxianus DMKU3-1042	BAO42473.1
Saccharomyces arboricola H-6	XP_011105266.1
Torulaspora delbrueckii	XP_003680506.1
Naumovozyma castellii CBS 4309	XP_003677547.1
Candida glabrata	XP_446420.1
Zygosaccharomyces rouxii	XP_002494450.1
Vanderwaltozyma polyspora	XP_001646133.1
Kazachstania africana	XP_003959314.1
Zygosaccharomyces bailii	CDH11277.1
Kazachstania naganishii	CCK71967.1
Ashbya gossypii	NP_983850.1
Kluyveromyces lactis	XP_455242.1
Schizosaccharomyces pombe	NP_596520.1
Candida albicans	KGU07888.1

Bibliography

Abrams, C.S., Zhao, W., Belmonte, E., and Brass, L.F. (1995). Protein kinase C regulates pleckstrin by phosphorylation of sites adjacent to the N-terminal pleckstrin homology domain. J Biol Chem *270*, 23317-23321.

Adhikari, A.N., Peng, J., Wilde, M., Xu, J., Freed, K.F., and Sosnick, T.R. (2012). Modeling large regions in proteins: applications to loops, termini, and folding. Protein Sci *21*, 107-121.

Alberti, S., Halfmann, R., King, O., Kapila, A., and Lindquist, S. (2009). A systematic survey identifies prions and illuminates sequence features of prionogenic proteins. Cell *137*, 146-158.

Baskaran, S., Ragusa, M.J., Boura, E., and Hurley, J.H. (2012). Two-site recognition of phosphatidylinositol 3-phosphate by PROPPINs in autophagy. Molecular cell *47*, 339-348.

Bonangelino, C.J., Nau, J.J., Duex, J.E., Brinkman, M., Wurmser, A.E., Gary, J.D., Emr, S.D., and Weisman, L.S. (2002). Osmotic stress-induced increase of phosphatidylinositol 3,5-bisphosphate requires Vac14p, an activator of the lipid kinase Fab1p. The Journal of cell biology *156*, 1015-1028.

Botelho, R.J., Efe, J.A., Teis, D., and Emr, S.D. (2008). Assembly of a Fab1 phosphoinositide kinase signaling complex requires the Fig4 phosphoinositide phosphatase. Mol Biol Cell *19*, 4273-4286.

Cheever, M.L., Sato, T.K., de Beer, T., Kutateladze, T.G., Emr, S.D., and Overduin, M. (2001). Phox domain interaction with PtdIns(3)P targets the Vam7 t-SNARE to vacuole membranes. Nat Cell Biol *3*, 613-618.

Civera, C., Simon, B., Stier, G., Sattler, M., and Macias, M.J. (2005). Structure and dynamics of the human pleckstrin DEP domain: distinct molecular features of a novel DEP domain subfamily. Proteins *58*, 354-366.

Cooke, F.T. (2002). Phosphatidylinositol 3,5-bisphosphate: metabolism and function. Arch Biochem Biophys *407*, 143-151.

Dove, S.K., Piper, R.C., McEwen, R.K., Yu, J.W., King, M.C., Hughes, D.C., Thuring, J., Holmes, A.B., Cooke, F.T., Michell, R.H., Parker, P.J., and Lemmon, M.A. (2004). Svp1p defines a family of phosphatidylinositol 3,5-bisphosphate effectors. Embo Journal *23*, 1922-1933.

Drozdetskiy, A., Cole, C., Procter, J., and Barton, G.J. (2015). JPred4: a protein secondary structure prediction server. Nucleic Acids Res *43*, W389-394.

Duex, J.E., Nau, J.J., Kauffman, E.J., and Weisman, L.S. (2006a). Phosphoinositide 5-phosphatase Fig 4p is required for both acute rise and subsequent fall in stress-induced phosphatidylinositol 3,5-bisphosphate levels. Eukaryotic cell *5*, 723-731.

Duex, J.E., Nau, J.J., Kauffman, E.J., and Weisman, L.S. (2006b). Phosphoinositide 5-phosphatase Fig 4p is required for both acute rise and subsequent fall in stress-induced phosphatidylinositol 3,5-bisphosphate levels. Eukaryot Cell *5*, 723-731.

Duex, J.E., Tang, F., and Weisman, L.S. (2006c). The Vac14p-Fig4p complex acts independently of Vac7p and couples PI3,5P2 synthesis and turnover. The Journal of cell biology *172*, 693-704.

Edgar, R.C., and Batzoglou, S. (2006). Multiple sequence alignment. Curr Opin Struct Biol *16*, 368-373.

Efe, J.A., Botelho, R.J., and Emr, S.D. (2005). The Fab1 phosphatidylinositol kinase pathway in the regulation of vacuole morphology. Curr Opin Cell Biol *17*, 402-408.

Ellson, C.D., Gobert-Gosse, S., Anderson, K.E., Davidson, K., Erdjument-Bromage, H., Tempst, P., Thuring, J.W., Cooper, M.A., Lim, Z.Y., Holmes, A.B., Gaffney, P.R., Coadwell, J., Chilvers, E.R., Hawkins, P.T., and Stephens, L.R. (2001). PtdIns(3)P regulates the neutrophil oxidase complex by binding to the PX domain of p40(phox). Nat Cell Biol *3*, 679-682.

Ferre, F., and Clote, P. (2006). DiANNA 1.1: an extension of the DiANNA web server for ternary cysteine classification. Nucleic Acids Res *34*, W182-185.

Gary, J.D., Sato, T.K., Stefan, C.J., Bonangelino, C.J., Weisman, L.S., and Emr, S.D. (2002). Regulation of Fab1 phosphatidylinositol 3-phosphate 5-kinase pathway by Vac7 protein and Fig4, a polyphosphoinositide phosphatase family member. Mol Biol Cell *13*, 1238-1251.

Gary, J.D., Wurmser, A.E., Bonangelino, C.J., Weisman, L.S., and Emr, S.D. (1998). Fab1p is essential for PtdIns(3)P 5-kinase activity and the maintenance of vacuolar size and membrane homeostasis. The Journal of cell biology *143*, 65-79.
Gillooly, D.J., Morrow, I.C., Lindsay, M., Gould, R., Bryant, N.J., Gaullier, J.M., Parton, R.G., and Stenmark, H. (2000). Localization of phosphatidylinositol 3-phosphate in yeast and mammalian cells. EMBO J *19*, 4577-4588.
Harlan, J.E., Hajduk, P.J., Yoon, H.S., and Fesik, S.W. (1994). Pleckstrin homology domains bind to phosphatidylinositol-4,5-bisphosphate. Nature *371*, 168-170.
Hayakawa, A., Hayes, S.J., Lawe, D.C., Sudharshan, E., Tuft, R., Fogarty, K., Lambright, D., and Corvera, S. (2004). Structural basis for endosomal targeting by FYVE domains. J Biol Chem *279*, 5958-5966.
Hu, M.H., Bauman, E.M., Roll, R.L., Yeilding, N., and Abrams, C.S. (1999). Pleckstrin 2, a widely expressed paralog of pleckstrin involved in actin rearrangement. J Biol Chem *274*, 21515-21518.
Ikeda, M., Arai, M., Okuno, T., and Shimizu, T. (2003). TMPDB: a database of experimentally-characterized transmembrane topologies. Nucleic Acids Res *31*, 406-409.
Jin, N., Chow, C.Y., Liu, L., Zolov, S.N., Bronson, R., Davisson, M., Petersen, J.L., Zhang, Y., Park, S., Duex, J.E., Goldowitz, D., Meisler, M.H., and Weisman, L.S. (2008a). VAC14 nucleates a protein complex essential for the acute interconversion of PI3P and PI(3,5)P(2) in yeast and mouse. EMBO J *27*, 3221-3234.
Jin, N., Chow, C.Y., Liu, L., Zolov, S.N., Bronson, R., Davisson, M., Petersen, J.L., Zhang, Y., Park, S., Duex, J.E., Goldowitz, D., Meisler, M.H., and Weisman, L.S. (2008b). VAC14 nucleates a protein complex essential for the acute interconversion of PI3P and PI(3,5)P(2) in yeast and mouse. The EMBO journal *27*, 3221-3234.
Kanai, F., Liu, H., Field, S.J., Akbary, H., Matsuo, T., Brown, G.E., Cantley, L.C., and Yaffe, M.B. (2001). The PX domains of p47phox and p40phox bind to lipid products of PI(3)K. Nat Cell Biol *3*, 675-678.
Kelley, L.A., Mezulis, S., Yates, C.M., Wass, M.N., and Sternberg, M.J. (2015). The Phyre2 web portal for protein modeling, prediction and analysis. Nat Protoc *10*, 845-858.
Kim, M.K., and Kang, Y.K. (1999). Positional preference of proline in alpha-helices. Protein Sci *8*, 1492-1499.
Kippert, F., and Gerloff, D.L. (2009). Highly sensitive detection of individual HEAT and ARM repeats with HHpred and COACH. PLoS One *4*, e7148.
Krick, R., Busse, R.A., Scacioc, A., Stephan, M., Janshoff, A., Thumm, M., and Kuhnel, K. (2012). Structural and functional characterization of the two phosphoinositide binding sites of PROPPINs, a beta-propeller protein family. Proceedings of the National Academy of Sciences of the United States of America *109*, E2042-2049.
Krogh, A., Larsson, B., von Heijne, G., and Sonnhammer, E.L. (2001). Predicting transmembrane protein topology with a hidden Markov model: application to complete genomes. J Mol Biol *305*, 567-580.
Lancaster, A.K., Nutter-Upham, A., Lindquist, S., and King, O.D. (2014). PLAAC: a web and command-line application to identify proteins with prion-like amino acid composition. Bioinformatics *30*, 2501-2502.
Levy, R., Edelman, M., and Sobolev, V. (2009). Prediction of 3D metal binding sites from translated gene sequences based on remote-homology templates. Proteins *76*, 365-374.
Lupas, A., Van Dyke, M., and Stock, J. (1991). Predicting coiled coils from protein sequences. Science *252*, 1162-1164.
McCartney, A.J., Zhang, Y., and Weisman, L.S. (2014). Phosphatidylinositol 3,5-bis phosphate: Low abundance. High significance. . Bioessays *36*, 52-64.
Michelitsch, M.D., and Weissman, J.S. (2000). A census of glutamine/asparagine-rich regions: implications for their conserved function and the prediction of novel prions. Proc Natl Acad Sci U S A *97*, 11910-11915.

Michell, R.H., Heath, V.L., Lemmon, M.A., and Dove, S.K. (2006). Phosphatidylinositol 3,5-bisphosphate: metabolism and cellular functions. Trends in biochemical sciences *31*, 52-63.
Morgenstern, B., Frech, K., Dress, A., and Werner, T. (1998). DIALIGN: finding local similarities by multiple sequence alignment. Bioinformatics *14*, 290-294.
Pace, N.J., and Weerapana, E. (2014). Zinc-binding cysteines: diverse functions and structural motifs. Biomolecules *4*, 419-434.
Passerini, A., Lippi, M., and Frasconi, P. (2011). MetalDetector v2.0: predicting the geometry of metal binding sites from protein sequence. Nucleic Acids Res *39*, W288-292.
Peng, J., and Xu, J. (2011). RaptorX: exploiting structure information for protein alignment by statistical inference. Proteins *79 Suppl 10*, 161-171.
Perutz, M.F. (1999). Glutamine repeats and neurodegenerative diseases: molecular aspects. Trends Biochem Sci *24*, 58-63.
Ponting, C.P., and Bork, P. (1996). Pleckstrin's repeat performance: a novel domain in G-protein signaling? Trends Biochem Sci *21*, 245-246.
Rao, V.D., Misra, S., Boronenkov, I.V., Anderson, R.A., and Hurley, J.H. (1998). Structure of type IIbeta phosphatidylinositol phosphate kinase: a protein kinase fold flattened for interfacial phosphorylation. Cell *94*, 829-839.
Ross, C.A., Margolis, R.L., Becher, M.W., Wood, J.D., Engelender, S., Cooper, J.K., and Sharp, A.H. (1998). Pathogenesis of neurodegenerative diseases associated with expanded glutamine repeats: new answers, new questions. Prog Brain Res *117*, 397-419.
Rudge, S.A., Anderson, D.M., and Emr, S.D. (2004). Vacuole size control: regulation of PtdIns(3,5)P2 levels by the vacuole-associated Vac14-Fig4 complex, a PtdIns(3,5)P2-specific phosphatase. Mol Biol Cell *15*, 24-36.
Sodhi, J.S., Bryson, K., McGuffin, L.J., Ward, J.J., Wernisch, L., and Jones, D.T. (2004). Predicting metal-binding site residues in low-resolution structural models. J Mol Biol *342*, 307-320.
Stenmark, H., Aasland, R., and Driscoll, P.C. (2002). The phosphatidylinositol 3-phosphate-binding FYVE finger. FEBS Lett *513*, 77-84.
Stenmark, H., Aasland, R., Toh, B.H., and D'Arrigo, A. (1996). Endosomal localization of the autoantigen EEA1 is mediated by a zinc-binding FYVE finger. J Biol Chem *271*, 24048-24054.
Strahl, T., and Thorner, J. (2007). Synthesis and function of membrane phosphoinositides in budding yeast, Saccharomyces cerevisiae. Biochim Biophys Acta *1771*, 353-404.
Thompson, J.D., Higgins, D.G., and Gibson, T.J. (1994). CLUSTAL W: improving the sensitivity of progressive multiple sequence alignment through sequence weighting, position-specific gap penalties and weight matrix choice. Nucleic Acids Res *22*, 4673-4680.
Tyers, M., Rachubinski, R.A., Stewart, M.I., Varrichio, A.M., Shorr, R.G., Haslam, R.J., and Harley, C.B. (1988). Molecular cloning and expression of the major protein kinase C substrate of platelets. Nature *333*, 470-473.
Uptain, S.M., and Lindquist, S. (2002). Prions as protein-based genetic elements. Annu Rev Microbiol *56*, 703-741.
Watanabe, Y., Kobayashi, T., Yamamoto, H., Hoshida, H., Akada, R., Inagaki, F., Ohsumi, Y., and Noda, N.N. (2012). Structure-based analyses reveal distinct binding sites for Atg2 and phosphoinositides in Atg18. The Journal of biological chemistry *287*, 31681-31690.
Xu, Y., Hortsman, H., Seet, L., Wong, S.H., and Hong, W. (2001). SNX3 regulates endosomal function through its PX-domain-mediated interaction with PtdIns(3)P. Nat Cell Biol *3*, 658-666.
Yang, J., Yan, R., Roy, A., Xu, D., Poisson, J., and Zhang, Y. (2015). The I-TASSER Suite: protein structure and function prediction. Nat Methods *12*, 7-8.

CHAPTER 3:

DOMINANT-ACTIVE MUTATIONS IN FAB1 REVEAL DOMAINS THAT ARE REQUIRED TO REGULATE PI(3,5)P_2 LEVELS

Introduction

Mechanisms that regulate the levels of PI(3,5)P_2 within the cell are not known. The Fab1 complex contains multiple proteins that regulate PI(3,5)P_2 levels; however, little is known about how this dynamic regulation occurs. Moreover, knowledge of the function of specific domains within Fab1 is limited to a handful of structure function studies (Gary *et al.*, 2002; Botelho *et al.*, 2008; Jin *et al.*, 2008a). For instance, of the six domains within Fab1 and eight domains within PIKfyve, detailed analysis of domain function has only been performed on two—the CCT domain and the kinase domain (Jin *et al.*, 2008b). Therefore, I sought to characterize other domains of Fab1 and to determine mechanisms within Fab1 that regulate PI(3,5)P_2 levels.

One effective approach to the study of domains of unknown function is to screen for dominant-active alleles that increase the activity of the protein of interest. This is in contrast with structure-function studies that rely on loss-of-function mutants. Loss-of-function mutations are often difficult to interpret because they often impair protein folding or stability. Multiple types of mutations would damage or decrease the activity of

protein; however, mutations that increase the activity of a protein will likely indicate regions of regulation.

The generation and characterization of dominant-active alleles has previously been used to probe the regulation of Fab1. Initially, a single Fab1 allele known as *Fab1-5* was able to bypass a *vac7Δ* strain. Vac7 is a positive regulator of Fab1 activity. Indeed, in a WT strain background with a *Fab1-5* allele, basal levels of PI(3,5)P_2 were elevated 40-fold over WT control (Gary *et al.*, 2002). However, the point mutations which contributed to this phenotype were not identified. Later, several dominant-active Fab1 alleles with multiple point mutations were identified using a similar screen (Duex *et al.*, 2006). However, these alleles were not dissected to determine the causative point mutation(s). Moreover, the mechanisms that these alleles affect was not determined. Recent studies have used two of these alleles, Fab1-E1822K, N1832Y and Fab1-E1822V, F1833L, T2250A to study the effect of PI(3,5)P_2 in detail in eukaryotic systems (Jin *et al.*, 2014; Li *et al.*, 2014; McCartney *et al.*, 2014b). Importantly, these yeast alleles are conserved in mammalian PIKfyve and have been used to successfully generate dominant-active PIKfyve alleles in human cells lines (McCartney *et al.*, 2014a). That dominant-active alleles of conserved residues can be made in both yeast Fab1 and mammalian PIKfyve indicates that some of the mechanisms of regulation may also be conserved across species. Understanding the mechanism(s) through which these and other alleles cause an elevation in PI(3,5)P_2 levels may generate additional genetic tools to better study

$PI(3,5)P_2$ within a cellular context. Additionally, the identification of novel alleles in domains of unknown function may provide mechanistic insight into the role of specific domains. Together, these studies demonstrate proof of concept that dominant-active alleles may be generated within Fab1. These studies lay the foundation to use a similar approach to identify mutations in additional domains of Fab1.

Description of gapped plasmid screen

To gain insight into the regulatory domains within the Fab1/PIKfyve protein, I performed five dominant-active gapped-plasmid screens. These screens were adapted from a previously published dominant-active screen of the kinase domain of Fab1 (Duex *et al.*, 2006). In this screen, a pRS416-Fab1 plasmid is gapped with a restriction enzyme digest at 37°C overnight, which cuts out a region of Fab1. The gapped plasmid is purified by agarose electrophoresis followed by DNA purification (Qiagen). Following this, primers that flank the gapped region are used to re-amplify this region along with 100 base pairs of overhang on either side of the cut site using native Taq polymerase (invitrogen). The gapped pRS416-Fab1 plasmid and the Taq-amplified gapped region are then co-transformed into an exponentially growing culture of *vac7Δ* (LWY2054). *vac7Δ* yeast are temperature-sensitive cells that grow slowly even at 25ºC. Co-transformant colonies that grow faster than pRS416-Fab1 WT control are picked and struck to single colonies. Following this, single colonies from freshly struck original transformant colonies are struck onto fresh plates and incubated at the non-permissive temperature of 37ºC. Colonies that by-pass the temperature sensitivity are selected as candidate dominant-active alleles. These candidate mutant Fab1 plasmids are extracted

from yeast, amplified in *E.coli*, and re-transformed into *vac7Δ*. Re-transformed dominant-active Fab1 candidate plasmids are then tested a second time for their ability to bypass the *vac7Δ* 37ºC temperature sensitivity phenotype. Plasmids that recapitulate the original finding are then transformed into a *fab1Δ* (LWY2055) strain and used in conjunction with the lipophilic dye FM4-64 to examine vacuole morphology by microscope. Often a highly fragmented vacuolar phenotype is suggestive of an elevation in $PI(3,5)P_2$ levels and a hyperactive mutation. Candidate plasmids that fragment the vacuole in *fab1Δ* yeast are sent for Sanger sequencing to reveal what mutations they harbor.

For the five screens that I performed, each was named for the first letter of the restriction enzyme used. Candidate plasmids isolated from screens are named first with the letter of the gapped plasmid screen they came from then with the mutant number from that screen. For instance, In Figure 3.2A candidate plasmid S58 comes from the S screen and is plasmid number 58. The S-screen was named for its use of the restriction enzyme Sph1, which gapped from residue 298 to residue 798 (Figure 3.1). Upon Sanger sequencing it was identified that this allele corresponded to a single mutation Fab1-M399T.

Taq polymerase inaccuracy is not the only cause of mutation within the gapped plasmid screen

Surprisingly, upon Sanger sequencing of candidate plasmids from screens, it was common to find point mutations outside of the gapped region of Fab1. More interesting

was the fact that sometimes these mutations were hundreds of base pairs upstream or downstream from the gapped region. For instance, Figure 3.3A, all of the alleles identified in the CCT domain that generate a dominant-active allele were more than 300 base pairs downstream from the gapped region of the plasmid—well outside of the restriction enzyme site and the overlapping Taq-generated PCR product. How do mutations outside of the gapped region occur?

The fidelity of the double-stranded DNA break repair mechanism likely increases the overall mutagenic ability of the gapped plasmid screens. The gapped-plasmid screens work through homologous recombination and the induction of the double-stranded break (DSB) repair mechanism. When a DSB occurs, single-stranded degradation of the DNA ends exposes 3'-OH termini (Aylon and Kupiec, 2004). Importantly: these 3'-OH ssDNA tails may be resected from a few hundred nucleotides to tens of kilobases (Aylon and Kupiec, 2004; Chung *et al.*, 2010). Following 5' resection that generates 3' ssDNA tails, the DNA is decorated with RPA and Rad51 thus generating a ssDNA nucleofilament (Aylon and Kupiec, 2004), which then searches for a homologous stretch of DNA. Rad51 continues to coat the ssDNA tail until the nucleofilament encounters a homologous DNA sequence and successful invasion of the homologous (donor) DNA molecule has been accomplished (Sugawara *et al.*, 2003). Following homology search and invasion of the donor DNA, DNA synthesis generates complimentary strains and Rad51 is removed upon DNA annealing and ligation. It is highly likely based on this information and the generation of dominant-active single-mutation alleles outside of the mutagenized area of my screens that the DSB repair mechanism has a sufficiently high

error rate during homologous recombination to generate meaningful mutant alleles in my screen.

Together, I performed a total of five gapped plasmid screens that spanned over 80% of Fab1. 56 novel mutations were identified that span every domain of Fab1 as well as unstructured areas between predicted domains. Below I present an analysis of identified alleles based on their location within Fab1 from N- to C-terminus.

The FYVE domain residue M238 is integral for the regulation of PI(3,5)P_2

Six Fab1 alleles harboring mutations in the Fab1 FYVE domain were isolated from gapped-plasmid screens that recue *vac7Δ* temperature sensitivity and that result in fragmented vacuoles in a *fab1Δ* strain, which suggests that these alleles are dominant-active. These are the first reported mutations in the FYVE domain of Fab1. Intriguingly, all mutant alleles harbor a mutation at methionine 238 (M238) (Figure 3.2A). M238 is the second residue of the Fab1 FYVE WxxD motif that coordinates the PI3P headgroup. All alleles rescue the *vac7Δ* temperature sensitivity growth defect (data not shown) as well as display a fragmented vacuolar morphology in a *fab1Δ* strain background compared to WT cells (Figure 3.2B). Given the known PI3P-coordinating role of the FYVE domain WxxD motif, I hypothesized that the putative dominant-active Fab1 M238 alleles would alter the binding specificity of Fab1 to PI3P.

As a first test, I modeled the Fab1 FYVE domain using the I-TASSER structure prediction software to assay if conformational changes existed in the PI3P binding

pocket of M238 alleles compared to WT Fab1. In alleles Fab1-M238T, Fab1-M238I, and Fab1-238L we see a significant change in the orientation of the WxxD aspartic acid Fab1-D260 (Figure 3.2C). That aspartic acid Fab1-D260 likely coordinates the inositol 4-OH of PI3P, and that it displays altered conformation in all Fab1-M238 mutant alleles strongly suggests that these alleles have altered PI3P binding specificity. Additionally, in alleles Fab1-M238T and Fab1-M238I we see a conformational change in the orientation of Fab1-R263, which is the PI3P 1-phosphate interacting arginine of the R(R/K)HHCR motif. There is not a drastic shift of Fab1-R263 in allele Fab1-M238L. Last, when assayed using this *in silico* I TASSER assay, we find Fab1-H261 (the inositol 5/6-OH coordinating residue) displays altered conformation in all Fab1-M238 mutant alleles again suggesting that these mutations likely alter the binding of the Fab1 FYVE domain with PI3P.

To gain further insight into the changes observed from these *in silico* assays, we monitored $PI(3,5)P_2$ levels over a hyperosmotic shock time course in yeast. We focused on Fab1-M238T due to the fact that it is the most divergent amino acid from the WxxD consensus motif—most second position amino acids of the WxxD motif are strongly hydrophobic (Stenmark *et al.*, 2002). We find in a Fab1-M238T mutant that under basal conditions $PI(3,5)P_2$ levels are higher than WT cells (N=2; error bars=SEM, Figure 3.3A). Additionally, we find that, in response to hyperosmotic shock, Fab1-M238T mutant yeast are unable to elevate $PI(3,5)P_2$ levels in response to a hyperosmotic shock stimulus; however, they appear to have similar rates of turnover of $PI(3,5)P_2$ after the 10-minute time point compared to WT (N=2, error bars=SEM, Figure 3.3B).

Together, this evidence indicates that Fab1-M238T is defective in the initial elevation of $PI(3,5)P_2$, but that it is comparatively WT in its ability to turn over $PI(3,5)P_2$ production after 10 minutes following a hyperosmotic shock (n=2). Combined with *in silico* experiments, this data indicates that Fab1-M238 alleles likely are defective in coordinating PI3P. Additional biochemical experiments are needed to confirm this hypothesis.

Unstructured regions of Fab1 regulate $PI(3,5)P_2$ levels

Classical structure-function experiments investigate the roles of predicted domains on the activity or function of a particular protein polypeptide. While Fab1 contains multiple domains, it also harbors large stretches of predicted unstructured, random-coiled regions. For instance, the region of yeast Fab1 spanning from residue 320 to residue 766 is predicted to have no stable structure (Figure 3.4A) (Drozdetskiy *et al.*, 2015). Intriguingly, eight putative dominant-active Fab1 alleles were isolated from gapped-plasmid screens that harbor mutations only in this unstructured region of Fab1, which strongly indicates that, despite a lack of predicted secondary structure, this polypeptide sequence is important for the activity of the Fab1 lipid kinase.

Three unstructured areas were identified that may harbor putative dominant-active alleles. First, at the extreme N-terminus of yeast Fab1 (residues 1-230), the point mutation Fab1-S81P rescues a *vac7Δ* growth defect, and in a *fab1Δ* strain background generates a fragmented vacuolar phenotype. Both of these results are consistent with an elevation in $PI(3,5)P_2$ levels; however, direct lipid measurements are necessary to

conclusively determine if this is a *bona fide* dominant-active allele. Fab1-S81 is not a previously cited phosphorylation site, nor is it conserved from yeast to humans. Due to the lack of literature on this residue and its lack of conservation we did not focus on characterizing it further.

A second set of putative, dominant-active mutations in unstructured areas of Fab1 can be found between residues 399 and 412 (Figure 3.4A). Four unique single point mutations cluster around a 13-residue patch of unconserved, unstructured amino acids. That the phosphorylatable residue Fab1-S409P is identified within this cluster, and that other mutations are gross mutations that add charge may indicate that Fab1-S409 is a phosphorylated residue and that its mutation or mutations within its surrounding epitope generate dominant-active Fab1 alleles.

The prion-like domain of Fab1 regulates PI(3,5)P_2 levels

A third set of alleles in an unstructured region are found within an unconserved area of Fab1 spanning from residue 456 to residue 607, which was identified in Chapter 2 as a prionogenic-like domain with no known function. Intriguingly, both alleles identified from gapped-plasmid screens in this area harbor a 6-residue or a 7-residue deletion of a 15-residue polyasparagine stretch (Figure 3.4B-C).

Figure 3.4B displays the polypeptide sequence along with the residues deleted in the dominant-active Fab1 alleles Fab1-S52 and Fab1-S79. Together this data indicates that Fab1 has an unstructured, prionogenic domain from residue 456 to residue 607. We

hypothesize that the PrD negatively regulates lipid kinase activity based on vacuolar morphology of PrD deletion mutants.

Fab1 CCT domain mutations alter vacuolar morphology without drastically altering PI(3,5)P_2 levels

Based on the similarity between Fab1 residues 819-1550 and the GroEL chaperonin, the CCT domain was proposed to associate with regulatory proteins (Efe *et al.*, 2005; Michell *et al.*, 2006; Botelho *et al.*, 2008). Indeed, the CCT domain is essential for the interaction of Fab1 with the scaffold protein Vac14 (Jin *et al.*, 2008b). Our gapped plasmid screens identify multiple point mutations, many of which are conserved from yeast to human, that display a fragmented vacuole phenotype and rescue the temperature sensitivity phenotype of the *vac7Δ* yeast strain (Chapter 3 Figure 3A). Indeed, in a *fab1Δ* strain background, compared to WT Fab1, CCT domain point mutations Fab1-E913K, Fab1-K917E, and the double point mutation Fab1-E913K-K917E display a fragmented vacuolar phenotype similar to the known dominant-active mutation Fab1-T2250A. We hypothesized that these putative dominant-active mutations may alter the binding capacity of the CCT domain with the scaffolding protein Vac14. To test this, we performed a yeast two-hybrid assay between the CCT domain and Vac14. We generated point mutations CCT-E913K, CCT-K917E, and CCT-E913K-K917E and assayed if the interaction between the CCT domain and Vac14 was altered. We find no change in the association between the CCT and Vac14 in dominant-active alleles compared to WT Fab1-CCT. This data may indicate that our yeast two-hybrid assay is not sensitive enough to assay differences in the association of this protein-protein

interaction. Alternatively, this data indicates that the fragmented vacuolar phenotype likely does not stem from the only known role of the Fab1 CCT domain—its association with Vac14. This data indicates that the CCT domain may harbor an additional role and that these mutations impact this role.

To more broadly characterize the CCT domain mutations, we sought to measure $PI(3,5)P_2$ levels. Under basal conditions the Fab1 CCT domain mutations K917E and E913K exhibit WT levels of $PI(3,5)P_2$ (Figure 3.5D). However, the double point mutation Fab1-E913K-K917E displays slightly elevated $PI(3,5)P_2$ levels—0.12% of total PI compared to 0.08% in WT cells. We next tested the ability of cells harboring these mutations to respond to a hyper-osmotic shock time course. Interestingly, while under basal conditions CCT domain mutants are able to generate normal levels or slightly elevated levels of $PI(3,5)P_2$, they fail to properly respond to hyperosmotic shock (Figure 3.5E). Mutant CCT domain alleles in a fab1Δ background fail to elevate $PI(3,5)P_2$ levels during a hyperosmotic shock time course and generate roughly half of WT $PI(3,5)P_2$ levels at the 5 minute and 10 minute time points. That CCT domain mutations (1) rescue a *vac7Δ* growth defect (2) display a fragmented vacuolar morphology yet (3) fail to elevate $PI(3,5)P_2$ levels under basal conditions or during hyperosmotic shock indicates additional roles for this domain in the regulation of Fab1 activity, $PI(3,5)P_2$ levels, and vacuole morphology.

Based on the observed data, we hypothesize that the CCT domain interacts directly or indirectly with Atg18. Atg18 is a negative regulator of $PI(3,5)P_2$ synthesis and a positive

regulator of vacuolar fission. An *atg18Δ* strain displays elevated levels of PI(3,5)P_2 and a large, swollen, single vacuole (Efe *et al.*, 2007; Jin *et al.*, 2008a). Moreover, Atg18 contains a WD40 repeat domain—a protein-protein interaction domain—and has been shown to interact with Vac14 (Jin *et al.*, 2008b). Based on this data we hypothesize that Atg18 inhibits Fab1 through association with the CCT domain and that dominant-active mutations in the CCT domain increase this inhibitory interaction. To test this hypothesis yeast two-hybrid assays should be performed as a first test to assay if a physical association between Atg18 and the CCT domain exists. Additionally, *in vitro* binding experiments provide an orthogonal approach to test this hypothesis. If an interaction exists, then dominant-active CCT domain mutations may be generated and tested for their ability to alter this interaction. Together, these experiments offer insights into the role of the CCT domain on the regulation of Fab1, PI(3,5)P_2 levels, and vacuole morphology.

Dominant-active CCR domain mutations are not conserved and occur in both structured and unstructured regions

The CCR domain is a region of unknown function that is critical for Fab1 activity (Botelho *et al.*, 2008). Nineteen dominant-active candidate plasmids were isolated from dominant-active gapped plasmid screens of Fab1. These nineteen candidate plasmids corresponded to fifteen unique alleles that display a fragmented vacuolar phenotype in a *fab1Δ* and that rescue a *vac7Δ* growth defect. Two groups of single CCR domain point mutation alleles were isolated: alleles within the predicted structured area of the CCR domain and alleles C-terminal to the areas of predicted secondary structure

(Figure 3.6A). We may hypothesize that the alleles within the areas of predicted secondary structure alter the domain's conformation and therefore alter Fab1 regulation. For alleles found between residue 1500 (the predicted end of the CCR domain) and residue D1568 (the most C-terminal mutation within this allele set) we may hypothesize two causes of a dominant-active phenotype. (1) That these mutations, despite being within an unstructured area, affect the conformation of either the CCR domain or of the entire Fab1 polypeptide such that it alters the activity of the kinase domain or (2) that these alleles affect a regulatory mechanism directly C-terminal to the CCR domain, such as reversible dephosphorylation.

To test if a regulatory phosphorylation event directly C-terminal to the CCR domain affects Fab1 activity the alleles identified in this screen can be better characterized. As a first assay, *in silico* experiments should be conducted to determine if any residue has previously been identified as phosphorylated. As a second assay, alleles such as P111, which harbors two phosphorylatable residues should be dissected into single mutants and assayed for their ability to fragment vacuoles and rescue *vac7Δ* temperature sensitivity. If the single mutation Fab1-T1553A is dominant-active this strongly suggests that it may be an inhibitory phosphorylation site. To further characterize Fab1-T1553, the non-phosphorylatable mutants Fab1-T1553D/E should be made. We hypothesize that Fab1-T1553A is dominant-active then these alleles should inhibit Fab1 activity. Last, phosphorylation-specific antibodies or mass spectroscopy may be used to determine if Fab1-T1553 is a *bona fide* phosphorylation site.

The generation of dominant-active alleles in predicted Fab1 domains L2 and L3 suggests that these are real, functional elements of Fab1 regulation

Previously our lab identified two additional, predicted domains within Fab1—the Fab1 L2 and Fab1 L3 domains (Jin *et al.*, 2016). However, despite having predicted secondary structure these regions had never been implicated in the regulation of Fab1 activity or $PI(3,5)P_2$ levels. The L2 domain is conserved only among fungi while the L3 domain is conserved among all Fab1. Interestingly, Fab1 gapped plasmid screens identify mutations within both domains.

Gapped plasmid screens identified fourteen unique alleles within the L2 domain of Fab1, which currently has no known function and is not conserved outside of fungi. That dominant-active alleles can be made indicates that this region holds functional value to the regulation of Fab1. Strikingly, all mutant alleles around this area tightly cluster to the predicted areas of secondary structure or slightly C-terminal to this region.

Gapped plasmid screens identified three unique alleles within the Fab1 L3 domain. One allele— Fab1-E1822K has previously been identified in a gapped plasmid screen (Duex *et al.*, 2006), but never before has it been isolated as a single point-mutation. This indicates that the Fab1-E1822K allele is a dominant-active allele by itself. An additional allele Fab1-S1828P was identified from three candidate plasmids (N13, N17, and N287). Moreover, that no other alleles besides Fab1-S1828P and Fab1-E1822K (or a triple mutation containing this mutation) indicates that gapped plasmid screens have likely been exhaustive in the identification of dominant-active alleles within this domain.

Dominant-active alleles in the Fab1 kinase domain reside in two distinct spatial clusters

Several dominant-active Fab1 alleles with multiple point mutations have been previously identified; however, in most cases the causative point mutation(s) were not determined (Duex *et al.*, 2006). The functional consequence of these alleles will be discussed in Chapter Four. In addition to these seven dominant-active Fab1 alleles, we find an additional eight alleles through the use of gapped plasmid screens.

As a first assay to better understand the possible functional consequence of the eight new dominant-active alleles in the kinase domain, we generated a predicted structure of the Fab1 kinase domain using Phyre2.0 secondary structure prediction and mapped the mutated residues onto this structure (Kelley and Sternberg, 2009; Kelley *et al.*, 2015) (Figure 3.9B Red residues). Interestingly, the eight residues share a common surface of the N-lobe of the predicted kinase domain structure surrounding a beta sheet. That these residues cluster to a specific area of the kinase domain indicates that this may be a surface with functional consequence in the regulation of Fab1. Importantly, many of these residues (such as Fab1-F2069 and Fab1-Q2102) are strongly conserved from yeast through humans indicating that their function may also be conserved.

To further assay the consequence of this second surface of the Fab1 kinase domain, more detailed functional characterization of these alleles should be performed. Specifically, $PI(3,5)P_2$ lipid level measurements should be performed both under basal

conditions and during a hyperosmotic shock response within yeast. Additionally, due to the conservation of some residues, the corresponding mutations should be made within a PIKfyve construct and tested for their ability to elevate PI(3,5)P_2 levels compared to WT PIKfyve, which is unable to elevate PI(3,5)P_2 levels in mammalian cells even when overexpressed (McCartney *et al.*, 2014a). These alleles offer additional conserved residues that may be used to study PIKfyve regulation in higher eukaryotes.

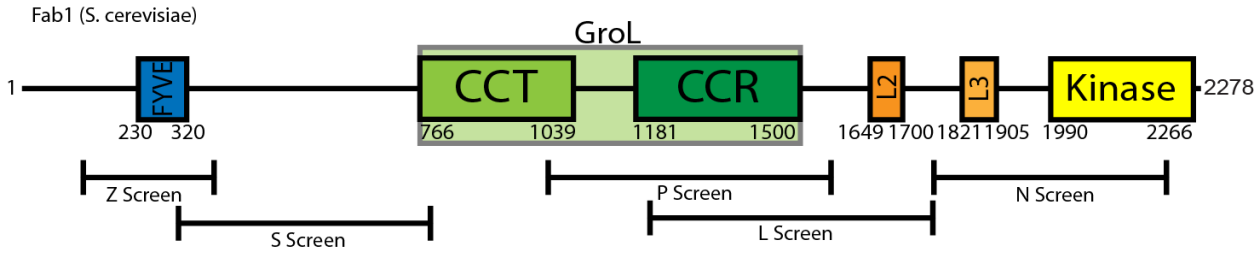

Figure 3.1. Five gapped plasmid screens of Fab1 were performed to generate dominant-active alleles. Screens are named after the first letter of the restriction enzyme used to gap a pRS416-Fab1 plasmid. From left to right: Z screen: Zra1 endonuclease; S screen: Sph1 endonuclease, P-screen: PflM1 endonuclease; L-screen: LpnPI Nru1 endonuclease; N-screen: Nru1 endonuclease.

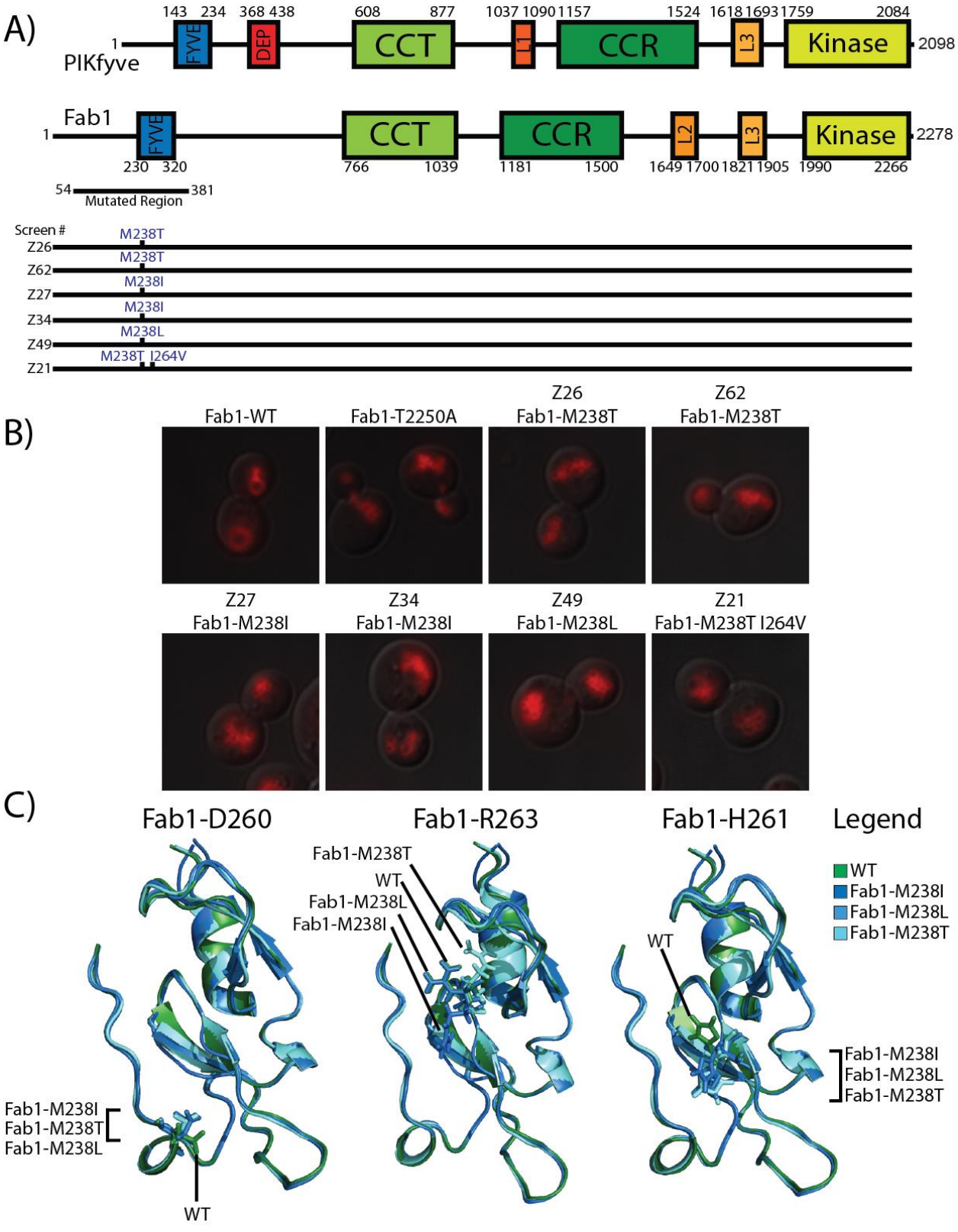
A)
PIKfyve
1
143 234
368 438
608 877
1037 1090 1157
1524 1618 1693 1759 2084
2098
FYVE
DEP
CCT
L1
CCR
L3
Kinase
Fab1
1
230 320
766 1039
1181 1500
1649 1700 1821 1905 1990 2266
2278
FYVE
CCT
CCR
L2
L3
Kinase
54
381
Mutated Region
Screen #
Z26 M238T
Z62 M238T
Z27 M238I
Z34 M238I
Z49 M238L
Z21 M238T I264V
B)
Fab1-WT
Fab1-T2250A
Z26 Fab1-M238T
Z62 Fab1-M238T
Z27 Fab1-M238I
Z34 Fab1-M238I
Z49 Fab1-M238L
Z21 Fab1-M238T I264V
C)
Fab1-D260
Fab1-R263
Fab1-H261
Legend
WT
Fab1-M238I
Fab1-M238L
Fab1-M238T
Fab1-M238T
WT
Fab1-M238L
Fab1-M238I
WT
Fab1-M238I
Fab1-M238T
Fab1-M238L
WT
Fab1-M238I
Fab1-M238L
Fab1-M238T

Figure 3.2. The FYVE domain residue M238 is integral in the regulation of $PI(3,5)P_2$. A) Schematic representation of dominant-active plasmid alleles identified from gapped plasmid screens. Screen # indicates the screen (letter) and candidate plasmid number (number). **B)** Compared to WT Fab1, all FYVE domain mutations fragment yeast vacuoles similar to the dominant-active kinase domain mutation Fab1-T2250A (N=3). **C)** Structural alignment of the yeast Fab1-FYVE domain from WT, M238I, M238T, and M238L FYVE Domains as predicted by I-TASSER. All mutations affect lipid head group coordinating residues Fab1-D260 (far left), Fab1-R263 (middle), and Fab1-H261 (far right) indicating that these mutations likely affect lipid binding of the Fab1-FYVE domain.

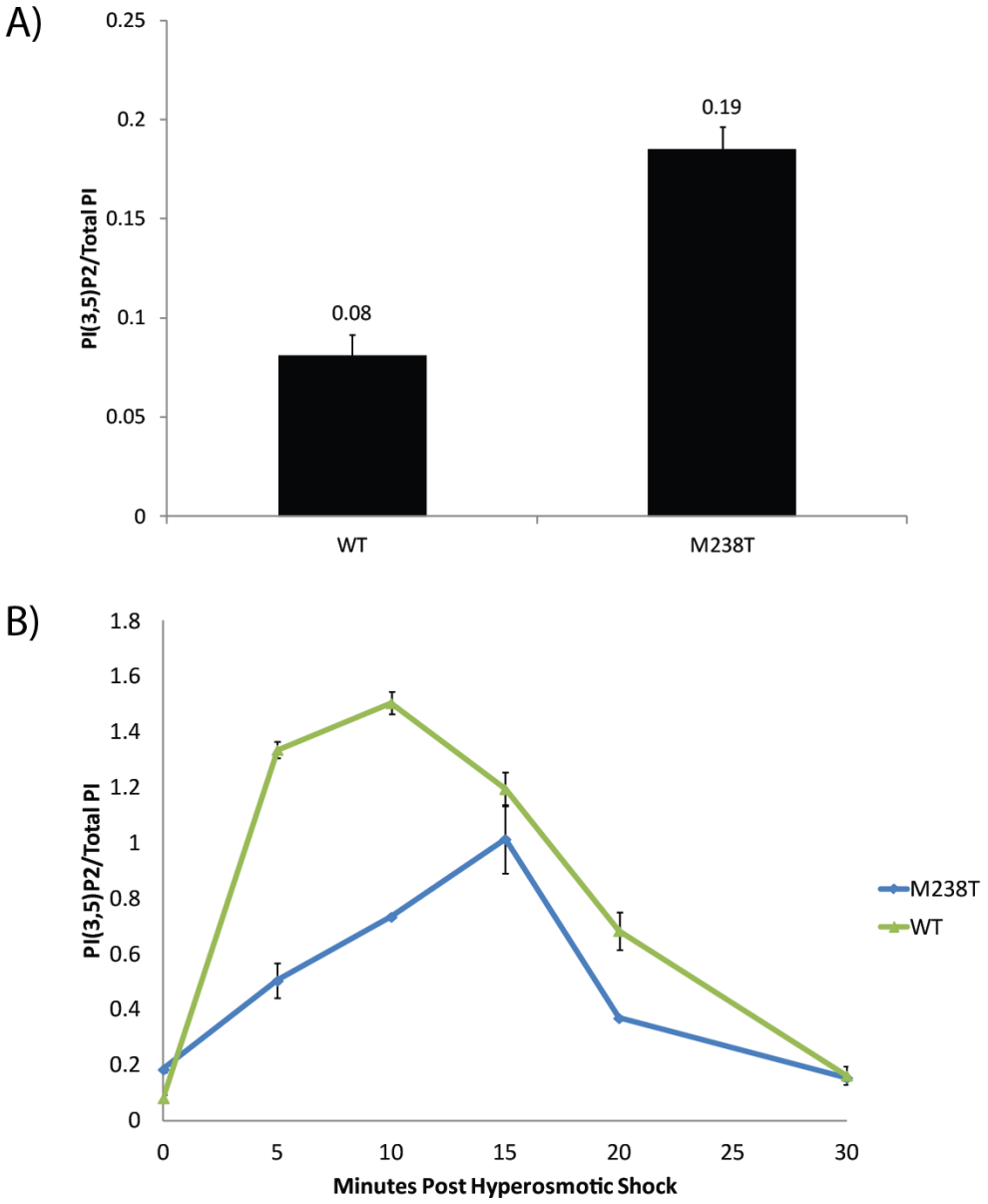

Figure 3.3. The Fab1 FYVE domain mutation M238T misregulates PI(3,5)P_2 levels. **A)** Under basal conditions, Fab1-M238T displays an elevation in PI(3,5)P_2 levels compared to WT (N=2, error bars=SEM). **B)** During stimulus-induced hyperosmotic shock, Fab1-M238T produces more PI(3,5)P_2 than WT Fab1 (minutes 5-15), but turns over PI(3,5)P_2 at rates comparable to WT Fab1 (minutes 15-30) (N=2, error bars=SEM).Together, this data suggests that Fab1-M238T is defective in the synthesis of PI(3,5)P_2 in response to an upstream stimulus possibly through a defect in phospholipid binding.

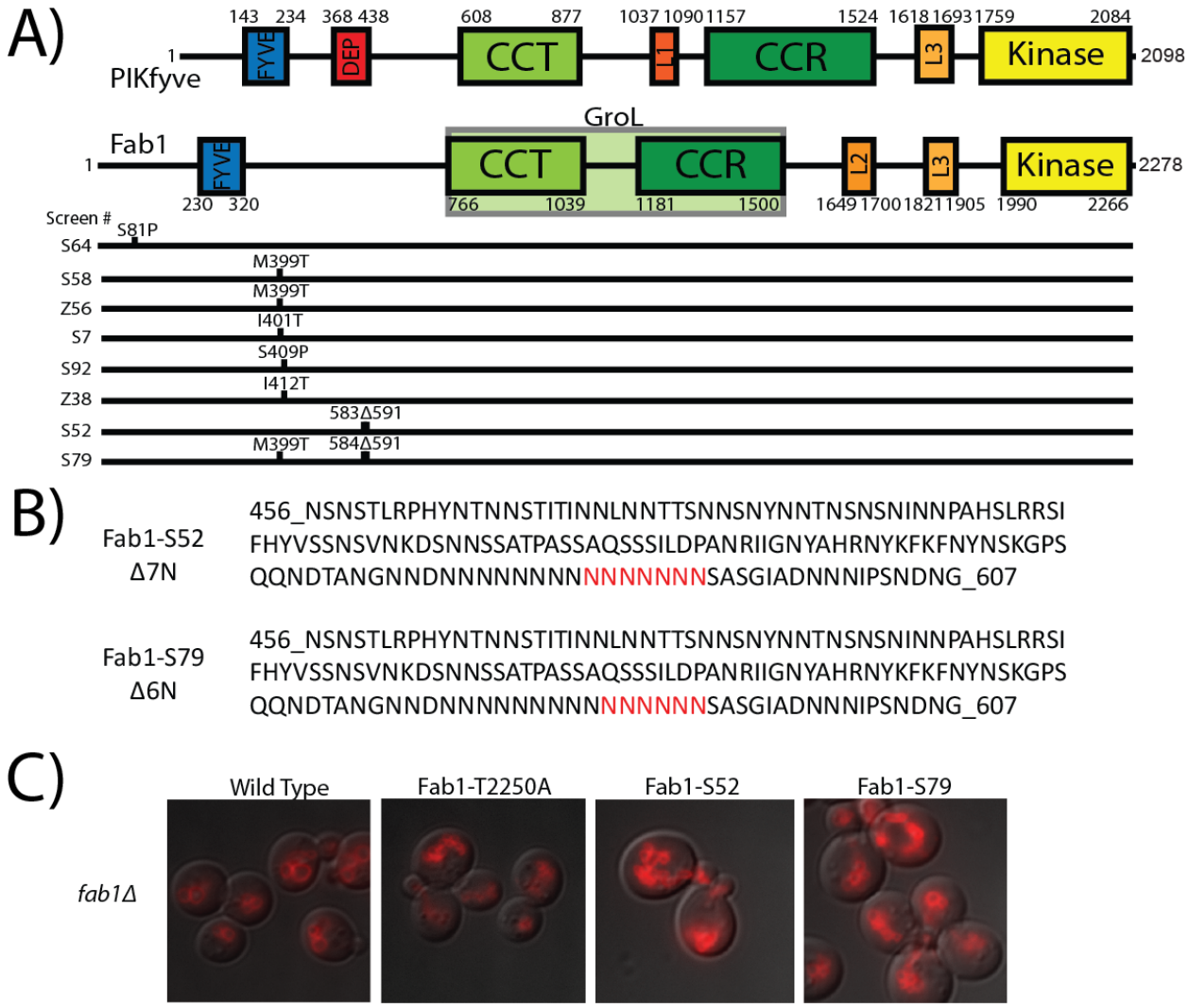

Figure 3.4. Unstructured regions of Fab1 regulate PI(3,5)P_2 levels. A) Schematic representation of dominant-active plasmid alleles identified from gapped plasmid screens. Screen # indicates the screen (letter) and candidate plasmid number (number). **B)** PrD domain (residues 456-607) is shown with multi-residue deletion of seven or six polyasparagines found in Fab1 dominant-active mutant S52 and S79, respectively. **C)** Compared to WT Fab1, both PrD domain mutations fragment yeast vacuoles similar to the dominant-active kinase domain mutation Fab1-T2250A (N=3).

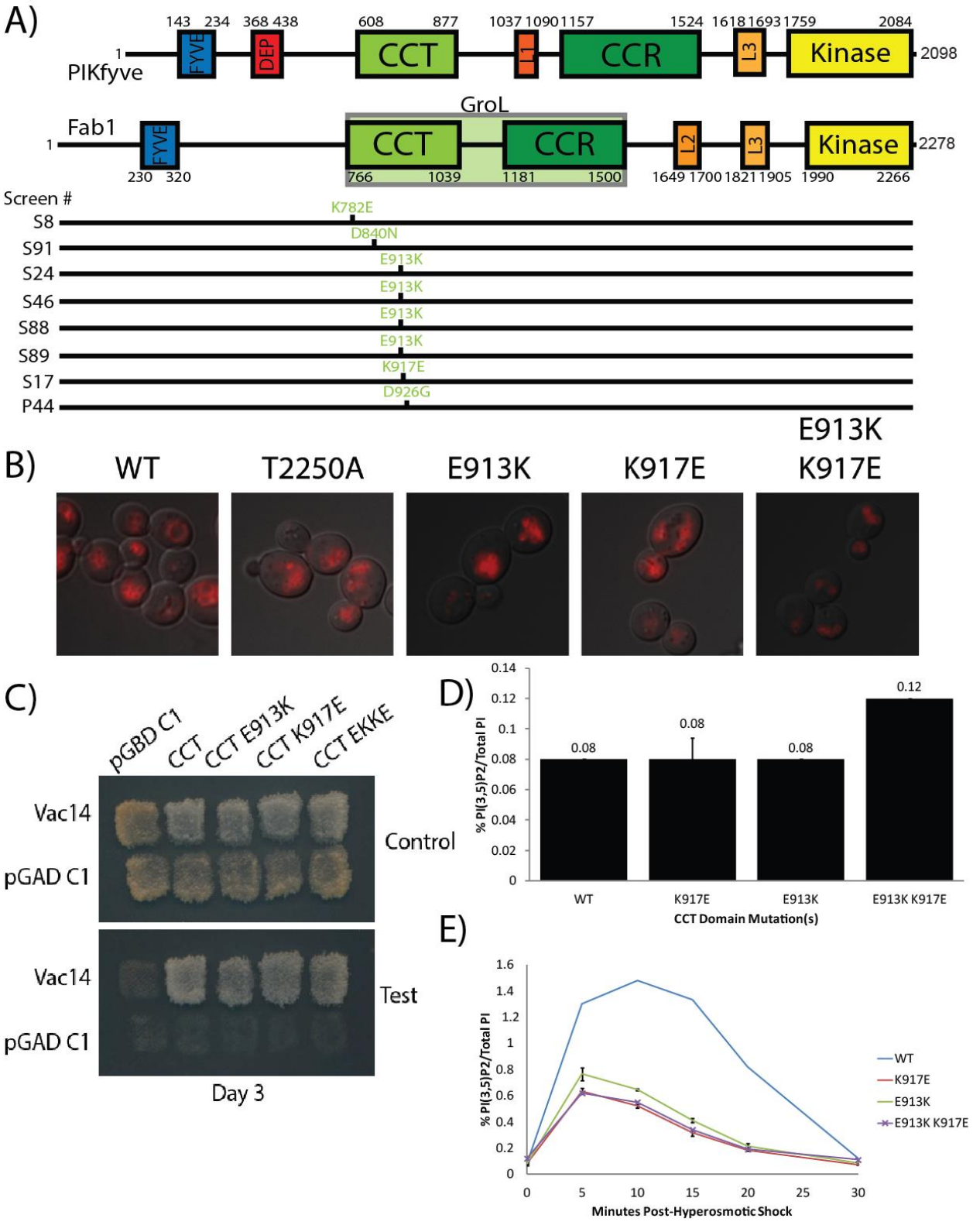
A)
PIKfyve
FYVE
DEP
CCT
L1
CCR
L3
Kinase
Fab1
GroL
L2
Screen #
S8
S91
S24
S46
S88
S89
S17
P44
K782E
D840N
E913K
K917E
D926G
B)
WT
T2250A
E913K
K917E
E913K K917E
C)
pGBD C1
CCT
CCT E913K
CCT K917E
CCT EKKE
Vac14
pGAD C1
Control
Test
Day 3
D)
% PI(3,5)P2/Total PI
CCT Domain Mutation(s)
E)
Minutes Post-Hyperosmotic Shock

Figure 3.5. Fab1 CCT domain mutations have fragmented vacuoles and a defect in the elevation of PI(3,5)P_2 levels during hyperosmotic stress. A) Schematic representation of dominant-active alleles identified from gapped plasmid screens. Screen # indicates the screen (letter) and candidate plasmid number (number). Green residues indicate mutations that lie within the predicted CCT domain (residues 766-1039). **B)** Compared to WT Fab1, the CCT domain mutations Fab1-E917K, Fab1-K917E, and the double mutant Fab1-E913K,K917E fragment yeast vacuoles similar to the dominant-active kinase domain mutation Fab1-T2250A. **C)** For yeast two-hybrid experiments transformants were patched onto SC-LEU-TRP, replica-plated onto SC-LEU-TRP (control) or SC-LEU-TRP-ADE-HIS (test). Yeast two-hybrid assay between the CCT domain and Vac14 indicating that CCT domain mutations do not alter the interaction of this domain with Vac14. Gal4-AD fused with Vac14 with Gal4-BD fused with either the Fab1-CCT domain (residues 538-1085), or this region with one of the following mutations: E913K, K917E, E913K K917E). Cell grown at 24°C for three days (N=6). **D)** Under basal conditions, two single CCT domain mutations (Fab1-E913K and Fab1-K917E) display no elevation in PI(3,5)P_2 levels compared to WT (N=2, error bars=SEM). The double mutation Fab1-E913K,K917E displays an elevation in PI(3,5)P_2 levels compared to WT under basal conditions (N=2, error bars=SEM). **E)** During stimulus-induced hyperosmotic shock, CCT domain mutants produce less PI(3,5)P_2 than WT Fab1 despite having normal basal levels of PI(3,5)P_2 (N=2, error bars=SEM).

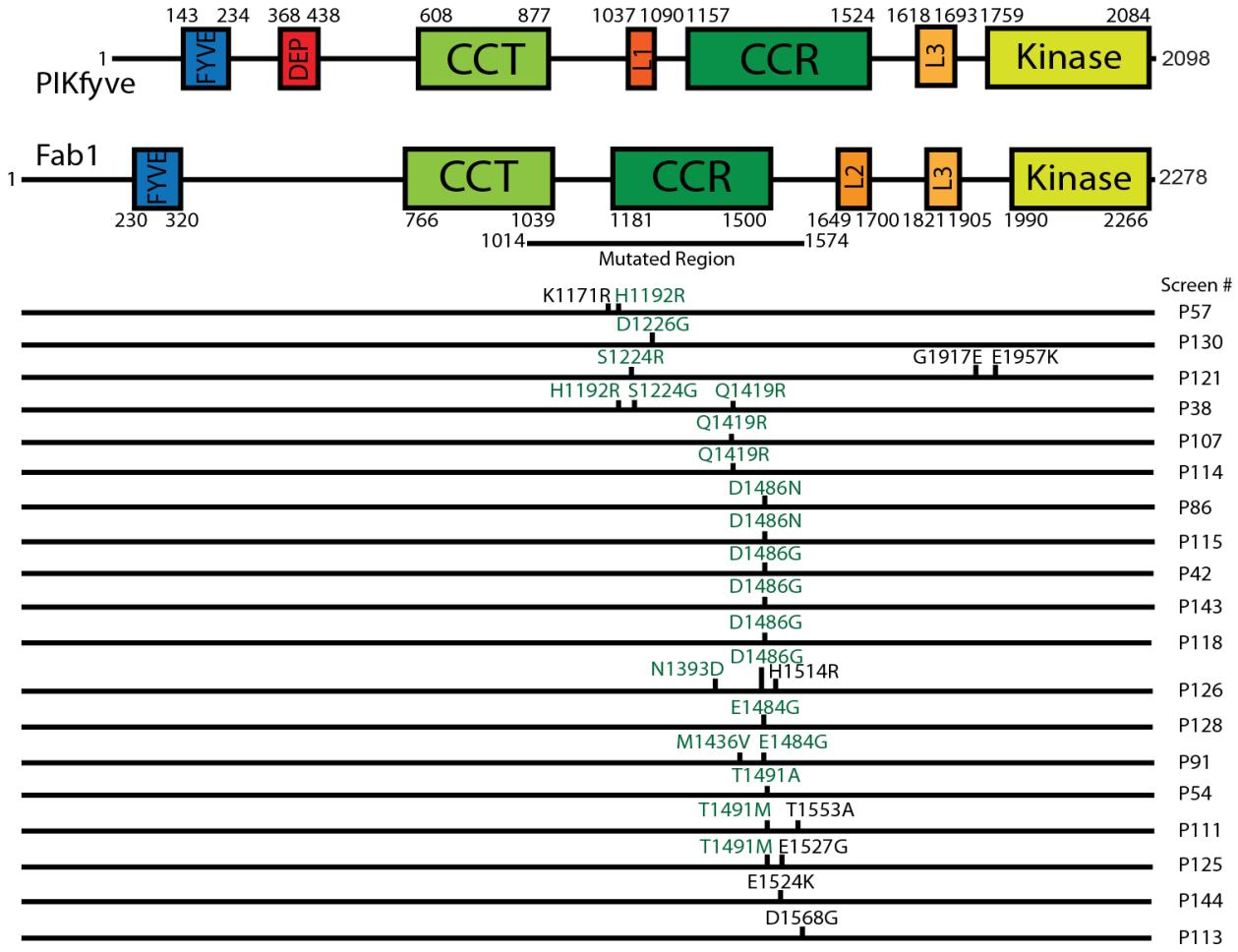

Figure 3.6. Dominant-active CCR domain mutations are not conserved and occur in both structured and unstructured regions. A) Schematic representation of dominant-active alleles identified from gapped plasmid screens. Screen # indicates the screen (letter) and candidate plasmid number (number). Green residues indicate mutations that lie within the predicted CCR domain (residues 1181-1500). Black residues indicate mutations that lie outside of the predicted domain either N- or C-terminally.

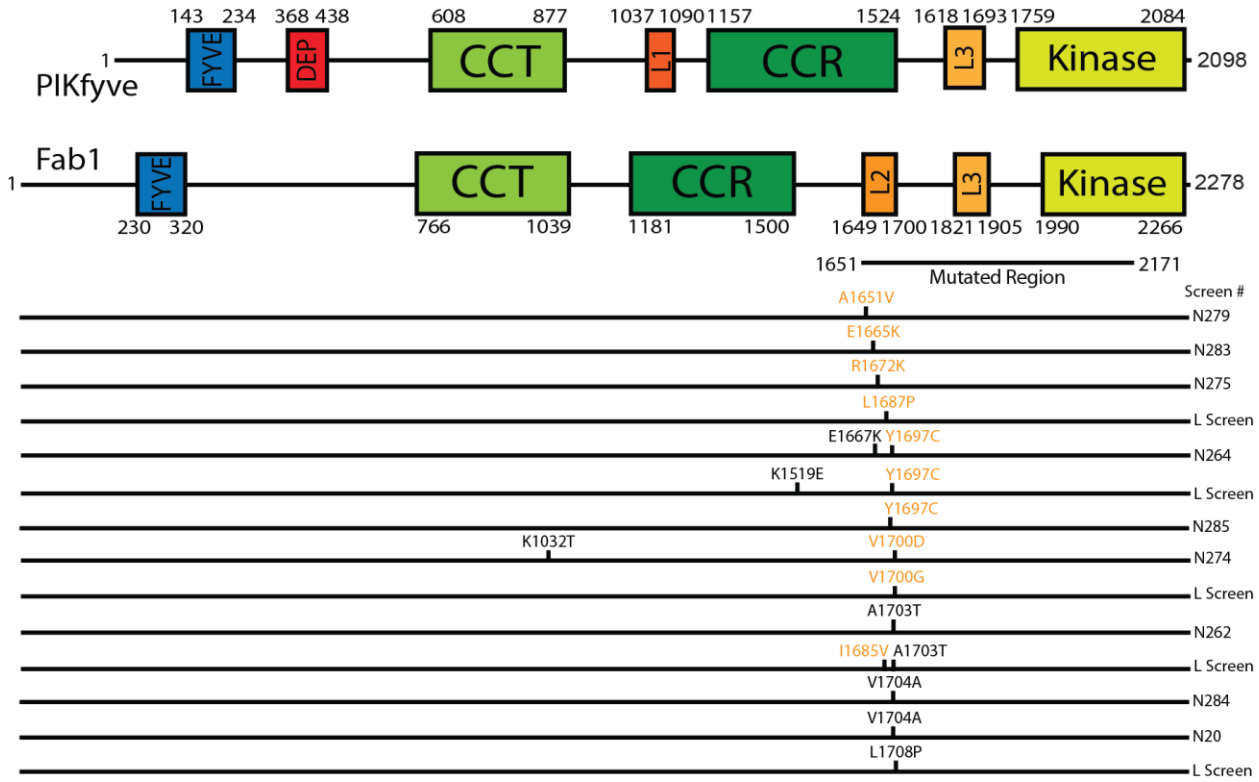

Figure 3.7. Gapped plasmid screens identified 14 unique alleles within the L2 domain of Fab1. A) Schematic representation of dominant-active alleles identified from gapped plasmid screens. Screen # indicates the screen (letter) and candidate plasmid number (number). Yellow residues indicate mutations that lie within the predicted L2 domain (residues 1649-1700). Black residues indicate mutations that lie outside of this predicted domain. That dominant-active mutations lie slightly outside of the C-terminus of the L2 domain may indicate that the domain is larger than predicted.

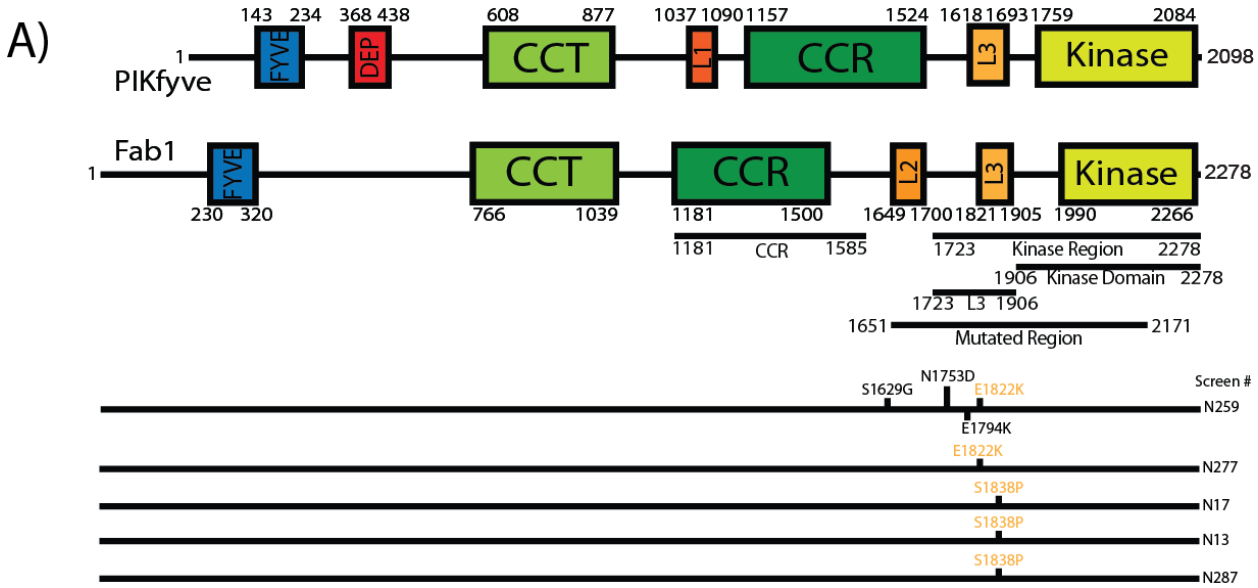

Figure 3.8. Gapped plasmid screens identified three unique alleles within the Fab1 L3 domain. A) Schematic representation of dominant-active plasmid identified from gapped plasmid screens. Screen # indicates the screen (letter) and candidate plasmid number (number). Yellow residues indicate mutations that lie within the predicted L3 domain (Residues 1821-1905). Black residues indicate mutations that lie outside of this predicted domain.

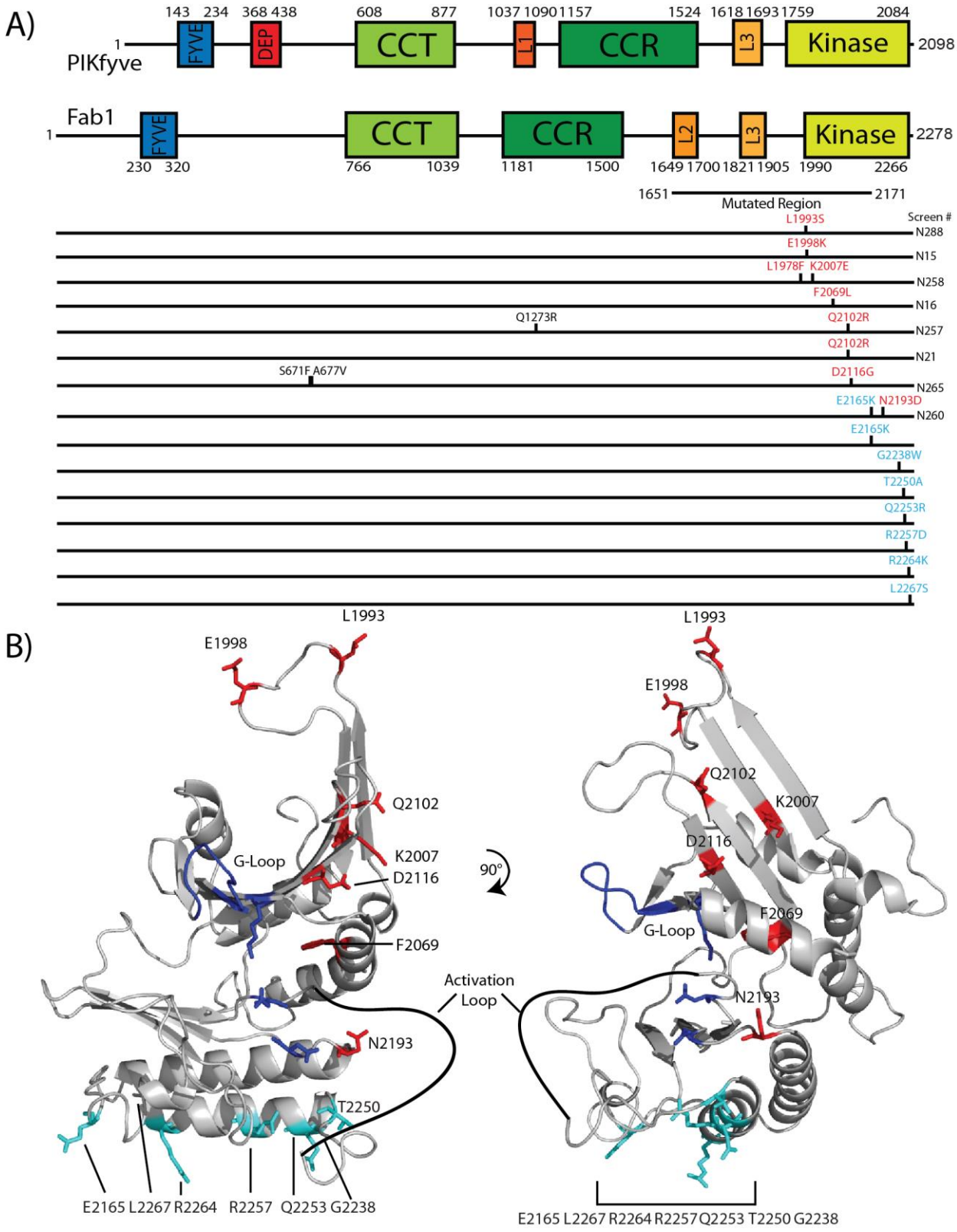
A)
PIKfyve
1
143 234
368 438
608 877
1037 1090 1157
1524 1618 1693 1759
2084
2098
FYVE
DEP
CCT
L1
CCR
L3
Kinase
Fab1
1
230 320
766 1039
1181 1500
1649 1700 1821 1905
1990 2266
2278
FYVE
CCT
CCR
L2
L3
Kinase
1651
2171
Mutated Region
Screen #
L1993S
N288
E1998K
N15
L1978F K2007E
N258
F2069L
N16
Q1273R
Q2102R
N257
Q2102R
N21
S671F A677V
D2116G
N265
E2165K N2193D
N260
E2165K
G2238W
T2250A
Q2253R
R2257D
R2264K
L2267S
B)
L1993
E1998
Q2102
K2007
D2116
G-Loop
F2069
N2193
T2250
Activation Loop
90°
E2165 L2267 R2264 R2257 Q2253 G2238
L1993
E1998
Q2102
K2007
D2116
F2069
G-Loop
N2193
E2165 L2267 R2264 R2257 Q2253 T2250 G2238

Figure 3.9. Dominant-active alleles in the Fab1 kinase domain reside in two distinct spatial clusters. A) Schematic representation of dominant-active alleles identified from gapped plasmid screens. Screen # indicates the screen (letter) and candidate plasmid number (number). Red and blue represent likely distinct dominant-active mutation clusters. Blue cluster mutations are discussed in Chapter 4. **B)** I-TASSER structure prediction of the Fab1 kinase domain. Red residues cluster to a solvent-exposed beta sheet on the N-lobe of the kinase domain proximal to the G-loop, which is required for ATP coordination. Blue residues are clustered near or on a solvent-exposed alpha helix discussed in Chapter 4.

Bibliography

Aylon, Y., and Kupiec, M. (2004). DSB repair: the yeast paradigm. DNA Repair (Amst) *3*, 797-815.
Botelho, R.J., Efe, J.A., Teis, D., and Emr, S.D. (2008). Assembly of a Fab1 phosphoinositide kinase signaling complex requires the Fig4 phosphoinositide phosphatase. Mol Biol Cell *19*, 4273-4286.
Chung, W.H., Zhu, Z., Papusha, A., Malkova, A., and Ira, G. (2010). Defective resection at DNA double-strand breaks leads to de novo telomere formation and enhances gene targeting. PLoS Genet *6*, e1000948.
Drozdetskiy, A., Cole, C., Procter, J., and Barton, G.J. (2015). JPred4: a protein secondary structure prediction server. Nucleic Acids Res *43*, W389-394.
Duex, J.E., Tang, F., and Weisman, L.S. (2006). The Vac14p-Fig4p complex acts independently of Vac7p and couples PI3,5P2 synthesis and turnover. The Journal of cell biology *172*, 693-704.
Efe, J.A., Botelho, R.J., and Emr, S.D. (2005). The Fab1 phosphatidylinositol kinase pathway in the regulation of vacuole morphology. Curr Opin Cell Biol *17*, 402-408.
Efe, J.A., Botelho, R.J., and Emr, S.D. (2007). Atg18 regulates organelle morphology and Fab1 kinase activity independent of its membrane recruitment by phosphatidylinositol 3,5-bisphosphate. Mol Biol Cell *18*, 4232-4244.
Gary, J.D., Sato, T.K., Stefan, C.J., Bonangelino, C.J., Weisman, L.S., and Emr, S.D. (2002). Regulation of Fab1 phosphatidylinositol 3-phosphate 5-kinase pathway by Vac7 protein and Fig4, a polyphosphoinositide phosphatase family member. Molecular biology of the cell *13*, 1238-1251.
Jin, N., Chow, C.Y., Liu, L., Zolov, S.N., Bronson, R., Davisson, M., Petersen, J.L., Zhang, Y., Park, S., Duex, J.E., Goldowitz, D., Meisler, M.H., and Weisman, L.S. (2008a). VAC14 nucleates a protein complex essential for the acute interconversion of PI3P and PI(3,5)P(2) in yeast and mouse. EMBO J *27*, 3221-3234.
Jin, N., Chow, C.Y., Liu, L., Zolov, S.N., Bronson, R., Davisson, M., Petersen, J.L., Zhang, Y., Park, S., Duex, J.E., Goldowitz, D., Meisler, M.H., and Weisman, L.S. (2008b). VAC14 nucleates a protein complex essential for the acute interconversion of PI3P and PI(3,5)P(2) in yeast and mouse. The EMBO journal *27*, 3221-3234.
Jin, N., Lang, M.J., and Weisman, L.S. (2016). Phosphatidylinositol 3,5-bisphosphate: regulation of cellular events in space and time. Biochem Soc Trans *44*, 177-184.
Jin, N., Mao, K., Jin, Y., Tevzadze, G., Kauffman, E.J., Park, S., Bridges, D., Loewith, R., Saltiel, A.R., Klionsky, D.J., and Weisman, L.S. (2014). Roles for PI(3,5)P2 in nutrient sensing through TORC1. (in revision).
Kelley, L.A., Mezulis, S., Yates, C.M., Wass, M.N., and Sternberg, M.J. (2015). The Phyre2 web portal for protein modeling, prediction and analysis. Nat Protoc *10*, 845-858.
Kelley, L.A., and Sternberg, M.J. (2009). Protein structure prediction on the Web: a case study using the Phyre server. Nat Protoc *4*, 363-371.
Li, S.C., Diakov, T.T., Xu, T., Weisman, L.S., Couoh-Cardel, S., Wilkens, S., and Kane, P.M. (2014). The signaling lipid PI(3,5)P2 stabilizes V1-Vo sector interactions and activates the vacuolar H+-translocating ATPase. . Molecular biology of the cell *(in revision)*.
McCartney, A.J., Zolov, S.N., Kauffman, E.J., Zhang, Y., Strunk, B.S., Weisman, L.S., and Sutton, M.A. (2014a). Activity-dependent PI(3,5)P2 synthesis controls AMPA receptor trafficking during synaptic depression. Proc Natl Acad Sci U S A *111*, E4896-4905.
McCartney, A.J., Zolov, S.N., Kauffman, E.J., Zhang, Y., Sutton, M.A., and Weisman, L.S. (2014b). Functional consequences of activity-dependent changes in PI(3,5)P2 in neurons. to be submitted.
Michell, R.H., Heath, V.L., Lemmon, M.A., and Dove, S.K. (2006). Phosphatidylinositol 3,5-bisphosphate: metabolism and cellular functions. Trends in biochemical sciences *31*, 52-63.

Stenmark, H., Aasland, R., and Driscoll, P.C. (2002). The phosphatidylinositol 3-phosphate-binding FYVE finger. FEBS Lett *513*, 77-84.
Sugawara, N., Wang, X., and Haber, J.E. (2003). In vivo roles of Rad52, Rad54, and Rad55 proteins in Rad51-mediated recombination. Mol Cell *12*, 209-219.

CHAPTER 4:

AN INTRAMOLECULAR INTERACTION WITHIN THE LIPID KINASE FAB1 REGULATES CELLULAR PHOSPHATIDYLINOSITOL 3,5-BISPHOSPHATE LIPID LEVELS[3]

Dominant-active mutations in the Fab1 kinase domain reveal a potential regulatory region

Several dominant-active Fab1 alleles with multiple point mutations have been identified; however, in most cases the causative point mutation(s) were not determined (Duex *et al.*, 2006b). Notably, ten of eleven alleles harbor at least one mutation at the C-terminal end of the kinase domain (Figure 4.1A, yellow), suggesting that this region may be critical for the regulation of Fab1 (Duex *et al.*, 2006b). We generated a model of the kinase domain using the Phyre 2.0 protein structure modeling program (Figure 4.1B) (Kelley *et al.*, 2015). Intriguingly, the C-terminal mutations cluster on a single surface of the predicted kinase domain. This surface is C-terminal to the activation loop. Within this surface, three of the residues—T2250, Q2253, and R2264—all reside on a predicted, solvent-exposed alpha helix (Figure 4.1B).

[3] This chapter is under review as a research article: Lang MJ, Azad A, Strunk BS, Petersen J, Weisman LS. 2016. An intramolecular interaction within the lipid kinase Fab1 regulates cellular phosphatidylinositol 3,5-bisphosphate lipid levels. MBoC (under review).

To test whether mutation of single residues on the predicted kinase domain surface results in dominant-active Fab1 alleles, we generated six single point mutations (Figure 4.2A). Vacuolar size is generally inversely correlated with $PI(3,5)P_2$ levels. For most cases fragmented vacuoles are indicative of elevated $PI(3,5)P_2$ levels, while mutations that negatively affect $PI(3,5)P_2$ levels lead to enlarged vacuoles. Each of the six point mutants exhibited fragmented vacuoles suggesting that each has elevated levels of $PI(3,5)P_2$. (Figure 4.2A). These results provide support for the hypothesis that the predicted surface of the kinase domain functions in the regulation of Fab1.

Based on the observation that most of these mutations cluster to on the surface of an alpha helix, we hypothesized that other residues on this helix may also be critical to the regulation of Fab1. We chose R2257, which is conserved among Fab1 homologues, and is predicted to be surface-exposed (Figure 4.6). We generated and tested the charge reversal mutation Fab1-R2257D and found that it also results in a dominant-active Fab1 allele and causes a fragmented vacuolar phenotype indicative of an elevation in $PI(3,5)P_2$ levels (Figure 4.2A).

As a second test, we directly measured $PI(3,5)P_2$ levels of two alleles—Fab1-R2257D and Fab1-T2250A. In yeast $PI(3,5)P_2$ levels transiently change in response to specific

stimuli. A prolonged single stimulus, introduction of yeast into hyperosmotic media, causes a transient elevation of $PI(3,5)P_2$ (Dove *et al.*, 1997). Within 5 minutes, $PI(3,5)P_2$ levels rise over 15-fold, plateau for 10 minutes, then precipitously return to basal levels (Duex *et al.*, 2006a). Under basal conditions, both Fab1-T2250A and Fab1-R2257D display elevated $PI(3,5)P_2$ levels compared to wild type (WT) (Figure 4.2C). Additionally, in response to a hyperosmotic stimulus, both mutants elevate $PI(3,5)P_2$ levels higher and continue to display elevated levels at the 30-minute time point compared to WT (Figure 4.2D). These results indicate that the C-terminal portion of the kinase domain acts in part to control both basal levels of $PI(3,5)P_2$ as well as the production of $PI(3,5)P_2$ in response to an extracellular stimulus. Importantly, this arginine is conserved among all type I and type II phosphatidylinositol phosphate kinases (PIPKs) (Rao *et al.*, 1998; Kunz *et al.*, 2000). This suggests that a similar mechanism may exist in other PIPKs.

The dominant-active mutations in the kinase region impair an interaction with the Fab1 CCR domain

We hypothesized that these dominant-active mutations disrupt a protein-protein interaction that modulates the kinase activity of Fab1. As an initial test we assayed the ability of the kinase domain to interact with other members of the Fab1 complex using the yeast two-hybrid (Y2H) test. The kinase region (residues 1723-2278, black line Figure 1A) does not interact with full-length Vac14, Fig4, Vac7, or Atg18 (Figure 4.3A). In addition, we tested whether the kinase region interacts with other domains within Fab1. Importantly, by day 4 of the assay, we find that the kinase region interacts with

Fab1$^{1181-1585}$, which includes the CCR domain, a region of unknown function that is critical for Fab1 activity (Botelho *et al.*, 2008). Additionally, by day 12 we see a very slight interaction of the kinase region with a much larger Y2H construct (Fab1$^{538-1917}$), which includes the CCT domain, the CCR domain, and the L2 and L3 domains (Figure 4.3C). That this interaction is less strong than the CCR domain alone is likely due to the large size of the construct. Note that this same construct, which includes the CCT domain, a known binding region for Vac14, shows even less interaction with Vac14. The CCT domain (Fab1$^{538-1085}$), and the L2 and L3 domains (Fab1$^{1373-1917}$) do not interact with the kinase region. Together, these results suggest that the CCR domain interacts with the kinase region of Fab1. In addition, we tested the ability of the Fab1 CCR domain (Fab1$^{1181-1585}$) to interact with Vac14, Fig4, Vac7, or Atg18 by the yeast two-hybrid assay (Figure 4.3B). The CCR domain does not interact with other known proteins within the Fab1 complex indicating that the CCR domain and the kinase region interact with each other but likely do not interact with other known regulators of Fab1.

We tested the ability of dominant-active kinase domain mutations to affect the interaction of the CCR domain with the kinase region. Notably, in a Y2H assay we find that all kinase domain mutations tested ablate its interaction with the CCR domain (Figure 4.3D). That dominant-active mutations ablate the interaction between the CCR domain and kinase region indicates that the CCR domain may inhibit Fab1 kinase activity.

The interaction of the CCR domain with the kinase region may either be intramolecular or between two Fab1 molecules. Fab1, Vac14, and Fig4 are each required for formation of a functional Fab1 complex. To test whether more than one Fab1 protein is present in each complex, we expressed Fab1-TAP and Fig4-Myc in *fig4Δ* mutant yeast harboring a Fab1-3xGFP genomic integrant and performed pull-down assays of TAP-tagged Fab1. Fab1-TAP pulls down Fig4-Myc indicating that the complex is intact; however, Fab1-TAP does not co-immunoprecipitate Fab1-3xGFP (Figure 4.3E). These findings are in agreement with previous reports that Fab1 does not dimerize and that only one Fab1 is present in each Fab1 complex (Bothelo 2008, Alghamdi 2013). Thus, this interaction is likely to be intramolecular.

To further test an interaction between the CCR domain and kinase region, we performed *in vitro* pulldown experiments with recombinant proteins. We co-expressed the CCR domain and kinase region as protein fusion constructs in *E. coli*. Due to the instability of multiple *Saccharomyces cerevisiae* (*S. cerevisiae)* Fab1 constructs tested, we used the thermophilic fungus *Chaetomium thermophilum*. Recombinant proteins from this organism are often more stable (Amlacher *et al.*, 2011; Baker *et al.*, 2015). *C. thermophilium* Fab1 has a similar domain architecture to both *S. cerevisiae* and *Homo sapiens* (*H. sapiens)* Fab1 and PIKfyve, respectively (Figure 4.4A). Based on the LALIGN sequence identity and similarity program (Huang and Miller, 1991) the CCR domains of *C. thermophilium* and *S. cerevisiae* Fab1 share 33.7% identity and 66.6% similarity, and the kinase region shares 46.8% identity and 73.9% similarity. Importantly, *S. cerevisiae* residues T2250 and R2257 are conserved in *C. thermophilium* as residues

S2509 and R2516, respectively. We generated MBP and GST fusion proteins with the CCR domain and also with the kinase region (Figure 4.4A). Expression of either construct with either tag yielded no soluble protein (data not shown); however, when co-expressed in *E. coli* the CCR domain with the kinase region yield stable proteins. Purification on amylose resin and then glutathione resin results in a final elution containing proteins of the expected predicted molecular weight (Figure 4.4B). Western blot analysis confirmed that the Coomassie band at 89.5kDa is the HIS-MBP-kinase region; the band at 75kDa is the GST-CCR domain (predicted molecular weight: 80.5kDa). Similar to the Y2H assays, the HIS-MBP-kinase region co-purifies with the GST-CCR domain (Figure 4.4B). Importantly, kinase domain mutations S2509A and R2516D reduce the *in vitro* affinity of the CCR domain and kinase region (Figure 4.4C). By the final purification WT CCR and kinase regions co-purify while the kinase domain carrying either mutation is unstable, likely due to dissociation of the complex. This assay demonstrates that the CCR domain and the kinase region of *C. thermophilium* Fab1 interact in an *in vitro* assay and that dominant-active kinase domain mutations reduce this interaction.

Dominant-active mutations in the CCR domain do not alter the interaction between the CCR domain and kinase region

That dominant-active mutations in the C-terminal portion of the kinase domain of Fab1 ablate its interaction with the CCR domain suggests the simple hypothesis that dominant-active mutations within the CCR domain would similarly impair the interaction

of the CCR domain with the kinase region. We performed random mutagenesis of the CCR domain and screened for dominant-active alleles of Fab1 with mutations in the CCR domain (Figure 4.8). Twenty-one mutant plasmids were isolated, which, when expressed in WT or *fab1Δ* cells, displayed a fragmented vacuolar phenotype. These mutants represent seven unique alleles of which only two contain multiple point mutations (Figure 4.1A, green). All seven alleles display a fragmented vacuolar phenotype indicative of elevated $PI(3,5)P_2$ levels (Figure 4.5A). We focused on three single-point mutations (Fab1-Q1419R, Fab1-D1486N, and Fab1-T1491A) and directly measured $PI(3,5)P_2$ levels. Compared to WT, both under basal conditions and during hyperosmotic shock all three mutants display elevated levels of $PI(3,5)P_2$ that are similar to the kinase domain mutation Fab1-T2250A (Figure 4.5C-D). These observations suggest that all four mutants disrupt the same regulatory mechanism. However, as measured by the Y2H assay, none of these CCR domain mutations or the other CCR domain mutations block the interaction of the CCR domain with the kinase region (Figure 4.5E). Note that K1171 lies outside of the Y2H CCR domain construct and was not tested. That these dominant-active CCR domain mutants do not dissociate the domain from the kinase region, suggests additional possible roles for the CCR domain in the regulation of $PI(3,5)P_2$ levels. Alternatively, the Y2H assay may not be sufficiently sensitive to detect differences in their interactions. Together, these studies suggest a model in which the Fab1 CCR domain and the C-terminal kinase domain region regulate $PI(3,5)P_2$ levels in a similar pathway and that the Fab1 CCR domain may play an additional regulatory role.

Structure-function studies that rely on loss-of-function mutants are often difficult to interpret because these mutations often impair protein folding or stability. These studies show that the generation and characterization of dominant-active mutations provide an effective approach to determine the function of specific protein domains. Through the characterization of dominant-active Fab1 alleles: (1) we identify a regulatory region on the putative surface of the C-terminal Fab1 kinase domain, which contains regulatory residues conserved among Fab1 proteins (2) we define an intramolecular interaction between this surface of the kinase domain and the upstream CCR domain (Figure 4.5F). Analogous genetic approaches with other genes that encode large proteins may be similarly informative. For instance, other proteins within the lipid kinase family such as Stt4 and Pik1 have several domains of unknown function (Foti *et al.*, 2001; Audhya and Emr, 2002; Strahl and Thorner, 2007; Baird *et al.*, 2008). If dominant-active alleles could be generated this would suggest that negative regulation occurs. Moreover, this type of mutant screen has the potential to reveal residues that are critical to the negative regulation of these kinases.

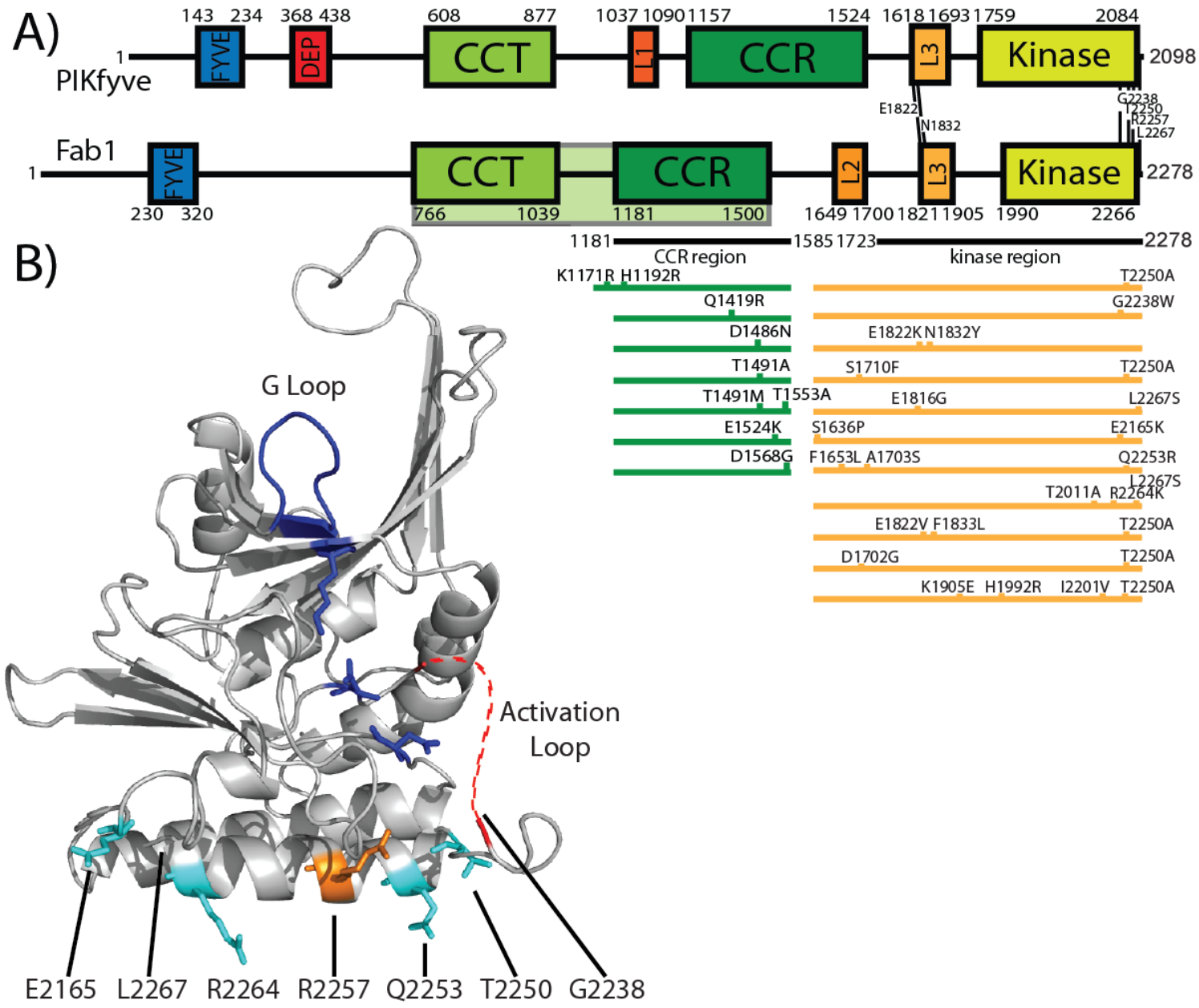
A)
PIKfyve
1
143 234
368 438
608 877
1037 1090 1157
1524
1618 1693 1759
2084
2098
FYVE
DEP
CCT
L1
CCR
L3
Kinase
E1822
N1832
G2238
T2250
R2257
L2267
Fab1
1
2278
FYVE
CCT
CCR
L2
L3
Kinase
230 320
766 1039
1181 1500
1649 1700 1821 1905
1990 2266
B)
1181
1585 1723
2278
CCR region
kinase region
K1171R H1192R
Q1419R
D1486N
T1491A
T1491M T1553A
E1524K
D1568G
T2250A
G2238W
E1822K N1832Y
S1710F
T2250A
E1816G
L2267S
S1636P
E2165K
F1653L A1703S
Q2253R
L2267S
T2011A R2264K
E1822V F1833L
T2250A
D1702G
T2250A
K1905E H1992R I2201V T2250A
G Loop
Activation Loop
E2165 L2267 R2264 R2257 Q2253 T2250 G2238

Figure 4.1. Mutations in the kinase and CCR domains result in dominant-active Fab1 alleles. **A)** Domain architecture of Fab1/PIKfyve indicating dominant-active alleles. Amino acid substitutions (yellow and green lines) indicate these alleles. Dominant-active mutations conserved between yeast Fab1 and mammalian PIKfyve indicated with contiguous lines between the two schematics. The CCR region and kinase region (black lines below schematic) correspond to yeast two-hybrid constructs. **B)** Mapping putative causative dominant-active mutations onto a predicted structure of the kinase domain suggests a surface critical for the regulation of Fab1. Structure prediction, using Phyre2 (Kelley *et al.*, 2015), based on the kinase domain of PIPKIIβ (Rao *et al.*, 1998). Most of the mutations (cyan) map to a surface of a predicted alpha helix proximal to the activation loop. Surface residue R2257 predicted to be part of the regulation of kinase activity and tested in Figure 2A-C, (orange). Residues G2238 and L2267 are outside of the predicted structure; approximate positions are indicated.

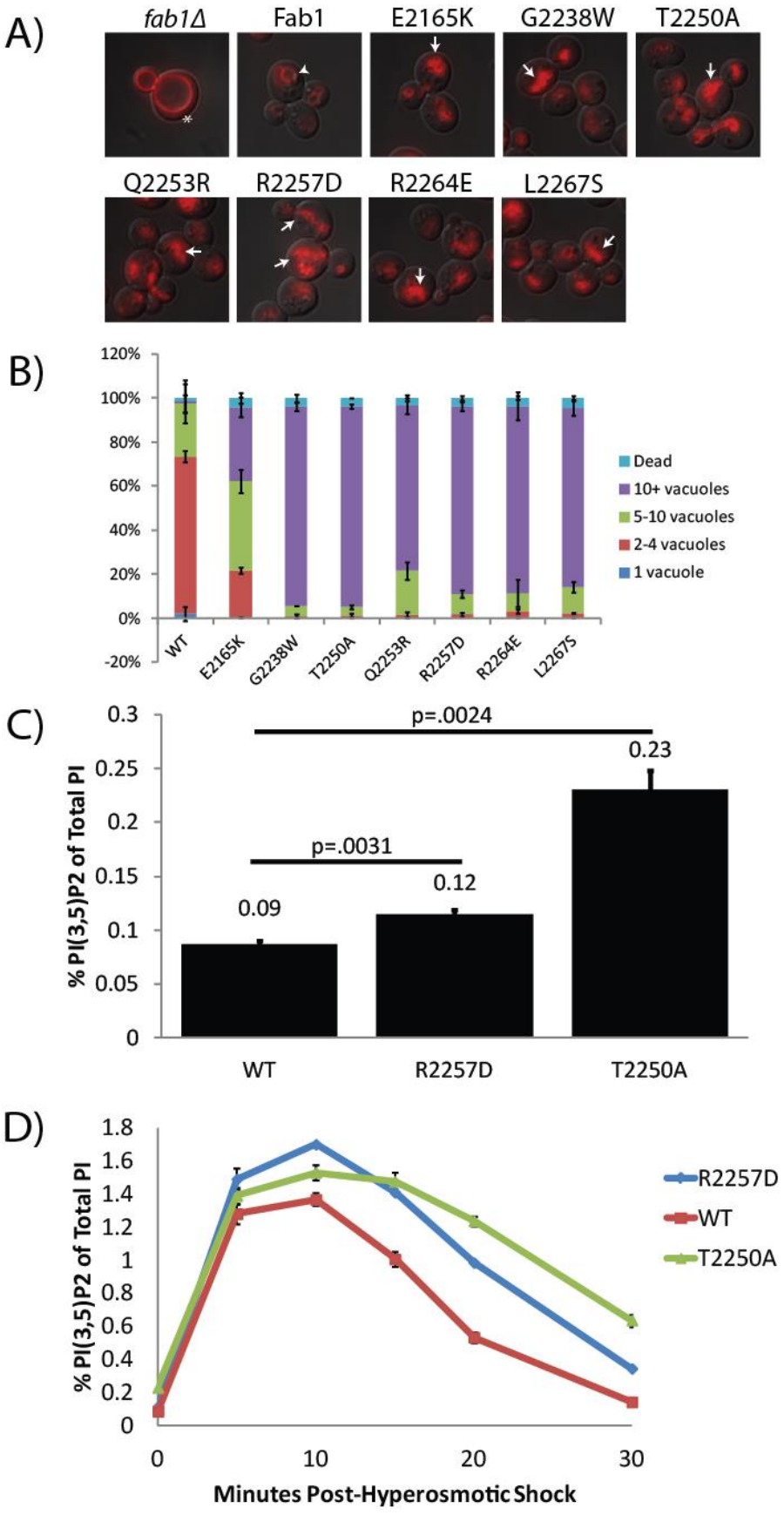
A)
fab1Δ
Fab1
E2165K
G2238W
T2250A
Q2253R
R2257D
R2264E
L2267S
B)
120%
100%
80%
60%
40%
20%
0%
-20%
WT
E2165K
G2238W
T2250A
Q2253R
R2257D
R2264E
L2267S
Dead
10+ vacuoles
5-10 vacuoles
2-4 vacuoles
1 vacuole
C)
% PI(3,5)P2 of Total PI
0.3
0.25
0.2
0.15
0.1
0.05
0
p=.0024
0.23
p=.0031
0.12
0.09
WT
R2257D
T2250A
D)
% PI(3,5)P2 of Total PI
1.8
1.6
1.4
1.2
1
0.8
0.6
0.4
0.2
0
0
10
20
30
Minutes Post-Hyperosmotic Shock
R2257D
WT
T2250A

Figure 4.2. Mutations of the C-terminal kinase domain result in dominant-active Fab1. A) Single point mutations show a fragmented vacuole phenotype (arrows) indicative of elevated PI(3,5)P_2 levels compared to WT Fab1 (arrowhead). The enlarged vacuole in *fab1Δ* (asterisk) is characteristic of reduced PI(3,5)P_2 levels. Vacuoles labeled with the lipophilic dye FM4-64 (red) (N=3). **B)** Quantification of vacuolar morphology of cells expressing Fab1 or the indicated kinase domain dominant-active allele. Dead cells scored if cell was ruptured or if FM4-64 filled cytoplasm (N=3, >100 cells per experiment, error bars=SEM). **C)** Under basal conditions, Fab1^{T2250A} and Fab1^{R2257D} produce elevated levels of PI(3,5)P_2. (N=3) **D)** During stimulus-induced hyperosmotic shock, these mutants produce more PI(3,5)P_2, and the levels of this lipid decline more slowly than in wild type yeast (N=3. error bars=SEM).

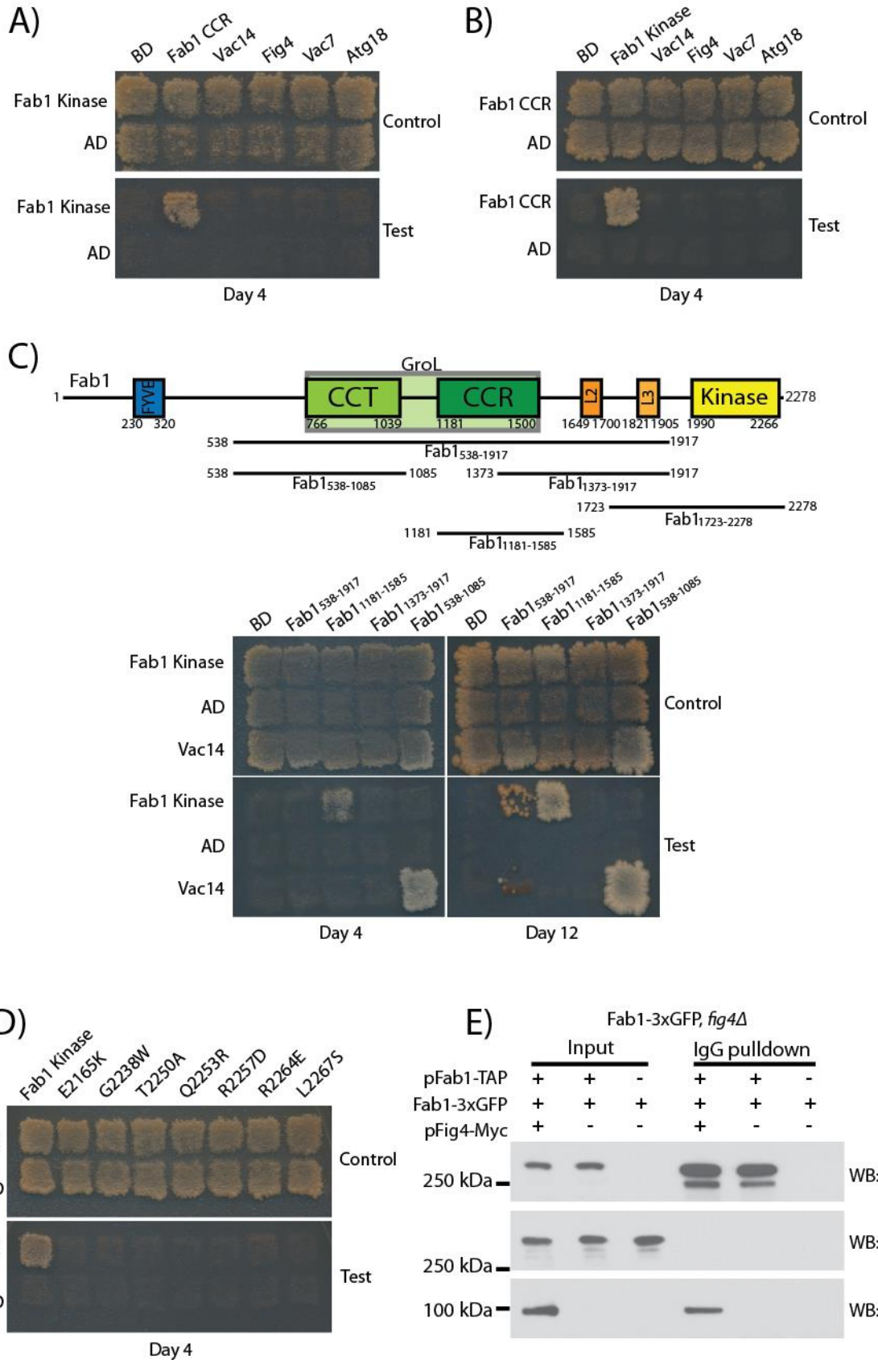
A)
BD
Fab1 CCR
Vac14
Fig4
Vac7
Atg18
Fab1 Kinase
AD
Control
Fab1 Kinase
AD
Test
Day 4
B)
BD
Fab1 Kinase
Vac14
Fig4
Vac7
Atg18
Fab1 CCR
AD
Control
Fab1 CCR
AD
Test
Day 4
C)
Fab1
GroL
1
FYVE
CCT
CCR
L2
L3
Kinase
2278
230 320
766 1039
1181 1500
1649 1700 1821 1905 1990 2266
538
1917
Fab1538-1917
538
1085
Fab1538-1085
1373
1917
Fab1373-1917
1723
2278
Fab1723-2278
1181
1585
Fab1181-1585
BD
Fab1538-1917
Fab1 1181-1585
Fab1 1373-1917
Fab1538-1085
BD
Fab1538-1917
Fab1 1181-1585
Fab1 1373-1917
Fab1538-1085
Fab1 Kinase
AD
Vac14
Control
Fab1 Kinase
AD
Vac14
Test
Day 4
Day 12
D)
Fab1 Kinase
E2165K
G2238W
T2250A
Q2253R
R2257D
R2264E
L2267S
Fab1 CCR
BD
Control
Fab1 CCR
BD
Test
Day 4
E)
Fab1-3xGFP, fig4Δ
Input
IgG pulldown
pFab1-TAP + + - + + -
Fab1-3xGFP + + + + + +
pFig4-Myc + - - + - -
250 kDa
WB:TAP
250 kDa
WB:GFP
100 kDa
WB:Myc

Figure 4.3. Via an intramolecular interaction, the Fab1 kinase region physically associates with the CCR region and dominant-active mutations ablate this interaction. For yeast two-hybrid (Y2H) experiments transformants were patched onto SC-LEU-TRP, replica-plated onto SC-LEU-TRP (control) or SC-LEU-TRP-ADE-HIS (test). **A)** The kinase region interacts with the Fab1 CCR domain. Gal4-Activation Domain (AD) fused with either the kinase region (residues 1723-2278) or empty vector tested against Gal4-Binding Domain (BD) fused with either the CCR region (residues 1181-1585), Vac14, Fig4, Vac7 (amino acids 394–918), or Atg18 (N=6). **B)** The Fab1 CCR domain interacts with the Fab1-kinase region. Gal4-AD fused with the CCR region (residues 1181-1585) or empty vector tested with Gal4-BD fused with either the kinase region (residues 1723-2278), Vac14, Fig4, Vac7 (amino acids 394–918), or Atg18 (N=6). **C)** The Fab1 kinase region interacts with the Fab1-CCR domain. Gal4-AD fused with either the kinase region (residues 1723-2278) or empty vector tested against Gal4-BD fused with Fab1-538-1917, Fab1-CCR domain, Fab1-1373-1917, or Fab1-538-1085 (N=6). **D)** Dominant-active kinase domain mutants ablate the interaction with the Fab1-CCR domain. Gal4-BD fused with the Fab1 CCR region with Gal4-AD fused with either the kinase region of Fab1, or this region with one of the following mutations: E2165K, G2238W, T2250A, Q2253R, R2257D, R2264E, L2267S (N=6). **E)** Fab1 does not co-immunoprecipitate with itself *in vivo*. Co-expression of Fab1-TAP, Fab1-3xGFP, and Fig4-myc in *S. cerevisiae*. Precipitation of Fab1-TAP with IgG pulls down a known Fab1 complex protein, Fig4-Myc, but fails to co-immunoprecipitate Fab1-3xGFP indicating that Fab1 does not form multimers *in vivo* (N=3. Experiment performed by Dr. Beth Strunk).

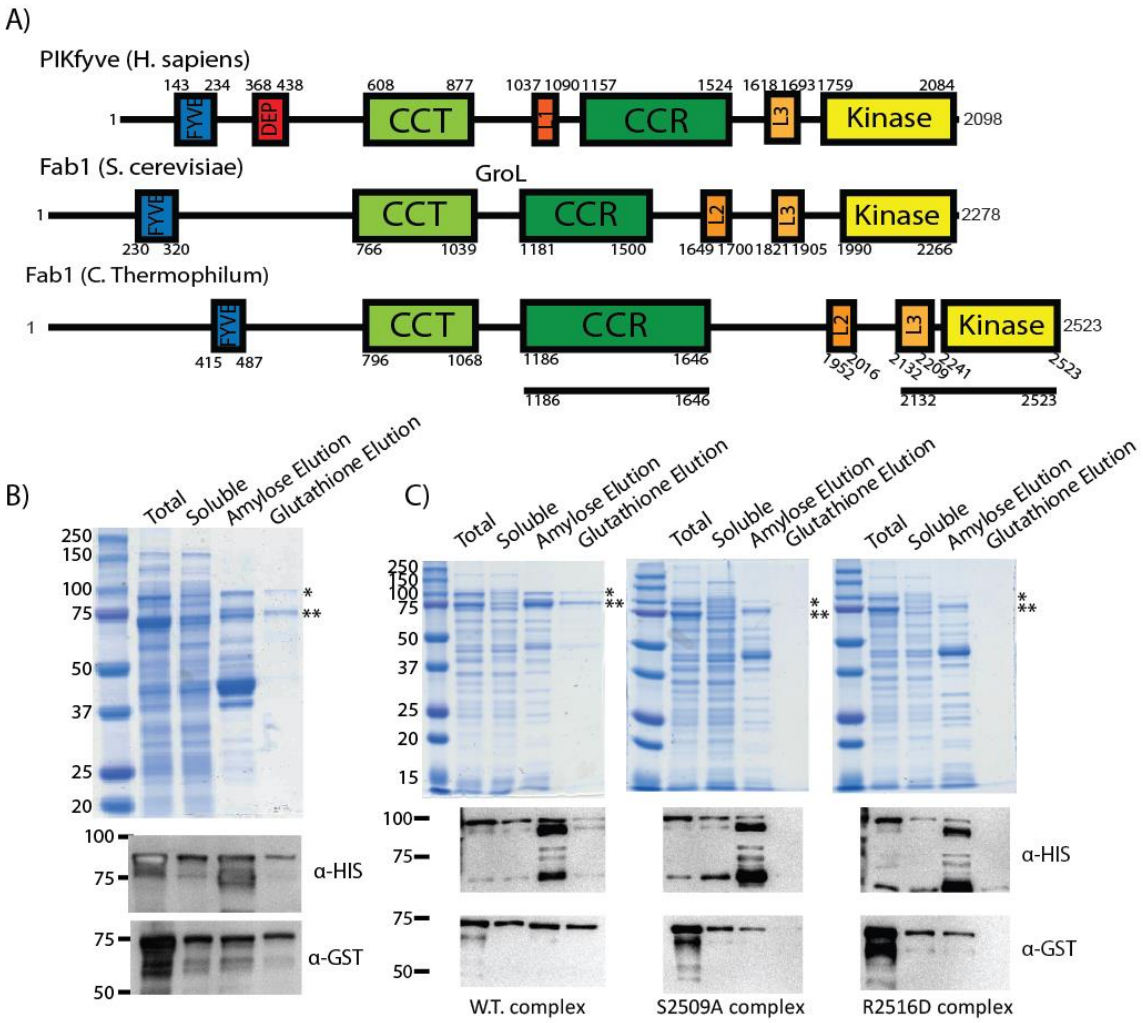

Figure 4.4. *C. thermophilum* Fab1 kinase region interacts with the CCR domain *in vitro*. A) Fab1 from *Homo sapiens* (PIKfyve), *S. cerevisiae*, or *C. thermophilum* indicate conserved domains. Black lines under *C. thermophilum* indicate polypeptides used for *in vitro* studies. **B)** Coomassie stain and western blot analysis indicate that the *C. thermophilum* CCR domain interacts with the kinase region. Co-expression of fusion protein constructs of 6X-HIS-Maltose Binding Protein (MBP) and Glutathione S transferase (GST) with CCR domain (1186-1646) and kinase region (2132-2523), respectively, were induced and purified from *E. coli*. Coomassie and western blot analysis indicates that the partially purified proteins associate as a complex (N=3). **C)** kinase domain mutants S2509A and R2516D (*S. cerevisiae* residues T2250 and R2257) reduce the interaction between CCR and kinase region *in vitro*. High salt purification (500mM NaCl) of the mutant complexes yields no CCR domain or kinase region by the final column purification step (N=3).

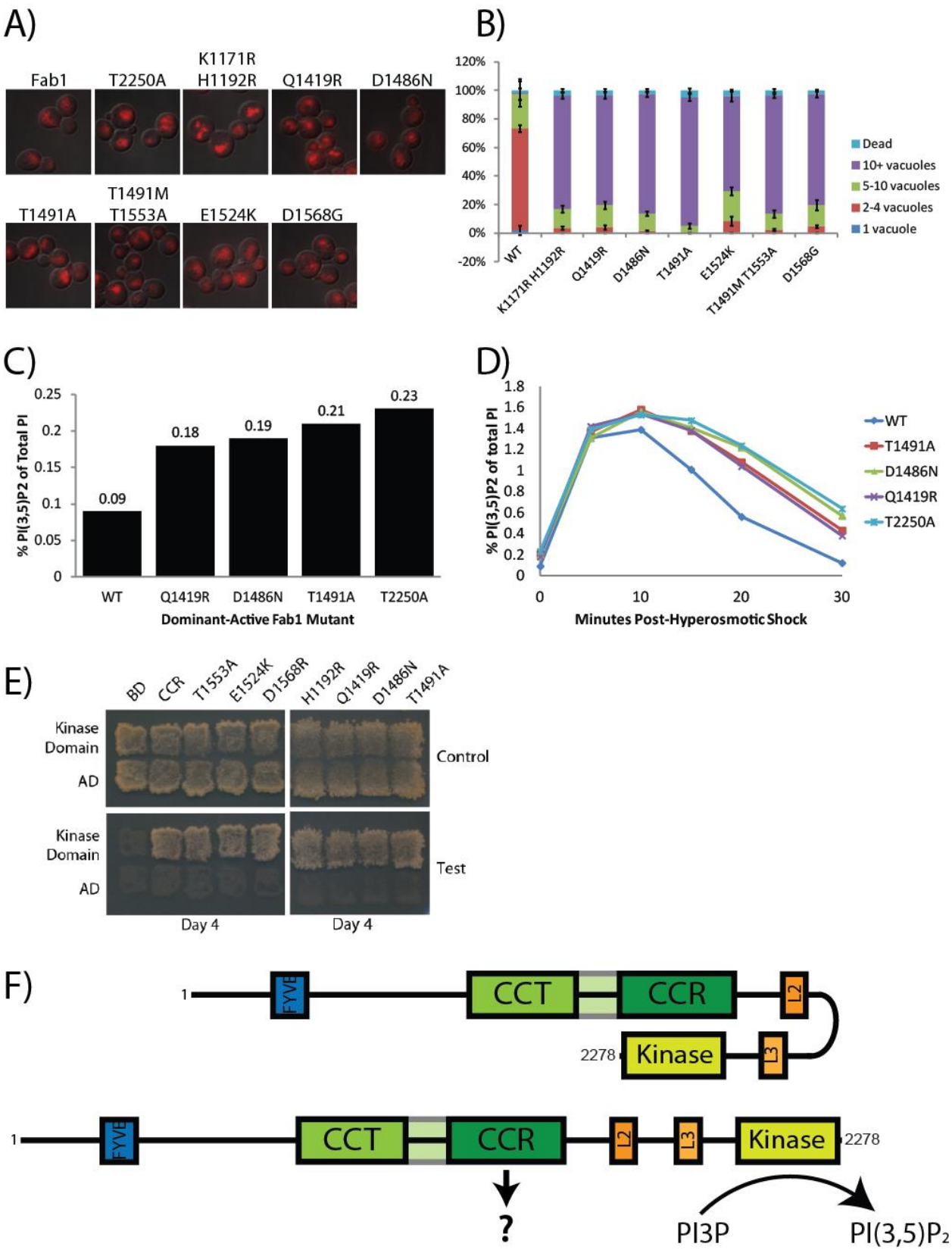
A)
Fab1
T2250A
K1171R H1192R
Q1419R
D1486N
T1491A
T1491M T1553A
E1524K
D1568G
B)
120%
100%
80%
60%
40%
20%
0%
-20%
WT
K1171R H1192R
Q1419R
D1486N
T1491A
E1524K
T1491M T1553A
D1568G
Dead
10+ vacuoles
5-10 vacuoles
2-4 vacuoles
1 vacuole
C)
% PI(3,5)P2 of Total PI
0.25
0.2
0.15
0.1
0.05
0
0.09
0.18
0.19
0.21
0.23
WT
Q1419R
D1486N
T1491A
T2250A
Dominant-Active Fab1 Mutant
D)
% PI(3,5)P2 of total PI
1.8
1.6
1.4
1.2
1
0.8
0.6
0.4
0.2
0
0
10
20
30
Minutes Post-Hyperosmotic Shock
WT
T1491A
D1486N
Q1419R
T2250A
E)
BD
CCR
T1553A
E1524K
D1568R
H1192R
Q1419R
D1486N
T1491A
Kinase Domain
AD
Control
Kinase Domain
AD
Test
Day 4
Day 4
F)
1
FYVE
CCT
CCR
L2
2278
Kinase
L3
1
FYVE
CCT
CCR
L2
L3
Kinase
2278
?
PI3P
PI(3,5)P2

Figure 4.5. Dominant-active mutations in the CCR region of Fab1 retain an interaction with the kinase domain. Notably, both the kinase and CCR dominant-active alleles respond similarly to hyperosmotic shock. A) Similar to the kinase domain mutation Fab1^{T2250A}, all CCR domain mutations exhibit fragmented vacuoles indicative of an elevation in PI(3,5)P_2 levels (N=3). **B)** Quantification of vacuolar morphology of cells expressing Fab1 or the indicated Fab1-CCR domain dominant-active allele. Dead cells scored when cell was ruptured or if FM4-64 filled cytoplasm (N=3, >100 cells per experiment, error bars=SEM). **C)** Under basal conditions, three CCR domain mutations (Fab1^{Q1419R}, Fab1^{D1486N}, and Fab1^{T1491A}) display an elevation in PI(3,5)P_2 levels. N=1. **D)** During stimulus-induced hyperosmotic shock, CCR domain mutants produce more PI(3,5)P_2 than WT Fab1, and the levels of PI(3,5)P_2 in these mutants decline more slowly than in wild-type yeast (N=1E. **D)** Dominant-active mutations in the CCR region do not interfere with the yeast two-hybrid interaction of the CCR region with the kinase region. Yeast two-hybrid tests of Gal4-AD fused with the kinase region (residues 1723-2278) with Gal4-BD fused with either the CCR region (residues 1181-1585), or this region with one of the following mutations: H1192R, Q1419R, D1486N, T1491A, T1491M, E1524K, T1553A, D1568R (N=6). **F)** Model for a regulatory intramolecular interaction within Fab1. Under basal conditions, the CCR domain interacts with the kinase region of Fab1 and inhibits its activity. We propose that during specific stimuli, post-translational modifications and/or binding of additional proteins transiently releases CCR domain inhibition of Fab1 kinase activity to promote PI(3,5)P_2 synthesis. The CCR domain likely has an additional role.

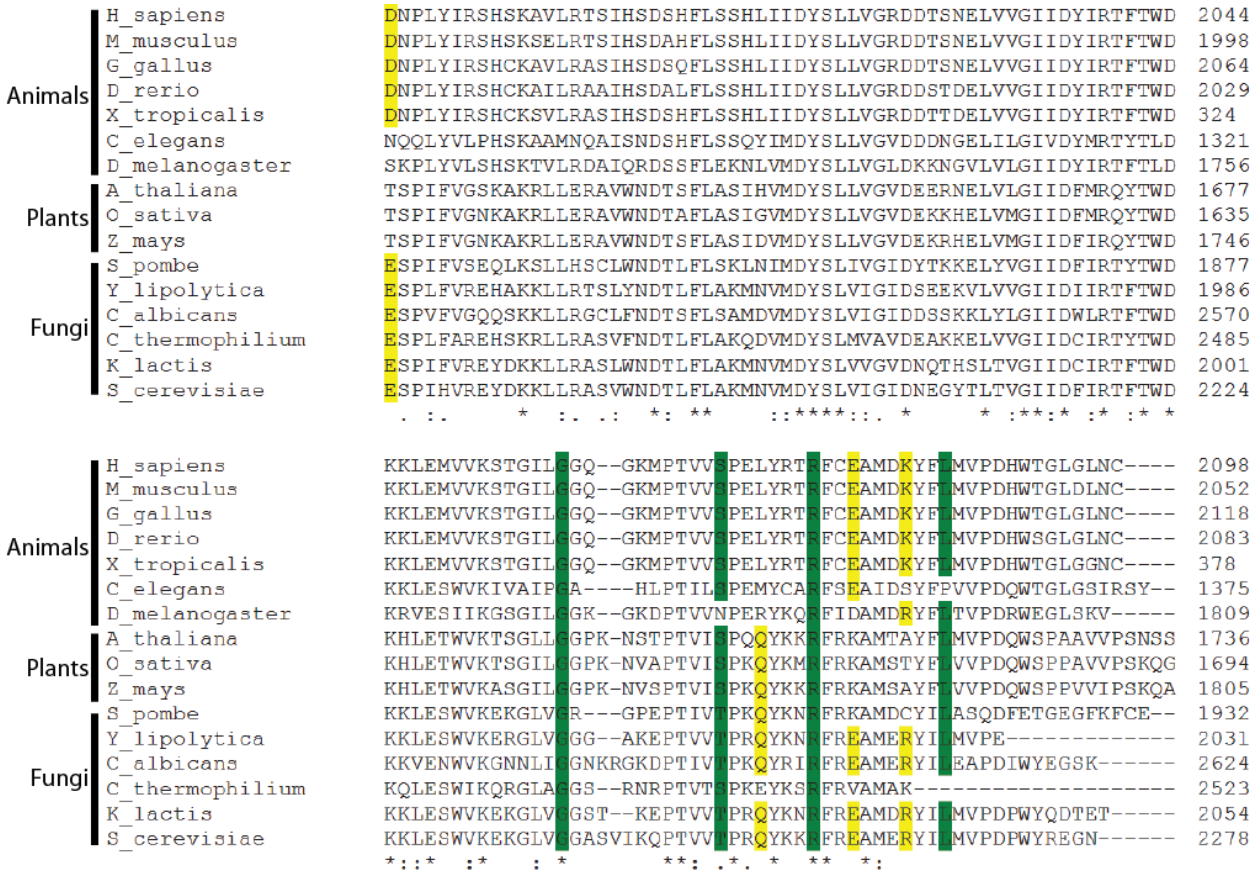

Figure 4.6. The C-terminal Fab1 kinase domain is conserved across multiple phyla. ClustalOmega alignment of the Fab1 compared to species indicated. **Yellow:** dominant-active mutations that are loosely conserved among species. **Green:** residues strongly conserved across all Fab1.

A)

```
Yeast_CCR              ------------------------------------------------------------
C.thermo_CCR           AFYSDMVAKYETRILSVSPFVRFTQPYLLMKAREQERRLEYLKRLRDQDQIQEPDQPDKP        1246

Yeast_CCR              ----------------------------------------------------SSSQNLLG        1188
C.thermo_CCR           EEFQLIKPEMIHQMGQKAPRKIMEVIHAVHDAEYDKALHNYLTQTKQWETYLQNCLDLFD        1305
                                                                          ... :*:

Yeast_CCR              TGSHQSITVLYSMVSTKTATPCVGPQIVTIDYF---------WDSDISIGQFIENVVGTA        1239
C.thermo_CCR           PYAHQNIVVLSSVTCTATQIPCVEPALMAIEFYNQHPDEGGFLDQDFTLGQYIEDICDTA        1365
                         :**.*.** *:..* *  *** * :::*:::          *.*:::**:**::  **

Yeast_CCR              RYPCQQ-GCNGLYLDHYRSYVHGSGKVDVLIEKFQT---RLP----------KLKDIILT        1285
C.thermo_CCR           NYVCTANNCGRKMYEHHRTFVHDNARLTIILKPSPQWPENFPEKPQERGGGDDEGTGICM        1425
                       .* *    *     :*:*::** ..:: ::::       .:*          .    *

Yeast_CCR              WSYCKKCGTSTPILQISEKTWNHSFGKYLEVMFWSYKDSVTGIGKCPHDFTKDHVKYFGY        1345
C.thermo_CCR           WNYCKVCDKHFGLMPMSVSTWKYSFGKYLELSFWNTGLRLHPETGCPHDHKKDHVRYFYY        1485
                       *.*** * .   :: :* .**::*******: **.    :     ****..****:** *

Yeast_CCR              --NDLVVRLEYSDLEVHELITPPRKIKWKPHIDIKLKVELYYKILEKINNFYGSVLSRLE        1403
C.thermo_CCR           TYLDIAVKVHYDPIDLYEIIVPRKRITWKVDIDLKLKNDVFTKAEERWNRFINSVKARLK        1545
                          *:.*::.*. ::::*:*.* ::*.** .**:*** ::: *  *: *.*  ** :**:

Yeast_CCR              RIKLDSMTKDKVLSGQAKIIELKSNATEEQKLMLQDLDTFYADSPCDQHLPLNLVIKSLY        1463
C.thermo_CCR           SIKIDSVLPEKAEDCKAEVDRLLEKAEEDHKEMIKVLQNAYMNSKYYEIIPFNVVFRQML        1605
                        **:**:  :*. . :*:: .* .:* *::* *:: *:. * :*   : :*:*:*::.:

Yeast_CCR              DKAVNWNSTFAIFAKSYLPSETDISRITAKQLKKLFY----- 1500
C.thermo_CCR           ERATEWDSAFTQFESKFLS-DKDVRQLTLIQLKKMFSDHEKD 1646
                       ::*.:*:*:*: * ..:*  :.*: ::*  ****:*
```

B)

```
Yeast_Kinase_Region            --EKSLLMKTLSNFWADRSAYLWKPLVYPTCPSEHIFTDSDVIIREDEPSSLIAFCLSTS 1879
C.thermo_Kinase_Region         KHQKKSLMDRLANFWAERSASSWPQLEYPVNMGDHVMFDSDVIVREDEPSSLVAYAMSLN 2191
                                 :*. **. *:****:***  *  * **.  .:*:: *****:********:*:.:* .

Yeast_Kinase_Region            DYRNKMMNLNVQQQQQQQTAEAAPAKTGGNSGGTTQTGDPSVNISPSVSTTSHNKGRDSE 1939
C.thermo_Kinase_Region         DYKEKLAAIRRDLRMS-------------NFGETDVSGDSLE------------------ 2220
                               **::*:  :. : : .             * * *  :**

Yeast_Kinase_Region            ISSLVTTKEGLLNTPPIEGARDRTPQESQTHSQANLDTLQELEKIMTKKTATHLRYQFEE 1999
C.thermo_Kinase_Region         ---------DNMGT----------PVDPEAAKERARKIDMELEKTLLRSTGTHVKYQFVH 2261
                                       : *          * : :: .:   .   **** : :.*.**::*** .

Yeast_Kinase_Region            GLTVMSCKIFFTEHFDVFRKICDCQENFIQSLSRCVKWDSNGGKSGSGFLKTLDDRFIIK 2059
C.thermo_Kinase_Region         GTAKMMCKIFFAEQFDALRRKCGAADRFVESLSRCLKWDSKGGKTKSVFLKTLDDRFVLK 2321
                               * : * *****:*:**.:*: * . :.*::*****:****:***: * *********::*

Yeast_Kinase_Region            ELSHAELEAFIKFAPSYFEYMAQAMFHDLPTTLAKVFGFYQIQVKSSISSSKSYKMDVII 2119
C.thermo_Kinase_Region         SLSVPETQSFLKFAPDYFNIMAEALFHELPSVIAKMLGFFRVHIKNPVTN-TDIKLDLLV 2380
                               .**  * ::*:****.**: **:*:**:**:.:**::**:::::*. ::. .. *:*:::

Yeast_Kinase_Region            MENLFYEKKTTRIFDLKGSMRNRHVEQTGKANEVLLDENMVEYIYESPIHVREYDKKLLR 2179
C.thermo_Kinase_Region         MENLFYDRTPSRTFDLKGSMRNRRIQSTGERDEVLLDENMVEYIYESPLFAREHSKRLLR 2440
                               ******::. :* **********:::.**: :*****************:..**:.*:***

Yeast_Kinase_Region            ASVWNDTLFLAKMNVMDYSLVIGIDNEGYTLTVGIIDFIRTFTWDKKLESWVKEKGLVGG 2239
C.thermo_Kinase_Region         ASVFNDTLFLAKQDVMDYSLMVAVDEAKKELVVGIIDCIRTYTWDKQLESWIKQRGLAGG 2500
                               ***:******** :******::.:*:    *.***** ***:****:****:*::**.**

Yeast_Kinase_Region            ASVIKQPTVVTPRQYKKRFREAMERYILMVPDPWYWEGN      2278
C.thermo_Kinase_Region         SR--NRPTVTSPKEYKSRFRVAMAK--------------      2523
                               :   ::***.:*::**.*** ** :
```

Figure 4.7. The CCR domain and kinase region of Fab1 are conserved in *C. thermophilum*. ClustalOmega alignment of the CCR domain and kinase region of *C. thermophilum* Fab1 compared to *S. cerevisiae*. **A)** Alignment of *C. thermophilum* and *S. cerevisiae* CCR domains. **B)** Alignment of *C. thermophilum* and *S. cerevisiae* kinase regions. Note that *S. cerevisiae* residues T2250 and R2257 are conserved in *C. thermophilum*, as S2509 and R2516 respectively.

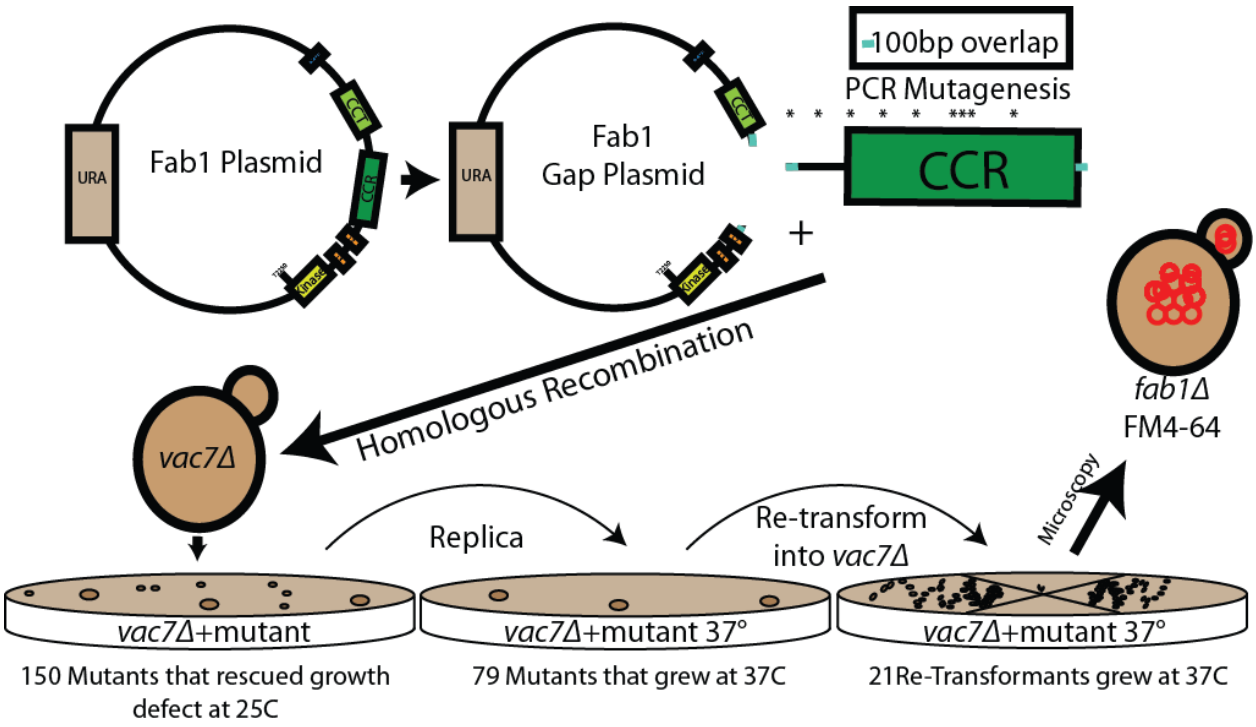

Figure 4.8. Schematic of a screen for dominant-active Fab1 alleles. Twenty-one dominant active mutants were recovered from a directed gapped-plasmid screen of Fab1.

Bibliography

Amlacher, S., Sarges, P., Flemming, D., van Noort, V., Kunze, R., Devos, D.P., Arumugam, M., Bork, P., and Hurt, E. (2011). Insight into structure and assembly of the nuclear pore complex by utilizing the genome of a eukaryotic thermophile. Cell *146*, 277-289.

Audhya, A., and Emr, S.D. (2002). Stt4 PI 4-kinase localizes to the plasma membrane and functions in the Pkc1-mediated MAP kinase cascade. Dev Cell *2*, 593-605.

Baird, D., Stefan, C., Audhya, A., Weys, S., and Emr, S.D. (2008). Assembly of the PtdIns 4-kinase Stt4 complex at the plasma membrane requires Ypp1 and Efr3. J Cell Biol *183*, 1061-1074.

Baker, R.W., Jeffrey, P.D., Zick, M., Phillips, B.P., Wickner, W.T., and Hughson, F.M. (2015). A direct role for the Sec1/Munc18-family protein Vps33 as a template for SNARE assembly. Science *349*, 1111-1114.

Botelho, R.J., Efe, J.A., Teis, D., and Emr, S.D. (2008). Assembly of a Fab1 phosphoinositide kinase signaling complex requires the Fig4 phosphoinositide phosphatase. Mol Biol Cell *19*, 4273-4286.

Dove, S.K., Cooke, F.T., Douglas, M.R., Sayers, L.G., Parker, P.J., and Michell, R.H. (1997). Osmotic stress activates phosphatidylinositol-3,5-bisphosphate synthesis. Nature *390*, 187-192.

Duex, J.E., Nau, J.J., Kauffman, E.J., and Weisman, L.S. (2006a). Phosphoinositide 5-phosphatase Fig 4p is required for both acute rise and subsequent fall in stress-induced phosphatidylinositol 3,5-bisphosphate levels. Eukaryotic cell *5*, 723-731.

Duex, J.E., Tang, F., and Weisman, L.S. (2006b). The Vac14p-Fig4p complex acts independently of Vac7p and couples PI3,5P2 synthesis and turnover. The Journal of cell biology *172*, 693-704.

Foti, M., Audhya, A., and Emr, S.D. (2001). Sac1 lipid phosphatase and Stt4 phosphatidylinositol 4-kinase regulate a pool of phosphatidylinositol 4-phosphate that functions in the control of the actin cytoskeleton and vacuole morphology. Mol Biol Cell *12*, 2396-2411.

Huang, X., and Miller, W. (1991). A time-efficient, linear-space local similarity algorithm. Advances in Applied Mathematics *12*, 337-357.

Kelley, L.A., Mezulis, S., Yates, C.M., Wass, M.N., and Sternberg, M.J. (2015). The Phyre2 web portal for protein modeling, prediction and analysis. Nat Protoc *10*, 845-858.

Kunz, J., Wilson, M.P., Kisseleva, M., Hurley, J.H., Majerus, P.W., and Anderson, R.A. (2000). The activation loop of phosphatidylinositol phosphate kinases determines signaling specificity. Mol Cell *5*, 1-11.

Rao, V.D., Misra, S., Boronenkov, I.V., Anderson, R.A., and Hurley, J.H. (1998). Structure of type IIbeta phosphatidylinositol phosphate kinase: a protein kinase fold flattened for interfacial phosphorylation. Cell *94*, 829-839.

Strahl, T., and Thorner, J. (2007). Synthesis and function of membrane phosphoinositides in budding yeast, Saccharomyces cerevisiae. Biochim Biophys Acta *1771*, 353-404.

CHAPTER 5

A REGULATORY MOTIF IS CONSERVED IN THE YEAST PHOSPHORYLATED PHOSPHATIDYLINOSITOL KINASES FAB1 AND MSS4

Introduction

Tight, dynamic regulation of $PI(3,5)P_2$ is essential for cellular homeostasis (Baulac *et al.*, 2014; McCartney *et al.*, 2014); therefore, it is likely that controlled regulation of other PPIs is important. Six lipid kinases exist in yeast (Strahl and Thorner, 2007). Most of the lipid kinases are essential or their deletion causes severe phenotypes that impair cellular growth (Flanagan *et al.*, 1993; Schu *et al.*, 1993; Cutler *et al.*, 1997; Desrivieres *et al.*, 1998). Importantly, alignments of kinase domains from both yeast and mammalian lipid kinases show that all contain a C-terminal alpha helix directly distal to the activation loop (Rao *et al.*, 1998). Therefore, I hypothesize the presence of a general mechanism of regulation for lipid kinases involving the C-terminal alpha helix of their kinase domains.

Some phosphatidylinositol kinases (PIKs) are controlled through physical associations of their kinase domains with regulatory domains

Two members of the phosphatidylinositol kinase (PIK) family (Vps34 and p110α) are regulated via a protein-protein contact on the kinase domain (Budovskaya *et al.*, 2002; Rostislavleva *et al.*, 2015). In the case of Vps34, regulation occurs in part via a physical

interaction of the C-terminal portion of its kinase domain with Vps15, a member of the Vps34 kinase complex (Budovskaya *et al.*, 2002). Recently, crystallization of this complex has been achieved and has demonstrated that an alpha helix C-terminal to the activation loop likely physically associates with the Vps15 kinase domain (Rostislavleva *et al.*, 2015). A physical association of Vps15 and Vps34 has been reported by yeast two-hybrid (Budovskaya *et al.*, 2002). Deletion mutations that remove multiple residues of polypeptide at the C-terminal Vps34 kinase domain ablate this yeast two-hybrid interaction. Specifically, these mutations ablate the C-terminal alpha helix of the Vps34 kinase domain. These mutations additionally deleteriously alter kinase activity—mutants fail to grow at 37ºC, have a defect in CPY maturation, and have decreased levels of PI3P (Budovskaya *et al.*, 2002). The authors propose a model in which the interaction between Vps15 and Vps34 is necessary for Vps34 kinase activity. However, it is possible that these multi-residue deletions of the C-terminal Vps34 kinase domain are negatively affecting kinase activity and the loss of an interaction with Vps15 is an artifact. Additional studies of the Vps34-Vps15 interaction may better highlight the importance of this physical interaction on the regulation of PI3P.

A second example of regulation of a PIK via a physical association of its kinase domain is the phosphatidylinositol 3-phosphate kinase, p110α, which exhibits an intramolecular interaction between its adaptor-binding domain (ABD) and its kinase domain (Huang *et al.*, 2007; Huang *et al.*, 2008). Oncogenic mutations in either the ABD or the kinase domain of p110α lead to elevated kinase activity (Zhao and Vogt, 2008), and are proposed to dissociate this intramolecular interaction (Zhao and Vogt, 2008). Together,

this data demonstrates that some phosphatidylinositol kinases are controlled by physical association of their kinase domains with regulatory domains.

Bioinformatic analysis of Mss4 and Fab1 identifies a putative regulatory motif in Mss4

The phosphorylated phosphoinositide kinases (PIPKs) of yeast, Fab1 and Mss4, share sequence similarity at the C-terminus of their kinase domains (Rao *et al.*, 1998). Interestingly, multiple residues, which in Fab1 can be mutated to generate a dominant-active Fab1 allele, are conserved in Mss4 (Figure 5.1B). Moreover, an I-TASSER structure prediction of the Mss4 kinase domain reveals a surface exposed alpha helix on which many of these residues lie (Figure 5.1C). The striking similarity between this analysis and the analysis of the Fab1 C-terminal kinase domain alleles in Chapter four suggests that a regulatory motif at the C-terminus of the Mss4 kinase domain may exist.

Dominant-active Mss4 alleles can be made based on dominant-active Fab1 alleles

As a first approach to test if a common regulatory motif is shared between yeast Fab1 and Mss4, I made point mutations in Mss4 predicted to result in a dominant-active allele. I acquired a pRS416-Mss4-GFP plasmid (generous gift from the laboratory of Dr. Scott Emr) and made point mutations Mss4-R747D based on the Fab1-R2257D allele, and Mss4-V756S based on the Fab1-L2267S dominant-active allele. Additionally, I generated mutants Mss4-Y744F and Mss4-F748A based on their position on the predicted regulatory alpha helix (Figure 5.1C) and conservation among all PIPKs (Rao *et al.*, 1998).

As a first test of the effect of these point mutations on Mss4, I analyzed these alleles in a WT background under the microscope. It is well established that WT Mss4 resides in distinct puncta on the plasma membrane of yeast while kinase dead Mss4 is cytosolic or degraded in the vacuole depending on the yeast strain background (Audhya and Emr, 2002). All alleles tested localized to punctate structures on the plasma membrane (Figure 5.2). This data indicates that these alleles do not perturb Mss4 localization and suggests that kinase activity is preserved.

Next, I sought to determine if putative dominant-active Mss4 alleles produced altered levels of PI(4,5)P_2 under basal conditions. I expressed vector alone, Mss4, or putative dominant-active Mss4 alleles in a WT strain background (LWY3250) and measured PPI levels as previously described (Bonangelino *et al.*, 2002; Duex *et al.*, 2006). WT Mss4 slightly elevates PI(4,5)P_2 levels compared to vector alone (Figure 5.3A). Mss4-R747D, based on the dominant-active Fab1-R2257D allele, is hypomorphic and produced reduced levels of PI(4,5)P_2 (data not shown). Mss4-Y744F, Mss4-F748A elevate PI(4,5)P_2 higher than WT Mss4 under basal conditions; however, these results are not statistically significant (Figure 5.3A). Excitingly, the allele Mss4-V756S elevates PI(4,5)P_2 higher than WT Mss4 under basal conditions in a statistically significant manner (N=3, p=.020) (Figure 5.3B). That Mss4-R747D is hypomorphic indicates that perfect conservation of the roles of specific residues is not maintained between Fab1 and Mss4. However, that Mss4-V756S is dominant-active under basal conditions indicates that the C-terminal alpha helix motif of Mss4 likely plays a regulatory role.

Stimulus-induced activation of Mss4 elevates $PI(4,5)P_2$ greater in cells expressing putative dominant-active alleles compared to WT Mss4. Upstream activating stimuli for PPI kinases are not well characterized. Therefore for stimulus-induced Mss4 activation I chose hyperosmotic shock, which has previously been shown to increase $PI(4,5)P_2$ levels 160% greater than basal levels at fifteen minutes post-hyperosmotic shock (Duex *et al.*, 2006). At fifteen minutes post-hyperosmotic shock, Mss4-Y744F, Mss4-F748A, and Mss4-V756S elevate $PI(4,5)P_2$ levels higher than WT Mss4 (Figure 5.3A). Mss4-V756S demonstrates a statistically significant 20% increase in $PI(4,5)P_2$ production compared to WT Mss4 at fifteen minutes post-hyperosmotic shock (Figure 5.3B). Elevated basal levels and stimulus-induced levels of $PI(4,5)P_2$ above WT strongly indicates that these alleles act in a dominant-active fashion. The mechanisms that regulate PIKs and PIPKs are not well understood and hyperosmotic shock may not be a major activator of Mss4 activity. Therefore, that similar residues can be mutated in the PI3P 5-kinase Fab1 and the PI4P 5-kinase Mss4 leading to an elevation in activity for both proteins indicates that a common mechanism of regulation may be present.

Discussion

The mechanisms that regulate lipid kinase activity both in yeast and higher eukaryotes are largely uncharacterized. Within this thesis, I provide evidence of an intramolecular interaction within the yeast PI3 5-kinase, Fab1. Additionally, in this chapter I demonstrate that the C-terminal portion of yeast PIPK kinase domains can be mutated in a similar fashion to increase their overall activity in response to an upstream stimulus.

Given that, in the PIPK Fab1, this dissociates the interaction of a negative modulator it is likely that in Mss4 it analogously inhibits binding of a negative regulator, such as the previously reported negative Mss4 regulator, Opy1 (Ling *et al.*, 2012). Genetic and biochemical evidence indicates that this C-terminal kinase domain motif may also be an important regulator of PIK activity as is the case for Vps34 (Budovskaya *et al.*, 2002) and p110α (Huang *et al.*, 2007). More detailed investigation into these biochemical and genetic observations may lead to a more comprehensive understanding of the role of C-terminal kinase domain regions on the regulation of lipid kinases or all kinases.

A)

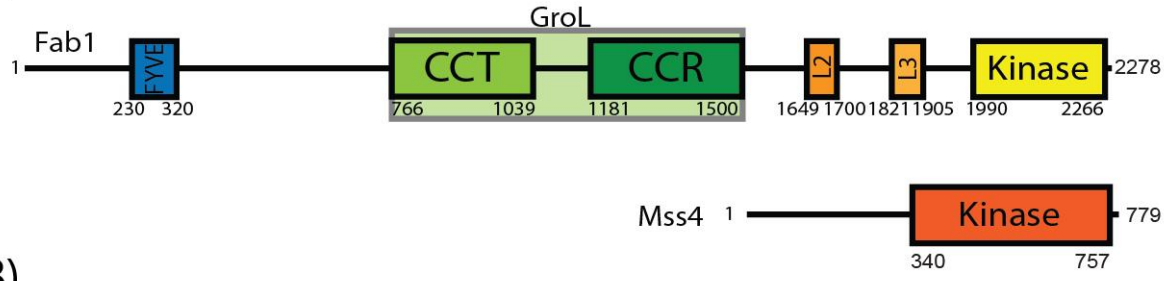

B)

```
Mss4      YYVGIIDFLTNYSVMKKLETFWRSLRH-----DTKLVSAIPPRDYANRFYEFIEDSVDPL     759
Fab1      LTVGIIDFIRTFTWDKKLESWVKEKGLVGGASVIKQPTVVTPRQYKKRFREAMERYILMV     2269
            ******: .::  ****:: :.          *  :.: **:* :** * :*  :  :

Mss4      PQKKTQSSYRDDPNQKNYKD    779
Fab1      PDPWYWE----GN-------    2278
          *:    .
```

C)

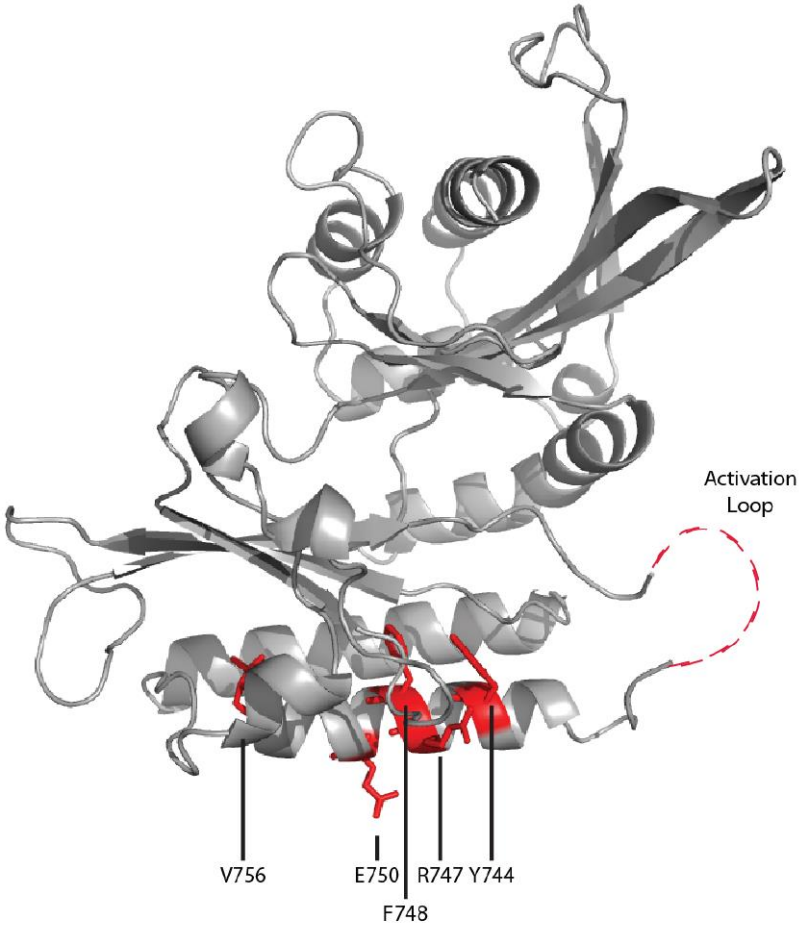

Figure 5.1. Dominant-active Fab1 kinase domain residues are conserved in Mss4. **A)** Domain architecture of Fab1/PIKfyve compared to Mss4. Boundaries of each domain were determined using a combination of Jpred4 secondary structure prediction and ClustalOmega multiple sequence alignment. **B)** ClustalOmega alignment of *S. cerevisiae* Fab1 and *S. cerevisiae* Mss4 indicate that multiple dominant-active residues in Fab1 are conserved with the PI4 5-Kinase Mss4. Red: residues chosen as candidate dominant-active residues based on sequence conservation in Fab1 and solvent-exposed placement on predicted Mss4 kinase domain structure in C. **C)** I-TASSER structure prediction of the Mss4 kinase domain reveals a solvent-exposed alpha helix C-terminal to the activation loop similar to Fab1. Red: five Mss4 residues chosen to test if dominant-active alleles can be made in Mss4.

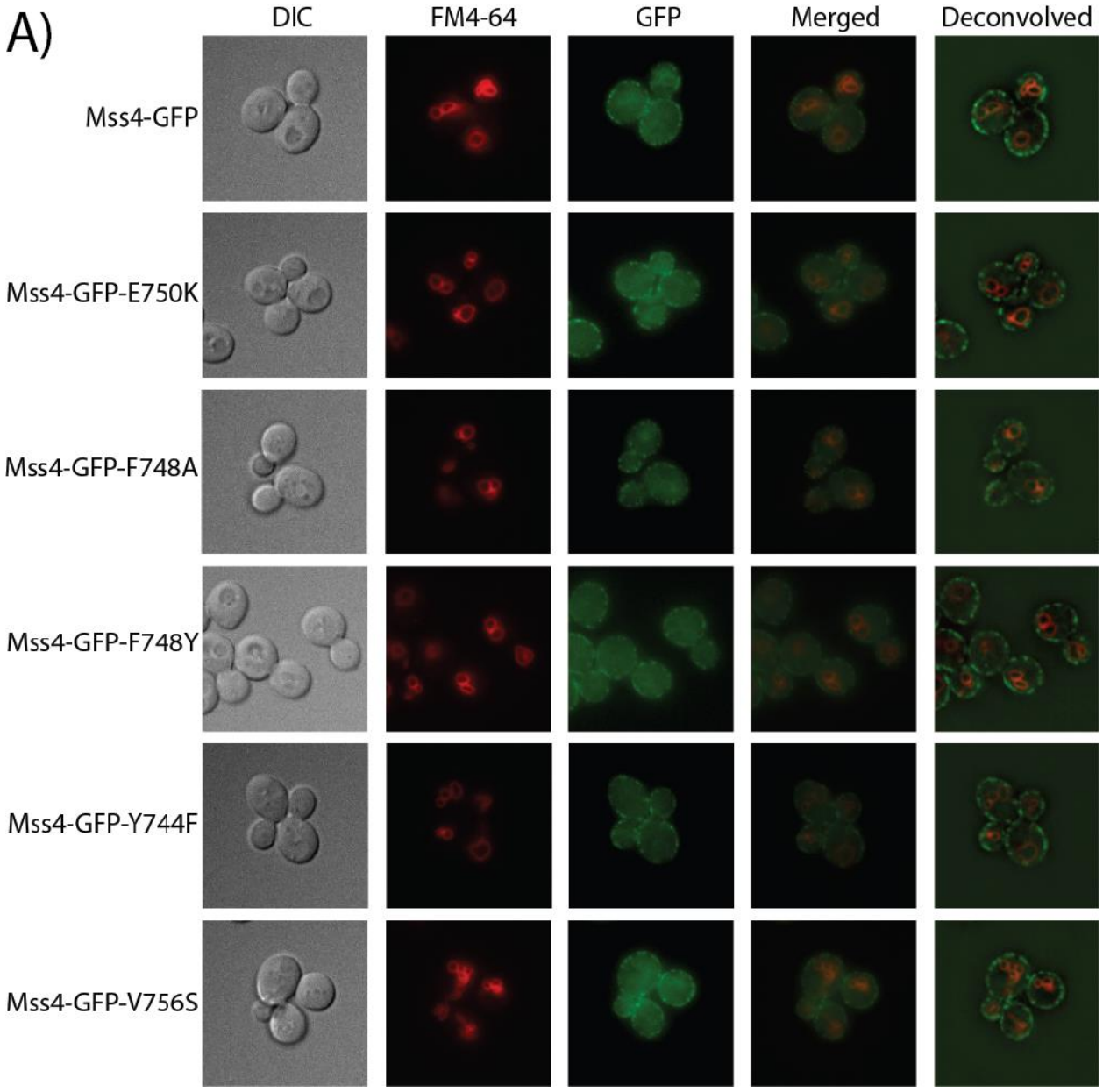

Figure 5.2. Mss4 as well as candidate dominant-active Mss4 alleles localize as punctate structures on the plasma membrane of yeast. A) WT yeast expressing either a pRS416-Mss4-GFP plasmid or the indicated candidate dominant-active allele were grown to log-phase and imaged under the microscope. From left to right: DIC image of the yeast; vacuolar staining (FM4-64); Mss4-GFP; merged FM4-64 and GFP signals; and a deconvolved image of the merge (N=3). The presence of punctate structures in both WT Mss4 and Mss4 candidate dominant-active alleles indicate that all mutants correctly localize to the plasma membrane.

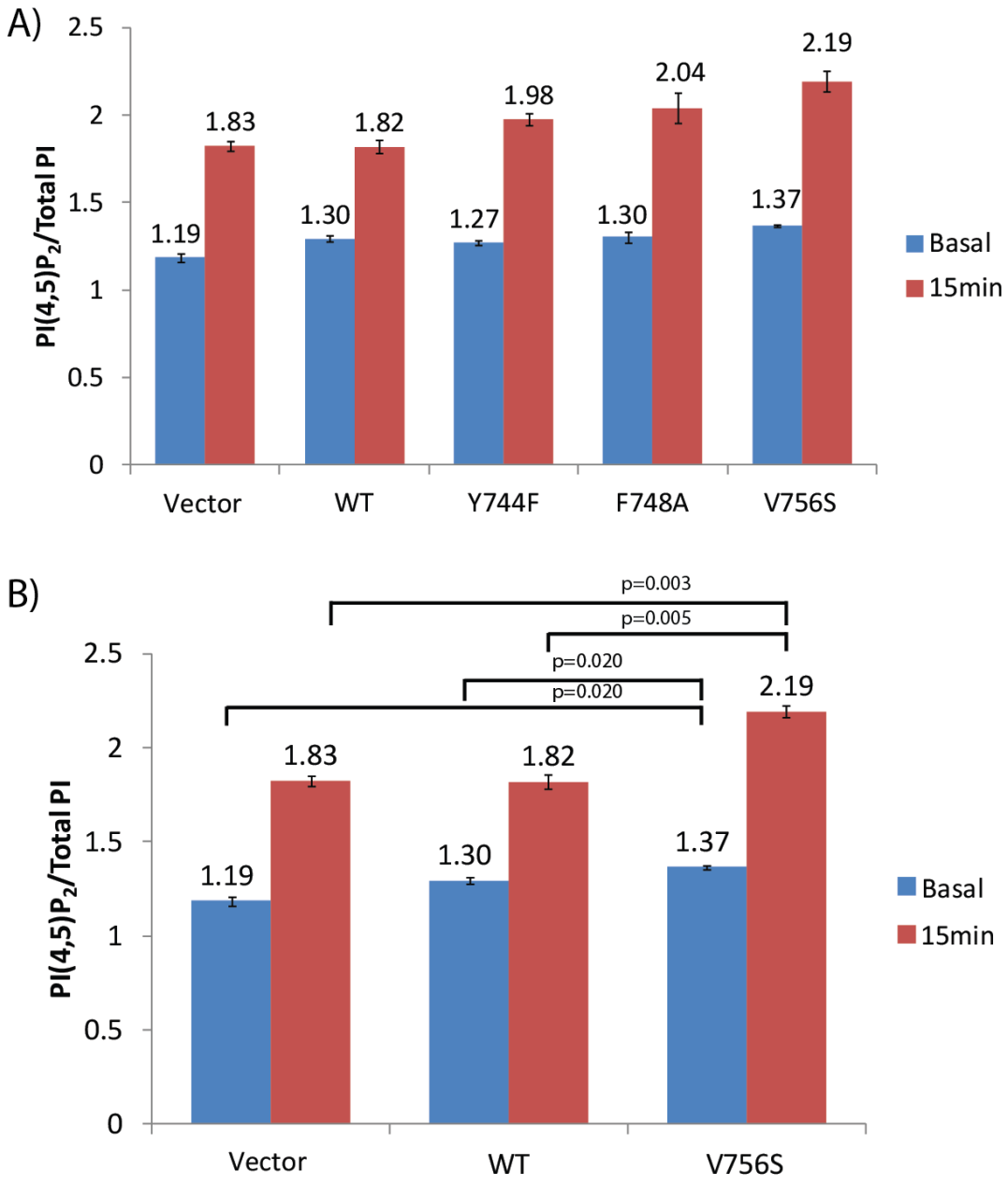

Figure 5.3. Kinase domain mutations conserved in Fab1 can be mutated in Mss4 to generate dominant-active Mss4 alleles. A) Three C-terminal Mss4 kinase domain mutations (Mss4-Y744F, Mss4-F748A, and Mss4-V756S) were expressed in WT cells and subjected to lipid labeling analysis under basal conditions and at 15-minutes post-hyperosmotic shock. Under basal conditions Mss4 and Mss4 mutants display elevated levels of PI(4,5)P_2 compared to vector control. At fifteen minutes post-hyperosmotic shock all three mutants display elevated levels compared to WT Mss4 and vector alone

(N=3, error bars=SEM). B) The dominant-active mutant Mss4-V756S displays elevated levels of PI(4,5)P2 under basal conditions and at the peak of PI(4,5)P_2 production during a hyperosmotic shock time course (N=3, error bars=SEM).

Bibliography

Audhya, A., and Emr, S.D. (2002). Stt4 PI 4-kinase localizes to the plasma membrane and functions in the Pkc1-mediated MAP kinase cascade. Dev Cell *2*, 593-605.

Baulac, S., Lenk, G.M., Dufresnois, B., Ouled Amar Bencheikh, B., Couarch, P., Renard, J., Larson, P.A., Ferguson, C.J., Noe, E., Poirier, K., Hubans, C., Ferreira, S., Guerrini, R., Ouazzani, R., El Hachimi, K.H., Meisler, M.H., and Leguern, E. (2014). Role of the phosphoinositide phosphatase FIG4 gene in familial epilepsy with polymicrogyria. Neurology.

Bonangelino, C.J., Nau, J.J., Duex, J.E., Brinkman, M., Wurmser, A.E., Gary, J.D., Emr, S.D., and Weisman, L.S. (2002). Osmotic stress-induced increase of phosphatidylinositol 3,5-bisphosphate requires Vac14p, an activator of the lipid kinase Fab1p. The Journal of cell biology *156*, 1015-1028.

Budovskaya, Y.V., Hama, H., DeWald, D.B., and Herman, P.K. (2002). The C terminus of the Vps34p phosphoinositide 3-kinase is necessary and sufficient for the interaction with the Vps15p protein kinase. J Biol Chem *277*, 287-294.

Cutler, N.S., Heitman, J., and Cardenas, M.E. (1997). STT4 is an essential phosphatidylinositol 4-kinase that is a target of wortmannin in Saccharomyces cerevisiae. J Biol Chem *272*, 27671-27677.

Desrivieres, S., Cooke, F.T., Parker, P.J., and Hall, M.N. (1998). MSS4, a phosphatidylinositol-4-phosphate 5-kinase required for organization of the actin cytoskeleton in Saccharomyces cerevisiae. J Biol Chem *273*, 15787-15793.

Duex, J.E., Nau, J.J., Kauffman, E.J., and Weisman, L.S. (2006). Phosphoinositide 5-phosphatase Fig 4p is required for both acute rise and subsequent fall in stress-induced phosphatidylinositol 3,5-bisphosphate levels. Eukaryotic cell *5*, 723-731.

Flanagan, C.A., Schnieders, E.A., Emerick, A.W., Kunisawa, R., Admon, A., and Thorner, J. (1993). Phosphatidylinositol 4-kinase: gene structure and requirement for yeast cell viability. Science *262*, 1444-1448.

Huang, C.H., Mandelker, D., Gabelli, S.B., and Amzel, L.M. (2008). Insights into the oncogenic effects of PIK3CA mutations from the structure of p110alpha/p85alpha. Cell Cycle *7*, 1151-1156.

Huang, C.H., Mandelker, D., Schmidt-Kittler, O., Samuels, Y., Velculescu, V.E., Kinzler, K.W., Vogelstein, B., Gabelli, S.B., and Amzel, L.M. (2007). The structure of a human p110alpha/p85alpha complex elucidates the effects of oncogenic PI3Kalpha mutations. Science *318*, 1744-1748.

Ling, Y., Stefan, C.J., Macgurn, J.A., Audhya, A., and Emr, S.D. (2012). The dual PH domain protein Opy1 functions as a sensor and modulator of PtdIns(4,5)P(2) synthesis. EMBO J *31*, 2882-2894.

McCartney, A.J., Zhang, Y., and Weisman, L.S. (2014). Phosphatidylinositol 3,5-bis phosphate: Low abundance. High significance. . Bioessays *36*, 52-64.

Rao, V.D., Misra, S., Boronenkov, I.V., Anderson, R.A., and Hurley, J.H. (1998). Structure of type IIbeta phosphatidylinositol phosphate kinase: a protein kinase fold flattened for interfacial phosphorylation. Cell *94*, 829-839.

Rostislavleva, K., Soler, N., Ohashi, Y., Zhang, L., Pardon, E., Burke, J.E., Masson, G.R., Johnson, C., Steyaert, J., Ktistakis, N.T., and Williams, R.L. (2015). Structure and flexibility of the endosomal Vps34 complex reveals the basis of its function on membranes. Science *350*, aac7365.

Schu, P.V., Takegawa, K., Fry, M.J., Stack, J.H., Waterfield, M.D., and Emr, S.D. (1993). Phosphatidylinositol 3-kinase encoded by yeast VPS34 gene essential for protein sorting. Science *260*, 88-91.
Strahl, T., and Thorner, J. (2007). Synthesis and function of membrane phosphoinositides in budding yeast, Saccharomyces cerevisiae. Biochim Biophys Acta *1771*, 353-404.
Zhao, L., and Vogt, P.K. (2008). Class I PI3K in oncogenic cellular transformation. Oncogene *27*, 5486-5496.

CHAPTER 6

CONCLUSION

Introduction

Phosphorylated phosphoinositide lipids (PPIs) are low-abundance signaling molecules that control signal transduction pathways and are necessary for cellular homeostasis. The PPI phosphatidylinositol (3,5)-bisphosphate ($PI(3,5)P_2$) is essential for multiple organ systems. $PI(3,5)P_2$ is generated from PI3P by the conserved lipid kinase Fab1/PIKfyve. Defects in the dynamic regulation of $PI(3,5)P_2$ are linked to human diseases. However, few mechanisms that regulate $PI(3,5)P_2$ have been identified. Therefore the identification and characterization of mechanisms of regulation are critical to our understanding of the role of $PI(3,5)P_2$ within the cell and its connection to human disease.

Our work provides valuable new insights into the dynamic regulation of $PI(3,5)P_2$ and advances the PPI field via multiple fronts. First, domain boundary identification of the Fab1 complex aids the field by defining regions of predicted secondary structure that may have functional consequence in $PI(3,5)P_2$ regulation. Second, our work has identified a set of dominant-active mutants specific to individual domains within Fab1, which provides a genetic toolkit to assay the functional contributions of individual domains on the activity of Fab1. Third, this dissertation outlines an intramolecular

interaction between the CCR domain and kinase region of Fab1. This physical interaction controls PI(3,5)P_2 levels. Additionally, this work defines a function to the CCR domain, which previously had no known function. Last, this work identifies a shared motif at the C-terminus of the kinase domains of Fab1 and the PI4 5-kinase, Mss4, which controls their dynamic regulation. The regulation of lipid kinases is poorly understood, and this work represents a major advance in the regulation of Fab1 and Mss4.

Domain boundary identification within the Fab1 complex guides structure-function studies

Our findings suggest new domain boundaries for all members of the Fab1 complex and that Fab1/PIKfyve contains previously unidentified areas of secondary structure. Fab1/PIKfyve is regulated through a large protein complex that includes at least three proteins in mammalian cells—PIKfyve, Vac14, and Fig4—and five proteins in yeast—Fab1, Vac14, Fig4, Vac7, and Atg18. How these proteins regulate Fab1 is not known. Proteins often regulate one another via physical association of protein domains. Therefore, understanding what domains exist within these proteins will guide functional studies of the Fab1 complex regulatory network. Our studies redefine the boundaries of the Fab1 complex compared to previous work (Efe *et al.*, 2005; Michell *et al.*, 2006). Our work will guide the analysis of the contributions of individual Fab1 complex domains toward the regulation of PI(3,5)P_2 by aiding in the design of protein constructs. Additionally, our studies identify new, uncharacterized regions of secondary structure within Fab1/PIKfyve which we coin the L1, L2, and L3 domains. That these conserved

regions exist indicates that they likely have a functional role within Fab1/PIKfyve. Additionally, that dominant-active mutations in Fab1-L2 and Fab1-L3 domains exist indicates that they have a functional role in the regulation of Fab1. This work advances the PPI field by defining the domains of known regulators of $PI(3,5)P_2$.

Dominant-active mutations in Fab1 reveal domains that are required to regulate $PI(3,5)P_2$ levels

Knowledge of the function of specific domains within Fab1 is limited to a handful of structure function studies (Gary *et al.*, 2002; Botelho *et al.*, 2008; Jin *et al.*, 2008a). For instance, of the six domains within Fab1 and eight domains within PIKfyve, detailed analysis of domain function has only been performed on two—the CCT domain and the kinase domain (Jin *et al.*, 2008b). The identification of novel dominant-active alleles in domains of unknown function may provide mechanistic insight into the role of specific domains. Importantly, these studies identify dominant-active alleles in multiple regions of Fab1—many of which reside in Fab1 domains. For instance, while the Fab1-FYVE domain is hypothesized to regulate PI3P binding, these studies have never been published. The identification of multiple mutations of a single residue—Fab1-M238—that resides within the Fab1-FYVE domain—indicates a novel residue integral for the regulation of $PI(3,5)P_2$ levels. Excitingly, dominant-active alleles with a mutation at Fab1-M238 elevate $PI(3,5)P_2$ levels under basal conditions; however, they fail to properly respond to hyperosmotic shock (Figure 3.3A-B). This may be due to decreased Pi3P affinity by the Fab1-FYVE domain. Further characterization of alleles with a mutation at residue Fab1-M238 may shed light on how the Fab1-FYVE domain works to

aid in the regulation of PI(3,5)P_2 levels. Together with the total set of single mutations within Fab1 outlined in Chapter three of this thesis, this work may be used as a toolkit to study the function of individual domains' functions within the Fab1 complex. Additionally, analysis of mutant alleles that are conserved in humans may shed light on the function of these residues within mammalian PIKfyve.

An intramolecular interaction within Fab1 regulates PI(3,5)P_2 levels

The CCR domain is conserved in all known Fab1 proteins (Efe et al., 2005; Michell et al., 2006). Based on the conservation between Fab1 residues 819-1550 and the GroEL chaperonin, the CCR domain was proposed to associate with regulatory proteins (Efe et al., 2005; Michell et al., 2006; Botelho et al., 2008). However, little is known about the CCR domain, which is required for Fab1 activity (Botelho et al., 2008). Mutation of a conserved cysteine within this domain does not perturb Fab1 localization; yet leads to loss of Fab1 function as exhibited by temperature sensitivity, a defect in vacuolar morphology, and greatly reduced PI(3,5)P_2 levels (Botelho et al., 2008). These findings indicate that the CCR domain is critical for the regulation of PI(3,5)P_2 levels. However, no known role is directly attributed to the CCR domain.

Our work reveals that the CCR domain contacts a C-terminal portion of Fab1 including the kinase domain and negatively regulates kinase activity. We find that dominant-active mutations of the kinase domain ablate this interaction. This interaction is likely to be intramolecular; Fab1 does not form multimers *in vivo*. We identify seven dominant-active alleles in the CCR domain that elevate PI(3,5)P_2 levels. However, none of these

mutants were defective in the interaction of the CCR domain with the kinase region. Together, these findings suggest that Fab1 is regulated in part via an interaction between the kinase region and CCR domain.

That mutations may be made in the CCR domain that do not alter its affinity to the kinase region suggests that the CCR domain plays more than one regulatory role. This leads to three possibilities for an additional role of the CCR domain: (1) the CCR domain regulates or is regulated by another member of the Fab1 complex (2) the CCR domain regulates or is regulated by an unknown factor such as an unidentified protein or (3) the CCR domain interacts with the kinase region in more than one manner. Using this hypothesis framework, future work may identify that the CCR domain has one of the above roles in addition to the physical association of the kinase region of Fab1.

Conservation of a regulatory motif between yeast Fab1 and Mss4 suggests a common mechanism of regulation for phosphorylated phosphoinositide kinases

Phosphorylated phosphoinositides are regulated via lipid phosphatases and lipid kinases. Six lipid kinases exist in yeast (Strahl and Thorner, 2007). Most yeast lipid kinases are essential or their deletion causes severe phenotypes that impair cellular growth (Flanagan et al., 1993; Schu et al., 1993; Cutler et al., 1997; Desrivieres et al., 1998). Importantly, alignments of kinase domains from both yeast and mammalian lipid kinases show that all contain a C-terminal alpha helix directly distal to the activation loop (Rao et al., 1998).

Our work identifies that the yeast lipid kinase, Mss4, shares a putative regulatory motif C-terminal to its kinase domain that closely aligns to yeast Fab1. Indeed, dominant-active Mss4 alleles can be made based on dominant-active Fab1 alleles. The dominant-active Mss4 allele Mss4-V756S is based off of the dominant-active Fab1 allele Fab1-L2267S. Mss4-V756S elevates PI(4,5)P_2 higher than WT Mss4 under basal conditions (Figure 5.3B). Moreover, Mss4-V756S demonstrates a statistically significant 20% increase in PI(4,5)P_2 production compared to WT Mss4 at fifteen minutes post-hyperosmotic shock (Figure 5.3B). That similar residues can be mutated in the PI3P 5-kinase Fab1 and the PI4P 5-kinase Mss4 leading to an elevation in activity for both proteins indicates that a common mechanism of regulation may be present. This is the first evidence of dominant-activity in Mss4. Additionally, this is the first evidence that a common mechanism of regulation may be present in yeast lipid kinases. The mechanisms that regulate lipid kinase activity both in yeast and higher eukaryotes are largely uncharacterized. Our work lays evidence that a common regulatory motif at the C-terminal kinase domain of these kinases may control kinase activity.

Bibliography

Botelho, R.J., Efe, J.A., Teis, D., and Emr, S.D. (2008). Assembly of a Fab1 phosphoinositide kinase signaling complex requires the Fig4 phosphoinositide phosphatase. Mol Biol Cell *19*, 4273-4286.
Efe, J.A., Botelho, R.J., and Emr, S.D. (2005). The Fab1 phosphatidylinositol kinase pathway in the regulation of vacuole morphology. Curr Opin Cell Biol *17*, 402-408.
Gary, J.D., Sato, T.K., Stefan, C.J., Bonangelino, C.J., Weisman, L.S., and Emr, S.D. (2002). Regulation of Fab1 phosphatidylinositol 3-phosphate 5-kinase pathway by Vac7 protein and Fig4, a polyphosphoinositide phosphatase family member. Molecular biology of the cell *13*, 1238-1251.
Jin, N., Chow, C.Y., Liu, L., Zolov, S.N., Bronson, R., Davisson, M., Petersen, J.L., Zhang, Y., Park, S., Duex, J.E., Goldowitz, D., Meisler, M.H., and Weisman, L.S. (2008a). VAC14 nucleates a protein complex essential for the acute interconversion of PI3P and PI(3,5)P(2) in yeast and mouse. EMBO J *27*, 3221-3234.
Jin, N., Chow, C.Y., Liu, L., Zolov, S.N., Bronson, R., Davisson, M., Petersen, J.L., Zhang, Y., Park, S., Duex, J.E., Goldowitz, D., Meisler, M.H., and Weisman, L.S. (2008b). VAC14 nucleates a protein complex essential for the acute interconversion of PI3P and PI(3,5)P(2) in yeast and mouse. The EMBO journal *27*, 3221-3234.
Michell, R.H., Heath, V.L., Lemmon, M.A., and Dove, S.K. (2006). Phosphatidylinositol 3,5-bisphosphate: metabolism and cellular functions. Trends in biochemical sciences *31*, 52-63.